JCMM

Journal of Computers, Mechanical and Management

Volume 1, Issue 1
2022

Journal of Computers, Mechanical and Management

Journal homepage: www.jcmm.co.in

Editorial Comments for the Inaugural Issue: JCMM Volume 1 Issue 1

Nanjangud Subbaro Mohan*[a,b]

[a]Editor-in-Chef, Journal of Computers, Mechanical and Management, GADL, Jalalpur Mafi, Uttar Pradesh, India 231304

[b]Department of Mechanical and Industrial Engineering, Manipal Institute of Technology, Manipal Academy of Higher Education, Manipal, Karnataka, India 576104

This is the first historical issue of the *Journal of Computers, Mechanical and Management (JCMM)*, a bimonthly publication of the *Global Academic Digital Library (GADL)*. Mechanical elements (from tiny screws to huge machines), computer knowledge (hardware and software) and application of the right management philosophy are the prime elements required to make the world look better. JCMM, an emerging multidisciplinary journal, has been thus launched to cover all the aspects of basic sciences, engineering sciences and management studies comprising the discussed prime elements.

The published papers are within the scope of JCMM and aim to enhance the international exchange of scientific activities on the applications of computers, mechanical components, materials and management techniques. The collaborative and international efforts were visible as authors from five countries (India, Germany, United States, Canada and Sri Lanka). The journal published seven articles, six full-length articles and one review article. Volume 1, issue 1 of JCMM started with the article by Bhat et al. [1], wherein the authors investigated the seawater's effect on the hardness of marine FRP composites of varying thicknesses and presented the experimental results indicating the effect. The authors also discussed the root cause concerning the chemistry behind it at the microstructural level using SEM and EDX analysis. Srikanth et al. [**?**] emphasized the application of simulation and modeling to determine the property enhancement and optimize the fiber content in concrete composites. The authors used the ANSYS simulation and modeling approach to optimize the polypropylene fibers in concrete to achieve better bending and uniaxial tensile strength. Banerjee and Dua [**?**] presented a framework based on trendy technologies, specifically extracting, transforming and integrating (ETI) processes, ontology graphs, and indexing resource description framework (RDF) using the wide-column not only structured query language (NoSQL) method. The authors performed numerous operations to evaluate the effectiveness of the proposed methodology in installing data sources, such as DBpedia and YAGO datasets and validated the developed model. Kumar et al. [**?**] touched upon a relatively hot topic in the welding process. The article focussed on friction stir welding of dissimilar aluminum-silicon alloys utilizing a vertical milling machine and altering process parameters. The authors provided optimum working conditions, yielding the welds exhibiting good tensile strength and surface finish. S. Deepa [**?**] proposed a meta-heuristics algorithm for regression testing. The author combined particle swarm optimization (PSO) with the bat algorithm to solve the problem of finding the best subset of regression test cases with multi objectives of reducing risk in skipping test cases, maximizing the number of faults within the time constraints. Bhiwaniwala et al. [**?**] developed a comprehensive model to assess the pandemic's impact on employees' lifestyles. The inferences highlighted the factors influencing employee morale and work culture and the parameters closely related to employee functioning in the organization that should not be affected. Volume 1, issue 1 of JCMM concluded with an extensive review article by Naik et al. [**?**], wherein the authors provided an in-depth overview of bioresin-based green composites so that the reader can better understand the mechanical properties, chemical treatment methods and processing techniques associated with these composites.

*Corresponding author: editor@jcmm.co.in
© 2023 Journal of Computers, Mechanical and Management.
Published: 01 November 2022
This is an open access article and is licensed under a Creative Commons Attribution-Non Commercial 4.0 International License.
DOI: 10.57159/gadl.jcmm.1.1.23014.

It is always opportune to remember that the JCMM will accept submissions as Original Articles, those documenting significant results that contribute to the extension of knowledge and promotion of the understanding, presented in such a way that qualified readers can replicate the key elements based on the information provided; Review Articles, which are about an extensive survey of one particular subject, in which the already published information is compiled, analyzed and discussed to achieve a balanced assessment and synthesis of knowledge. With the publication of this first issue, I, on behalf of the JCMM team, call the authors forward their original works so that we can make JCMM, as soon as possible, an international publication of the highest level.

References

[1]

[2] V. Rai and V. R. Chauhan, *Market Penetration through Digital Marketing: A Case Study of a Tractor Dealership During Covid-19 Pandemic*, Journal of Computers, Mechanical and Management, 2 (2), 2023, doi:10.57159/gadl.jcmm.2.2.23042.

[3] B. Z. Hameed et al., *The Impact of the COVID-19 Pandemic and Associated Lockdowns on the Mental and Physical Health of Urologists*, Journal of Computers, Mechanical and Management, 2 (2), 2023, doi:10.57159/gadl.jcmm.2.2.23045.

[4] P. Gayathri, A. Dhavileswarapu, S. Ibrahim, R. Paul, and R. Gupta, *Exploring the Potential of VGG-16 Architecture for Accurate Brain Tumor Detection Using Deep Learning*, Journal of Computers, Mechanical and Management, 2 (2), 2023, doi:10.57159/gadl.jcmm.2.2.23056.

[5] B. Z. Hameed et al., *Mitigating Psychological Impacts of Quarantine During Pandemics: A Mini Review*, Journal of Computers, Mechanical and Management, 2 (2), 2023, doi:10.57159/gadl.jcmm.2.2.23043.

[6] Y. Kaushik, N. Sooriyaperakasam, U. Rathee, and N. Naik, *A Mini Review of Natural Cellulosic Fibers: Extraction, Treatment and Characterization Methods*, Journal of Computers, Mechanical and Management, 2 (2), 2023, doi:10.57159/gadl.jcmm.2.2.23057.

Journal of Computers, Mechanical and Management

Journal homepage: www.jcmm.co.in

Volume 1 Issue 1

Influence of Seawater Absorption on the Hardness of Glass Fiber/Polyester Composite

Ritesh Bhat*[a], Nanjangud Mohan[a], Sathyashankara Sharma[a], and Suma Rao[b]

[a]Department of Mechanical and Industrial Engineering, Manipal Institute of Technology, Manipal Academy of Higher Education, Manipal, India 576104

[b]Department of Chemistry, Manipal Institute of Technology, Manipal Academy of Higher Education Manipal, India 576104

Abstract

In the marine industry, glass fibers are commonly used to reinforce polyesters for ship hulls, submarine components, and other marine structures. Isophthalic polyesters are a feasible alternative due to their superior mechanical qualities and added end-of-life scenarios compared to orthophthalic polyesters. However, like other fiber composite systems, glass fiber reinforced polymer (GFRP) composites are also water sensitive. Here, GFRP composites of three different thicknesses are aged under three different immersion periods in seawater (20, 40 and 60 days). All samples are evaluated for hardness following aging. Significant emphasis is placed on the presence of calcium carbonate, over which increases in moisture content irrevocably reduce the composite's hardness. Compared to untreated material, the hardness of 6, 8 and 10 mm composites decreased by 25.64, 10.92 and 4.63% after the 60-day aging period. This drop is mostly the result of microstructure evolution manifesting as an increase in porosity. Consequently, fiber deterioration, fiber cracks, and degradation of polymer-fiber bonding emerge in the composite, decreasing hardness.

Keywords: Degradation; Hydrolysis; Polyester Composites; Hardness; Material Chemistry

1 Introduction

Components and structures functioning in the marine environment are subjected to high stresses caused by wind, waves, and tides. In addition, they must contend with hostile and harsh environmental circumstances throughout their existence, as they are placed in the splash zone if not submerged in saltwater. The application of polymer composites in maritime systems has been the subject of significant research over the past few decades, showing the potential benefits of replacing numerous components, including ship hulls, domes and non-pressure hull decking for submarines, propeller blades, wind turbine blades, and tidal turbine blades, to name a few [1–3]. To be precise, it is since the mid-1980s that the usage of composite materials in marine constructions has expanded dramatically, and the global industry anticipates an annual growth rate of 5.8% as an alternative to galvanic corrosion-prone classical materials [4, 5]. However, fiber reinforced polymer (FRP) composite materials are sensitive to moisture and temperature, and prolonged exposure to such a harsh environment degrades the material's mechanical characteristics. The seawater environment tends to chemically alter the composition of FRP composites [6–8]. Therefore, to anticipate the service life of structures and the functional stability of the composites, it is vital to understand the robustness and life cycle of composites in terms of their mechanical, chemical, and thermal properties [9]. In other words, it is crucial to assess the degradation of mechanical properties caused by exposure to seawater for marine composites [9]. Hardness, a mechanical attribute of the material, is its ability to resist deformation and is determined by a standard test that measures the surface resistance to indentation [10–12].

*Corresponding author: ritesh.bhat@manipal.edu

Received: 24 August 2022; **Accepted:** 04 September 2022; **Published:** 30 October 2022

© 2022 Journal of Computers, Mechanical and Management.

This is an open access article and is licensed under a Creative Commons Attribution-Non Commercial 4.0 International License.

DOI: 10.57159/gadl.jcmm.1.1.23003.

Hardness not only affects the tribological performance of a material [13] but also is an important factor to be considered while machining, in particular drilling, as the drill tool life is found to be a strong function of it [14, 15]. A mechanical connection is required between FRP composites and other metal or composite structures. As a crucial final manufacturing stage for composite laminates, drilling is widely employed to facilitate riveted and bolted joints for attaching the composite structure to other components [16]. The most prominent concerns in FRP composite drilling are delamination and hole surface roughness. It has been discovered that tool wears greatly contributes to both problems [17–20]. From the literature reviewed, hardness is determined to be an important mechanical property to be investigated as it holds significance in machining materials, particularly the drilling of composites. It is also learned that seawater exposure has adverse effects on the FRP composites, leading to an alteration in the material chemistry resulting in material degradation. Though several researchers have been focusing on investigating the various mechanical properties of the marine FRP composites, there is no document that exclusively discusses the investigation of seawater immersion effect on the FRP composite hardness. Thus, filling the literature gap and emphasizing the non-addressed but important mechanical property, this study aims to investigate seawater's effect on the hardness of marine FRP composites of varying thicknesses. The present study not only experimentally indicates the effect but also discusses the root cause concerning the chemistry behind it at the microstructural level using SEM and EDX analysis.

2 Materials and Methods

2.1 Composite composition and fabrication

The glass fiber reinforced polymer (GFRP) composite material used in this investigation consisted of chopped stranded mats containing discontinuous E-glass fibers with a density of 1.56 gcm-2. The matrix phase is composed of thermoset polymer resins with a density of 2.56 g/cm2, which are unsaturated (isophthalic) polyesters. Methyl-ethyl-ketone peroxide (MEKPO) is used as a hardener, also known as a curing agent or catalyst, to enhance the crosslinking of unsaturated polyesters (curing) [21, 22]. The composites produced contained 33.4 wt.% of fibers. When creating composites, a hardener-to-resin ratio of 0.0012:1 and a matrix-to-fiber ratio of 2:0 was considered. For manufacturing GFRP composites, the manual open-mold hand-layup approach [23] was adopted. Before applying the mold release agent, the plywood mold was thoroughly cleaned. As a release agent for the mold, wax and polyvinyl acetate was utilized [24, 25]. The liquid polyester was used to create the gel coating, followed by applying the first layer of the fiber mat. The matrix consisting of the polyester-hardener mixture was then brushed over it, and the second layer of glass fiber was deposited on top. The matrix was distributed evenly throughout the composite using a hand roller. Thus, the described layer-by-layer hand-layup technique was employed to manufacture 6, 8, and 10 mm thick GFRP composites.

2.2 Seawater treatment and mass gain determination

Seawater was produced in the laboratory following ASTM D1141-98 Standard practice for the preparation of substitute ocean water [26, 27]. Seawater is slightly alkaline, with pH values between 8.0 and 8.5 [28]; hence the pH of the prepared seawater was maintained between 8.3 to 8.5. The chemicals used and their proportion for making 10 liters of seawater is as shown in Table 1.

Table 1: Chemical composition for preparing 10 liters of seawater as per ASTM D1141-98 standard.

Composition (chemical formula)	**Fraction (g/10 liters)**
Sodium chloride (NaCl)	245.34
Magnesium chloride ($MgCl_2$·6H2O)	111.12
Anhydrous sodium sulfate (Na_2SO_4)	40.94
Anhydrous calcium chloride ($CaCl_2$)	11.58
Potassium chloride (KCl)	6.95
Sodium bicarbonate ($NaHCO_3$)	2.01
Potassium bromide (KBr)	1.00
Boric acid (H_3BO_3)	0.27
Strontium chloride ($SrCl_2$·$6H_2O$)	0.42
Sodium fluoride (NaF)	0.03
0.1 N Sodium hydroxide (NaOH) solution	Added in quantity sufficient to get the pH level to 8.3 ±0.2

All chemicals utilized during the research were of research grade. Thus prepared, seawater was poured into three separate 10-liter-capacity containers. In addition, three different colors of buckets were used to distinguish between the specimen contained in each container, based on the material thicknesses. A precise digital weighing balance with a weight limit of 10 kg and an accuracy of 1 gram was used to weigh the aged GFRP composite slabs of every thickness at 20-day intervals up to 60 days to determine the water absorption by the material periodically. Before weighing, tissue paper was used to wipe the surface of the samples.

Using Eq. [1], the relative mass change m (%) was calculated, where mi and mf represent the initial and final mass of the material, respectively [29]. The weight variations of GFRP composites with thicknesses of 6, 8, and 10 mm were determined by weighing five replicates of each thickness.

$$m(\%) = \frac{m_f - m_i}{m_i} \times 100 \tag{1}$$

2.3 Hardness measurement

The ASTM D2583-07 standard test method for indentation hardness of rigid plastics [30] is used to perform Barcol hardness tests with the Barber Colman impresser. The hardness measurement characterizes the indentation strength of components as assessed by the indenter point's penetration depth. The test was conducted for untreated and treated composite samples. Five Barcol hardness measurements were taken for each GFRP slab of every thickness, and the average value was chosen for each specimen's final Barcol hardness measurement.

2.4 Material characterization

The material characterization was accomplished using scanning electron microscopy (SEM) and energy dispersive X-ray (EDX) analysis. The SEM was employed to investigate the microstructural damage caused in all the composite samples of different thicknesses. The diameters for untreated and treated fibers were measured using the ImageJ software to check for degradation in terms of diameter reduction. The EDX analysis was used not only to check the probability of the presence of salts like potassium chloride [KCl], potassium bromide [KBr] and sodium chloride [NaCl] but also to determine the atomic weight percentage reduction in Silica [SiO_2]and other constituents of the E-glass fiber (magnesium and aluminum oxides) due to degradation in the seawater treated composites. The presence of calcium carbonate [$CaCO_3$] is also investigated using the EDX analysis. Zeiss Evo MA18 with Oxford EDS(X-act) equipment installed in the Central Instrumentation Facility (CIF), MIT, Manipal, India, was used to conduct both SEM and EDX analysis.

3 Results and Discussion

Figure 1 represents the hardness reduction (%) of 6, 8 and 10 mm thick GFRP composite at different immersion periods. The negative sign in Figure represents that reduction in the hardness value. A trendline is obtained for each represented graph considering a third-order polynomial equation.

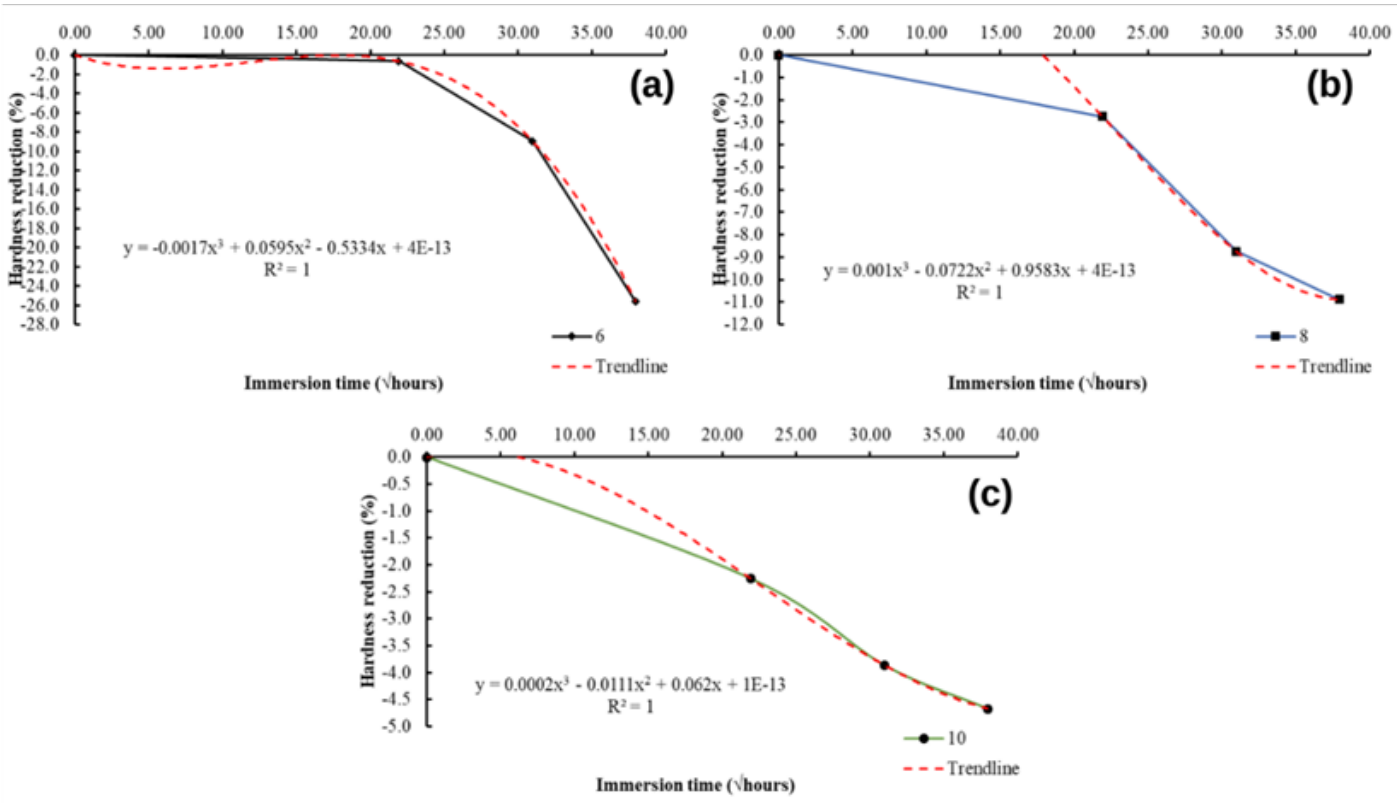

Figure 1: Results of hardness reduction for **(a)** 6mm; **(b)** 8 mm; **(c)** 10 mm GFRP composites.

The developed equation for 6, 8 and 10 mm GFRP composites are given by Eqs. [2], Eq. [3] and Eq. [4], respectively. The term y_i in the equations represents the hardness reduction (%) value for i^{th} thickness, and x represents the immersion period (square root of hours). All the developed equations possess high prediction accuracy ($R^2 = 1$) within the experimented limits. The average standard deviations are recorded as 0.531, 0.601 and 0.515 for 6, 8 and 10 mm GFRP composites.

$$y_6 = -0.0017x^3 + 0.0595x^2 - 0.5334x - 4e^{-13} \tag{2}$$

$$y_8 = 0.001x^3 - 0.0722x^2 + 0.9583x - 4e^{-13} \tag{3}$$

$$y_{10} = 0.00025x^3 - 0.0111x^2 - 0.062x - 1e^{-13} \tag{4}$$

The average Barcol hardness was recorded as 43.3, 46.7 and 49.7 BHN for 6, 8 and 10 mm thick fabricated untreated GFRP samples, respectively. A continuous drop was later observed in the hardness value irrespective of the thickness of the GFRP composites, and the decrement continued with the increase in the immersion period. Table 2 details the average hardness value for 6, 8 and 10 mm GFRP considering the three selected immersion times.

Table 2: Hardness test results for 6, 8 and 10 mm seawater treated GFRP composites.

Immersion time (days)	**Composite thickness (mm)**	**BHN of untreated specimen**	**BHN of seawater treated specimen**	**Reduction(%)**
20 days	6	43.3	43.0	0.69
	8	46.7	45.4	2.78
	10	49.7	48.6	2.21
40 days	6	43.3	39.4	9.01
	8	46.7	42.6	8.78
	10	49.7	47.8	3.82
60 days	6	43.3	32.2	25.64
	8	46.7	41.6	10.92
	10	49.7	47.4	4.63

Figure 2 represents the mass gain rate (%) of 6, 8 and 10 mm thick GFRP composite at different immersion periods. A trendline is obtained for each represented graph considering a third-order polynomial equation.

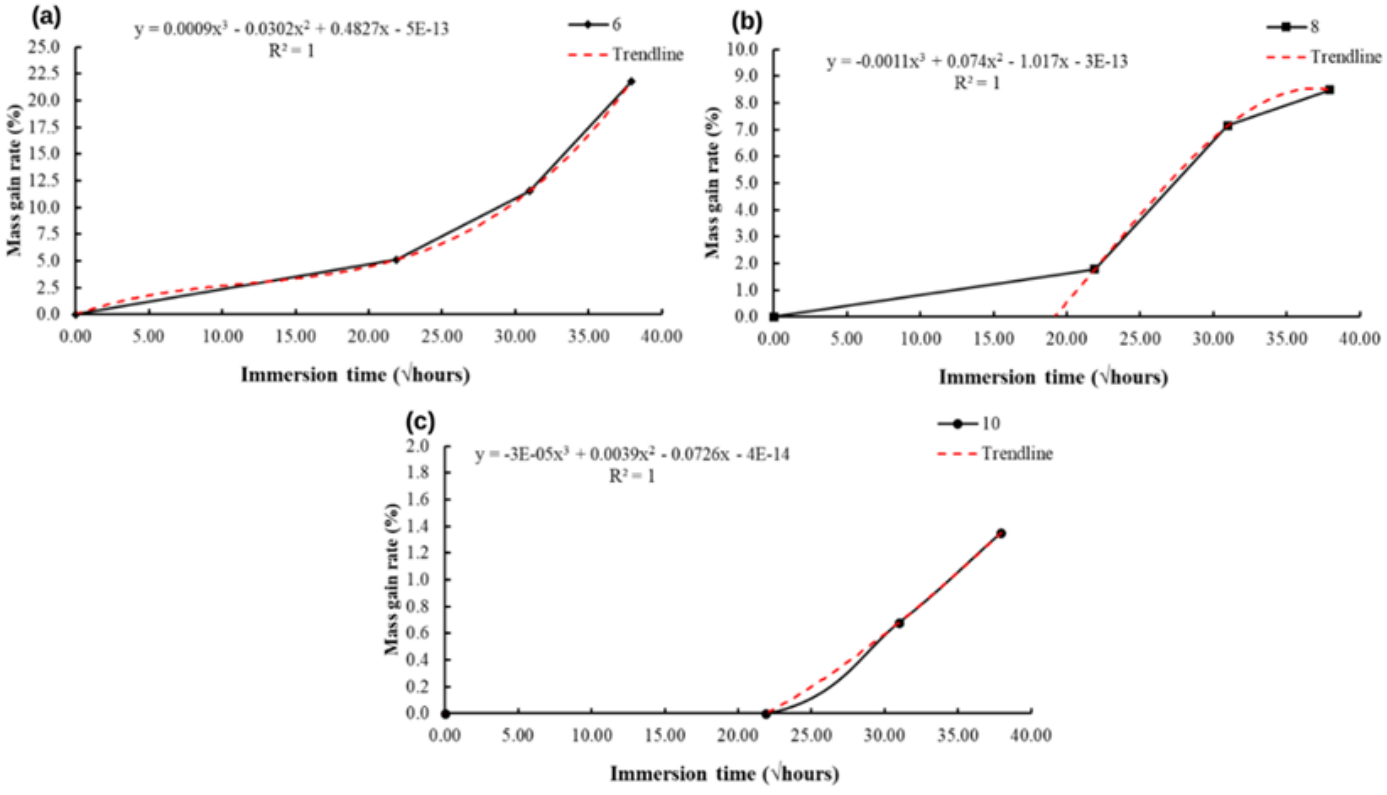

Figure 2: Results of mass gain rate for **(a)** 6mm; **(b)** 8 mm; **(c)** 10 mm GFRP composites.

The developed equation for 6, 8 and 10 mm GFRP composites are given by Eq. [5], Eq. [6] and Eq. [7], respectively. The term y_i in the equations represents the mass gain rate (%) value for ith thickness, and x represents the immersion period (square root of hours). All the developed equations possess high prediction accuracy (R^2 = 1) within the experimented limits. The average standard deviations are determined to be 0.634, 0.436 and 0.031 for 6, 8 and 10 mm GFRP composites. When immersed in seawater, the composites absorb water molecules and release the soluble solid particles. Therefore, the mass gain rate represents the net effect of mass gained due to water absorption and the mass lost due to the oozing out of soluble solid particles from the composite. The average mass was recorded as 78, 112 and 148 g for 6, 8 and 10 mm thick fabricated untreated GFRP samples.

$$y_6 = 0.0009x^3 - 0.03025x^2 + 0.4827x - 5e^{-13} \tag{5}$$

$$y_8 = -0.001x^3 + 0.074x^2 - 1.107x - 3e^{-13} \tag{6}$$

$$y_{10} = -0.0003x^3 + 0.0039x^2 - 0.072x - 4e^{-14} \tag{7}$$

Table 3 provides the results for mass change in composites due to water absorption. The thinner composites were seen to absorb more amount of water. Therefore, it could be said that the thicker composites with a greater number of lamina layers prevent the degradation as the salt particles do not tend to penetrate much in such compositions. The unit used for the immersion period in Figure 1 and Figure 2 is the square root of hours, as it provides a neat and regular curve. Moreover, the prediction within the experimental limits of response value for a small immersion period gets easier. The reduction in the hardness value and increase in the water absorption values with the increase in the immersion period is mostly the result of microstructure evolution manifesting as an increase in porosity. The microstructural analysis was conducted using the SEM and EDX analysis to affirm the assumption.

Table 3: Mass gain rate results for 6, 8 and 10 mm seawater treated GFRP composites.

Immersion time (days)	**Composite thickness (mm)**	**Mass of untreated specimen (g)**	**Mass of seawater treated specimen (g)**	**Mass gain rate(%)**
20	6	78	82	5.13
	8	112	114	1.79
	10	148	148	0.00
40	6	78	87	11.54
	8	112	120	7.14
	10	148	149	0.68
60	6	78	95	21.79
	8	112	122	8.93
	10	148	150	1.35

The results of the SEM analysis for 6, 8 and 10 mm thick GFRP composites concerning different seawater immersion periods are depicted in Figure 3, Figure 4 and Figure 5 respectively. Irrespective of the thickness, the severity of the composite degradation is observed to increase with the increasing period of immersion. The fiber cracks are visible in the presented SEM images. The SEM images were also analyzed using the ImageJ software to determine the degradation of fibers characterized by the change in the diametric values. The average diameter of the fibers in untreated samples was 16 µm. The average diameter value was reduced to 15.5, 14 and 11 µm considering the GFRP samples subjected to 20, 40 and 60 days of seawater immersion. Changes in diameter values were reported to be greatest in samples with a thickness of 6 mm and smallest in samples with a thickness of 10 mm. On average, the reduction in diametric values was observed to be 3.13, 12.5 and 31.25%. The fiber cracks and the reduction of diametric value confirm the degradation of the fibers used in the composites. Moreover, the SEM images also evidently show the severe matrix erosion at the surface and matrix-fiber debonding. The matrix degradation in the GFRP samples was because of the leaching action, wherein the distributed salt particles (present in the seawater) leach away to form a porous structure [31]. Irrespective of the thickness, the matrix degradation is observed to have initiated in the 20 days aged samples. Nevertheless, the matrix erosion was low in the case of 10 mm samples compared to the counterparts for any given period of immersion time. The phenomenon observed in all the samples was the leaching of the matrix due to salt present in the seawater medium, causing porosity and leading to further penetration of the seawater into the composites. The second stage is wherein the matrix-fiber debonding occurs, and the component functional stability starts weaking. In this phase, the matrix degrades and exposes the fibers to the seawater medium, which causes cracks in them. With a further increase in immersion time, the matrix erosion increases, causing greater damage to the composites. The salt particles could not damage the 10 mm thick composites much, probably due to the higher amount of fibers and matrix layers than their counterparts. However, an increased immersion time than the selected period in the current study can cause damage to it and thus can be considered as a future scope of the present work. The matrix degradation is also caused due to the hydrolysis (breaking of the crosslinking bondage) of polyesters caused due to the presence of sodium hydroxide and potassium salt [28, 32]. The reinforcing phase provides the mechanical strength in a fiber composite compared to the matrix material [33]. In this study, it is the glass fibers. Therefore, to further examine the reason for the reduction of hardness caused due to severe degradation of fiber material, particularly after 60 days of immersion period, EDX analysis was conducted. Glass fibers are made up of silica [SiO_2] and other material oxides like calcium [CaO], magnesium [MgO]and aluminum [Al_2O_3][33]. The EDX analysis aimed to observe the reduction in the atomic weights of these elements and to check for the formation of calcium carbonate [$CaCO_3$].

The data obtained from the supplier for the glass fibers were taken as the benchmark for its various constituents. The glass fiber used in the present study comprised 55.2 % silica, 18.7 % calcium oxide [CaO], 8% aluminium oxide [Al_2O_3], 7.3 % of lithium oxide [Li_2O], and 4.6 % magnesium oxide [MgO] as its major constituents. As assumed, the atomic weight of silica and magnesium and aluminum oxides has decreased in the seawater-treated specimen irrespective of the composite thickness.

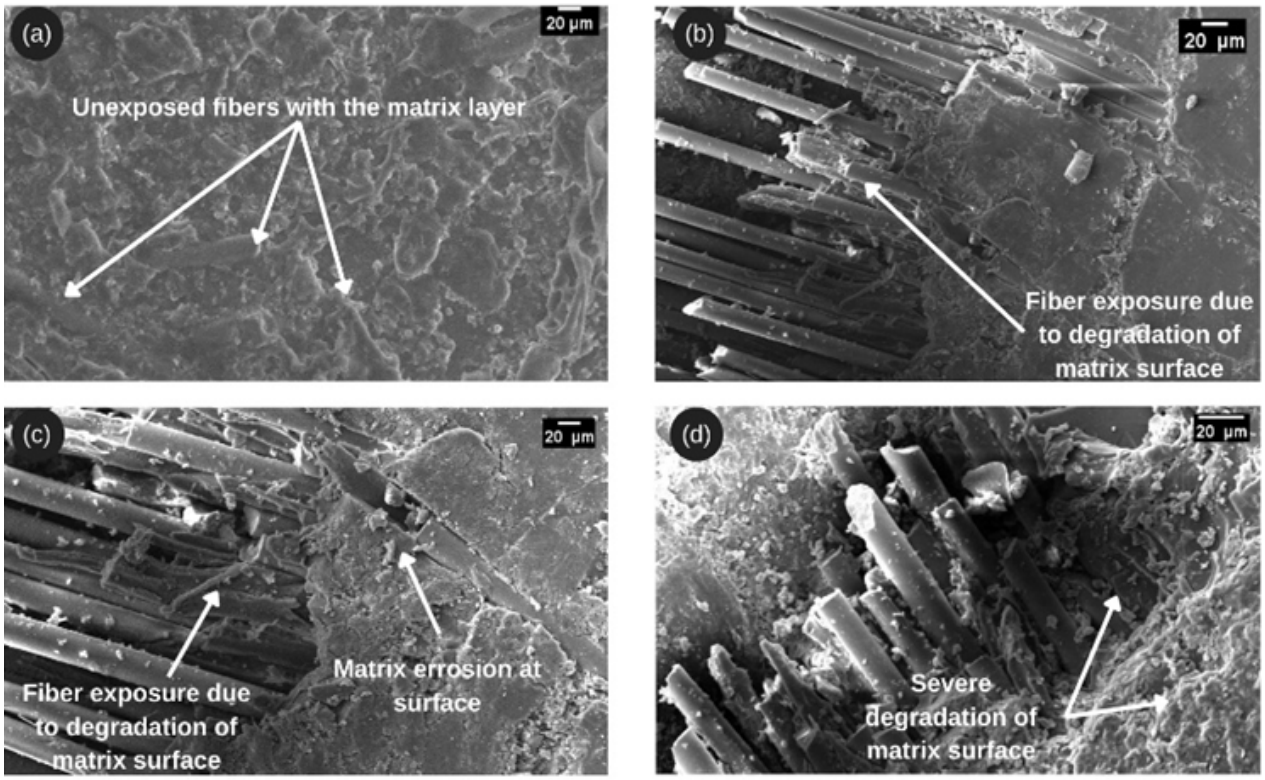

Figure 3: SEM results for 6 mm GFRP: **(a)** untreated; **(b)** 20 days seawater treated; **(c)** 40 days seawater treated; **(d)** 60 days seawater treated.

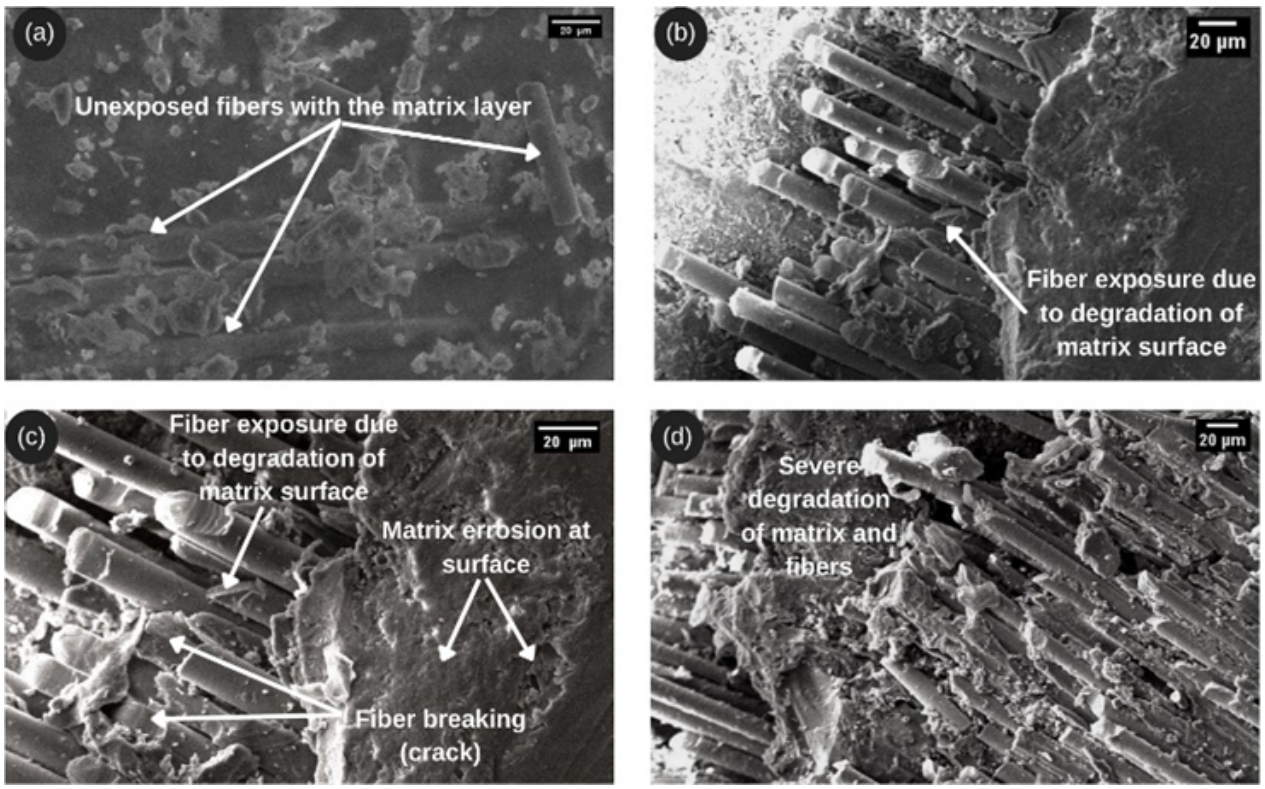

Figure 4: SEM results for 8 mm GFRP: **(a)** untreated; **(b)** 20 days seawater treated; **(c)** 40 days seawater treated; **(d)** 60 days seawater treated.

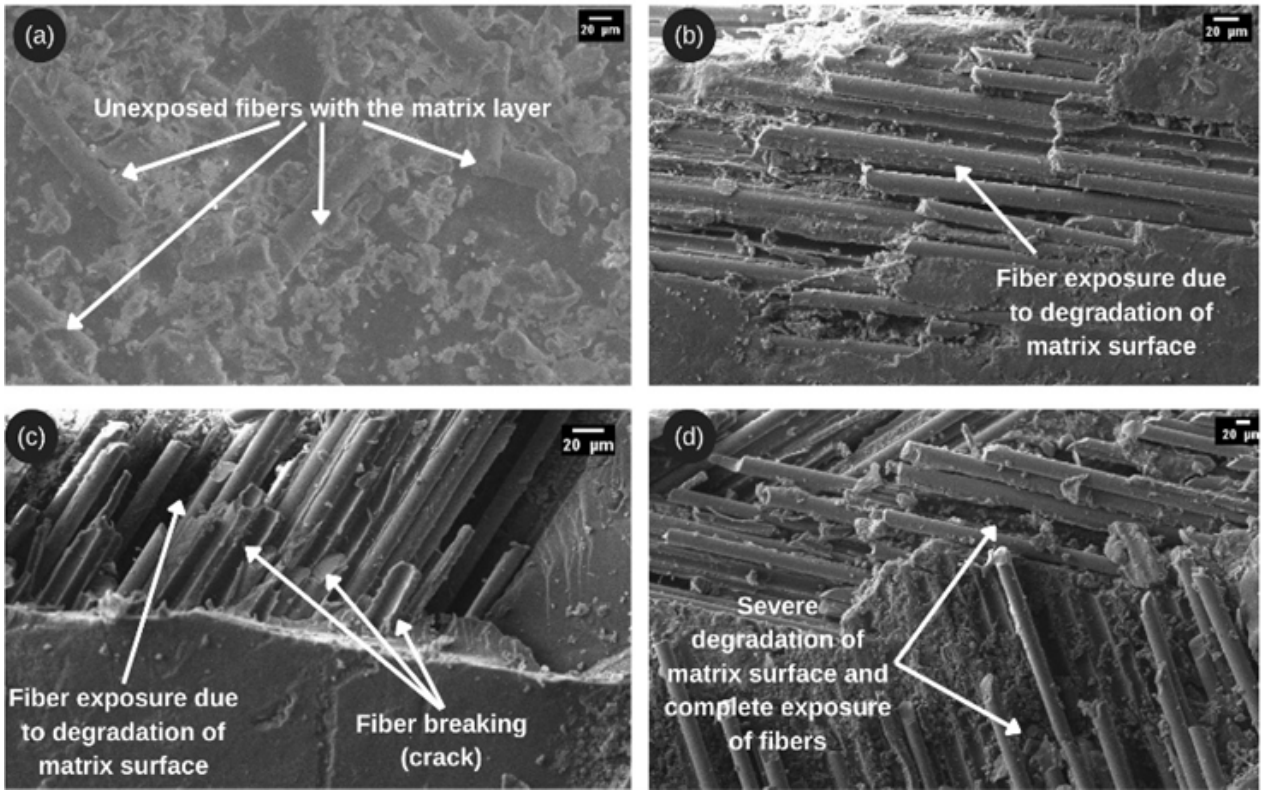

Figure 5: SEM results for 10 mm GFRP: **(a)** untreated; **(b)** 20 days seawater treated; **(c)** 40 days seawater treated; **(d)** 60 days seawater treated.

The loss was seen to be higher for the 6 mm thick composite, followed by the 8 and then the 10 mm thick samples. The EDX results support all the results obtained for the hardness test and SEM analysis. The results justify the decrease in the diameter values of the fibers, increasing the porosity. The atomic weight of silica is seen to reduce on average by 45.50, 42.75 and 36.68 % in 6, 8 and 10 mm composites. The average reduction in the atomic weight of aluminum oxide is by 3.08, 2.16 and 1.73 % for 6, 8 and 10 mm thick composites. Considering the average reduction in the atomic weights of magnesium oxide for 6, 8 and 10 mm composites, it was recorded as 2.47, 0.825 and 0.65 %. The traces of potassium chloride [KCl] and potassium bromide [KBr] salts in good percentages were found in 6 and 8 mm thick composites, which might have caused the leaching effect. As mentioned earlier, the salts could not penetrate much into the 10 mm thick material. Figure 6, Figure 7 and Figure 8 illustrate the results of the discussed EDX analysis. In addition, the calcium carbonate is in higher proportion in the 6 mm composites and least in the 10 mm composite. The average atomic weight of the CaCO3 is determined to be 34.49, 33.49 and 23.25 % in the 6, 8 and 10 mm composites, respectively. The EDX results and all other tests justify the degradation in the GFRP composites subjected to seawater conditions. The EDX results also justify the importance of the thickness of the composites when used for marine conditions.

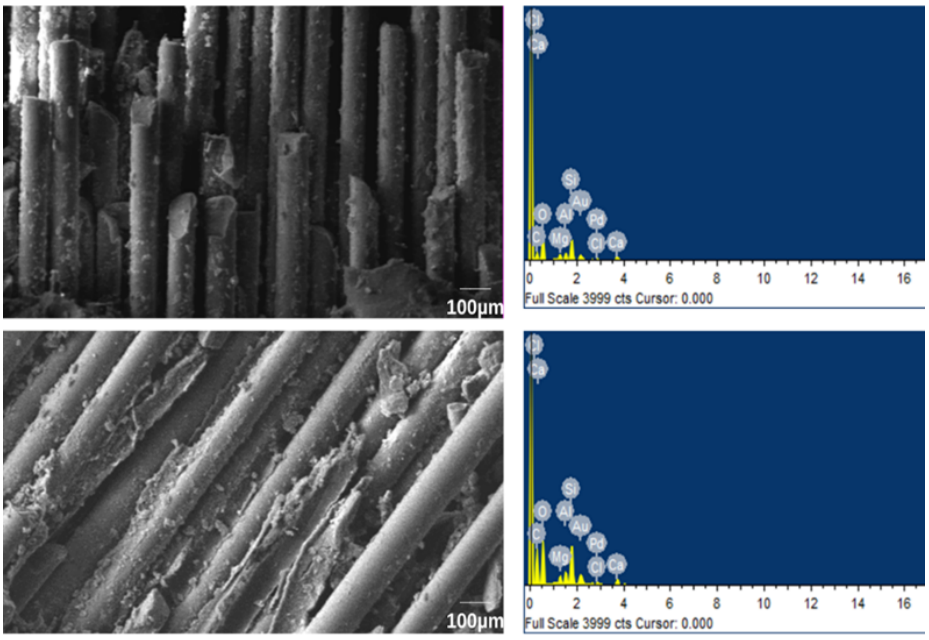

Figure 6: EDX results for 60 days seawater treated 6 mm GFRP at two different positions.

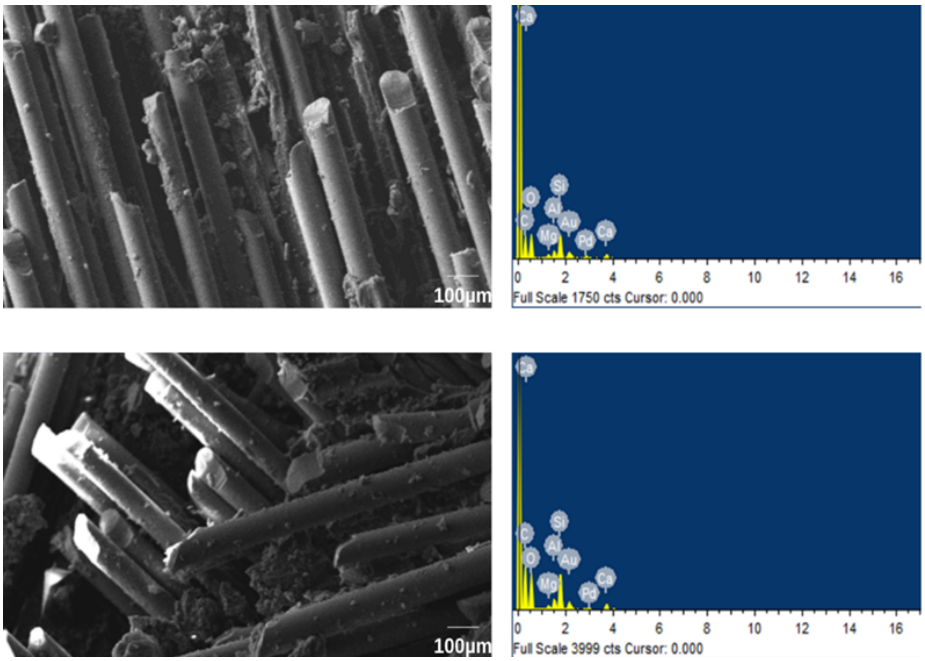

Figure 7: EDX results for 60 days seawater treated 8 mm GFRP at two different positions.

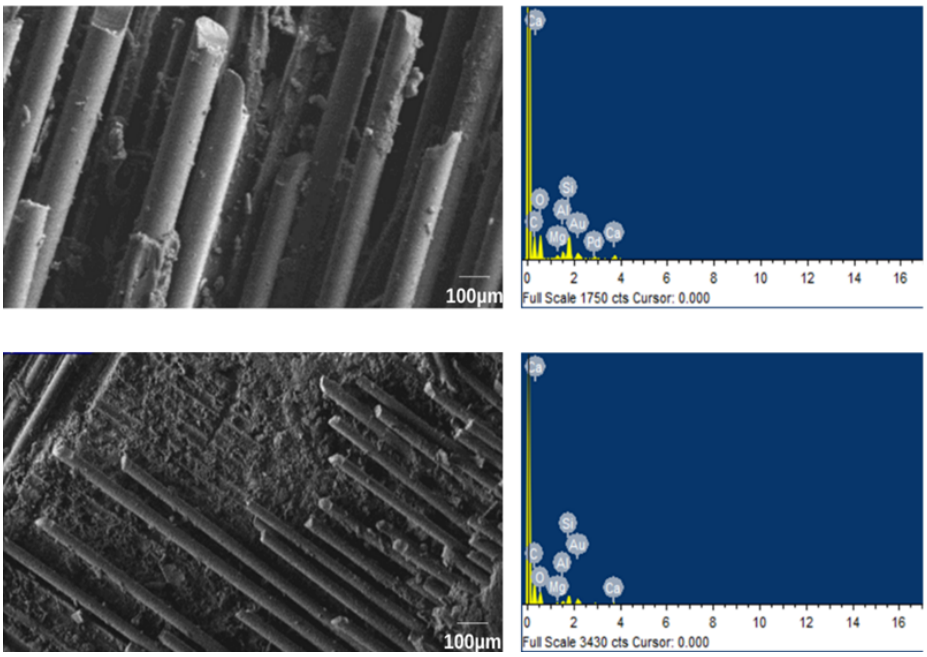

Figure 8: EDX results for 60 days seawater treated 10 mm GFRP at two different positions.

4 Conclusion

This research aimed to determine the influence of seawater on the hardness of 6, 8, and 10 mm thick composites made of glass fiber and isophthalic polyester, a new generation of marine composites. This is one of the first studies to explore the impact of seawater immersion on marine composites' hardness. The investigation revealed the vulnerability of polyester resin to hydrolysis, which resulted in the leaching out of ester species with hydroxyl end groups and debonding at the matrix-fiber interfacial region. The change in the mass of glass fiber reinforced unsaturated polyester composites after immersion in seawater was due to two effects: water absorption and soluble particle extraction. The matrix swelled and eroded due to the absorbed moisture. The matrix erosion due to leaching exposed the glass fibers, which were then damaged by the salts in the artificially prepared seawater. Due to the dissolving of silica and its other primary elements, the exposure of the fibers to seawater caused a reduction in their diameter. The material's loss of functional stability resulted from physical damage and/or irreversible chemical deterioration, as demonstrated by the material's progressively decreasing hardness values after prolonged exposure to seawater. The SEM and EDX analyses of the specimen after immersion in seawater revealed that the fiber/matrix interface had been severely degraded, with the degree of damage increasing with immersion time.

Declaration of Competing Interests

The authors declare that they have no known competing financial interests or personal relationships that could have appeared to influence the work reported in this paper.

Funding Declaration

This research did not receive any grants from governmental, private, or nonprofit funding bodies.

Author Contribution

Ritesh Bhat: Conceptualization, Methodology, Data curation, Writing- Original draft preparation, Visualization, Validation. **Nanjangud Mohan**: Supervision, Validation, Writing- Reviewing and Editing. **Sathyashankara Sharma**: Supervision, Validation, Writing- Reviewing and Editing. **Suma Rao**: Supervision, Validation, Writing- Reviewing and Editing.

References

[1] F. Rubino, A. Nisticò, F. Tucci, and P. Carlone, "Marine Application of Fiber Reinforced Composites: A Review," *Journal of Marine Science and Engineering*, vol. 8, p. 26, jan 2020.

[2] A. W. Horsmon, "Composites for Large Ships," *Journal of Ship Production*, vol. 10, pp. 274–280, nov 1994.

[3] S. Selvaraju and S. Ilaiyavel, "Applications of composites in marine industry," *Journal of Engineering ...*, vol. II, no. II, pp. 89–91, 2011.

[4] A. Siriruk and D. Penumadu, "Degradation in fatigue behavior of carbon fiber–vinyl ester based composites due to sea environment," *Composites Part B: Engineering*, vol. 61, pp. 94–98, may 2014.

[5] R. Sen, "Durability of advanced composites in a marine environment," *International Journal of Materials and Product Technology*, vol. 19, no. 1/2, p. 118, 2003.

[6] H. Gu, "Dynamic mechanical analysis of the seawater treated glass/polyester composites," *Materials & Design*, vol. 30, pp. 2774–2777, aug 2009.

[7] H. Gu, "Behaviours of glass fibre/unsaturated polyester composites under seawater environment," *Materials & Design*, vol. 30, pp. 1337–1340, apr 2009.

[8] A. Kootsookos and A. Mouritz, "Seawater durability of glass- and carbon-polymer composites," *Composites Science and Technology*, vol. 64, pp. 1503–1511, aug 2004.

[9] H. B. Mayya, D. Pai, V. M. Kini, and P. N H, "Effect of Marine Environmental Conditions on Physical and Mechanical Properties of Fiber-Reinforced Composites—A Review," *Journal of The Institution of Engineers (India): Series C*, vol. 102, pp. 843–849, jun 2021.

[10] P. Smith, "Metallic Materials for Piping Components," in *The Fundamentals of Piping Design*, ch. 3, pp. 115–136, Houston: Elsevier, 2007.

[11] M. Patel G. C., G. R. Chate, M. B. Parappagoudar, and K. Gupta, "Optimization of Machining of Hard Material," in *SpringerBriefs in Applied Sciences and Technology*, pp. 103–128, 2020.

[12] P. B. Anand, A. Lakshmikanthan, M. P. Gowdru Chandrashekarappa, C. P. Selvan, D. Y. Pimenov, and K. Giasin, "Experimental Investigation of Effect of Fiber Length on Mechanical, Wear, and Morphological Behavior of Silane-Treated Pineapple Leaf Fiber Reinforced Polymer Composites," *Fibers*, vol. 10, p. 56, jun 2022.

[13] "Hardness," in *Tribology Handbook* (M. Neale, ed.), ch. 3, p. E3.1, Elsevier, 2 ed., 1995.

[14] S. Rawat and H. Attia, "Wear mechanisms and tool life management of WC–Co drills during dry high speed drilling of woven carbon fibre composites," *Wear*, vol. 267, pp. 1022–1030, jun 2009.

[15] K. Subramanian and N. H. Cook, "Sensing of Drill Wear and Prediction of Drill Life," *Journal of Engineering for Industry*, vol. 99, pp. 295–301, may 1977.

[16] D. Geng, Y. Liu, Z. Shao, Z. Lu, J. Cai, X. Li, X. Jiang, and D. Zhang, "Delamination formation, evaluation and suppression during drilling of composite laminates: A review," *Composite Structures*, vol. 216, pp. 168–186, may 2019.

[17] C. Tsao and H. Hocheng, "Effect of tool wear on delamination in drilling composite materials," *International Journal of Mechanical Sciences*, vol. 49, pp. 983–988, aug 2007.

[18] R. Bhat, N. Mohan, S. Sharma, A. U. Kini, S. Shivakumar, and N. Naik, "Multi response parametric optimisation in machining of marine application based GFRP composite with HSS drill: Application of TOPSIS approach," *Materials Today: Proceedings*, vol. 28, pp. 2077–2083, jan 2020.

[19] I. Ullah, M. Wasif, M. Tufail, M. A. Khan, and S. A. Iqbal, "Experimental Investigation of Cutting Parameters Effects on the Surface Roughness and Tools Wear during the Drilling of Fiber Reinforced Composite Materials," *Mehran University Research Journal of Engineering and Technology*, vol. 38, pp. 717–728, jul 2019.

[20] U. Aich, R. R. Behera, and S. Banerjee, "Modeling of delamination in drilling of glass fiber-reinforced polyester composite by support vector machine tuned by particle swarm optimization," *International Journal of Plastics Technology*, vol. 23, pp. 77–91, jun 2019.

[21] C. Bora, P. Bharali, S. Baglari, S. K. Dolui, and B. K. Konwar, "Strong and conductive reduced graphene oxide/polyester resin composite films with improved mechanical strength, thermal stability and its antibacterial activity," *Composites Science and Technology*, vol. 87, pp. 1–7, oct 2013.

[22] R. Akter, R. Sultana, Z. Alam, R. Qadir, M. Begum, and A. Gafur, "Fabrication and Characterization of Woven Natural Fibre Reinforced Unsaturated Polyester Resin Composites," *International Journal of Engineering & Technology IJET-IJENS*, vol. 13, no. 2, pp. 122–127, 2013.

[23] M. Elkington, D. Bloom, C. Ward, A. Chatzimichali, and K. Potter, "Hand layup: understanding the manual process," *Advanced Manufacturing: Polymer & Composites Science*, vol. 1, p. 2055035915Y.000, may 2015.

[24] C. Arumugam, S. Arumugam, and S. Muthusamy, "Mechanical, thermal and morphological properties of unsaturated polyester/chemically treated woven kenaf fiber/AgNPs@PVA hybrid nanobiocomposites for automotive applications," *Journal of Materials Research and Technology*, vol. 9, pp. 15298–15312, nov 2020.

[25] W. Hall and Z. Javanbakht, "How to Make a Composite—Wet Layup," in *Advanced Structured Materials*, vol. 158, pp. 33–53, 2021.

[26] J. H. Xin, Y. Zhang, Q. Huang, and N. Y. Cheng, "The research about ultimate load of CFRP repaired pipes under long-term seawater immersion and bending moment," *IOP Conference Series: Materials Science and Engineering*, vol. 634, p. 012028, oct 2019.

[27] M. K. Singh and S. Zafar, "Wettability, absorption and degradation behavior of microwave-assisted compression molded kenaf/HDPE composite tank under various environments," *Polymer Degradation and Stability*, vol. 185, p. 109500, mar 2021.

[28] G. Wang, D. Huang, J. Ji, C. Völker, and F. R. Wurm, "Seawater-Degradable Polymers—Fighting the Marine Plastic Pollution," *Advanced Science*, vol. 8, p. 2001121, jan 2021.

[29] O. Starkova, S. Gaidukovs, O. Platnieks, A. Barkane, K. Garkusina, E. Palitis, and L. Grase, "Water absorption and hydrothermal ageing of epoxy adhesives reinforced with amino-functionalized graphene oxide nanoparticles," *Polymer Degradation and Stability*, vol. 191, p. 109670, sep 2021.

[30] D. Das, S. K. Pradhan, R. K. Nayak, B. K. Nanda, and B. C. Routara, "Influence of curing time on properties of CFRP composites: A case study," *Materials Today: Proceedings*, vol. 26, pp. 344–349, 2020.

[31] A. Pandya, P. Upadhaya, S. Lohakare, T. Srivastava, S. Mhatre, S. Pulakkat, and V. B. Patravale, "Nanobiomaterials for regenerative medicine," in *Nanotechnology in Medicine and Biology* (H. H. Liu, T. Shokuhfar, and S. Ghosh, eds.), ch. 6, pp. 141–187, Elsevier, 2022.

[32] G. P. Karayannidis, A. P. Chatziavgoustis, and D. S. Achilias, "Poly(ethylene terephthalate) recycling and recovery of pure terephthalic acid by alkaline hydrolysis," *Advances in Polymer Technology*, vol. 21, no. 4, pp. 250–259, 2002.

[33] K. K. Chawla, *Composite Materials*. New York, NY: Springer New York, 3 ed., 2012.

Journal of Computers, Mechanical and Management

Journal homepage: www.jcmm.co.in

Volume 1 Issue 1

Finite Element Modelling and Analysis of Fiber Reinforced Concrete Under Tensile and Flexural Loading

V. Srikanth[a], Suhas Kowshik*[a], Dhanraj Narasimha[b], Santosh Patil[c], Kaustubh Samanth[d], and Udit Rathee[e]

[a]Department of Mechanical and Industrial Engineering, Manipal Institute of Technology, Manipal Academy of Higher Education, Manipal, Karnataka, India 576104
[b]Department of Environment Impact Assessment, Horizon Ventures, Bengaluru, Karnataka, India 560094
[c]Department of Mechanical Engineering, School of Automobile, Mechanical and Mechatronics Engineering, Manipal University Jaipur, Rajasthan, India 303007
[d]Department of Aerospace and Geodesy, Technical University of Munich, Ottobrunn, Munchen, Germany 85521
[e]Clemson University International Center for Automotive Research, Clemson University, Clemson, SC, United States 29634

Abstract

Concrete is a material exhibiting high compressive strength but about tenfold lower tensile strength. Its brittle property also prohibits the transmission of stresses after cracking. Thus, steel, polymer, polypropylene, glass, carbon, and other fibers are added to concrete to form fiber-reinforced concretes (FRC), having enhanced mechanical properties. The utilization of fiber-reinforced concrete is widespread. Identifying the mechanical properties of fiber-reinforced cement composites under dynamic loading, establishing relationships between their composition, structure, and properties, justifying the correct mathematical model, and determining its parameters are challenging. Utilizing finite elemental modeling and analysis to comprehend the mechanical characteristics of the FRC addition to concrete bricks has shown considerable benefit. In the present study, polypropylene microfibers are included in fiber-reinforced concrete composites, and their performance is compared to that of unreinforced concrete bricks. Under FEA analysis, three-point bending and uniaxial tensile tests were conducted. The results indicate that using fiber reinforcements increases the tensile strength and endurance of the brick.

Keywords: Concrete; Composite; Polymer; Mechanical Strength; ANSYS

1 Introduction

Concrete is a material with high compressive strength but has about tenfold lower tensile strength. In addition, it exhibits a brittle characteristic and prohibits the transmission of stresses after cracking. It is feasible to incorporate fibers into the concrete mixture to prevent brittle failure and increase mechanical qualities, producing fiber-reinforced concrete (FRC), a cementitious composite material with a distributed reinforcement in the form of fibers, steel, polymers, glass, carbon, and others [1]. AC1 116R, cement and concrete terminology, defines FRC as concrete having scattered, randomly oriented fibers. More than 30 years have elapsed since the present age of FRC research and development began [2].

*Corresponding author: suhas.kowshik@manipal.edu
Received: 28 August 2022; **Accepted:** 17 September 2022; **Published:** 30 October 2022
© 2022 Journal of Computers, Mechanical and Management.
This is an open access article and is licensed under a Creative Commons Attribution-Non Commercial 4.0 International License.
DOI: 10.57159/gadl.jcmm.1.1.23004.

Many scholarly articles have recently focused on creating new cement matrix compositions and using modified multicomponent fibers in concrete compositions for static and dynamic loads [3]. Identifying the mechanical properties of fiber-reinforced cement composites under dynamic loading, establishing relationships between their composition, structure, and properties, justifying the correct mathematical model, and determining its parameters are challenging. If this problem can be resolved, the efficiency of building structures operating under dynamic loads can be increased, i.e., from an economic standpoint, due to a reduction in material consumption and the accurate findings of analytical and numerical approaches [4]. Polypropylene fibers (PPF) are a type of polymer fiber composed of straight or distorted fragments of extruded, orientated, and cut polymer material. PPF was previously referred to as Stealth. These micro reinforcement fibers are homopolymer polypropylene graded monofilament fibers made entirely from virgin polypropylene. PPF does not contain any reprocessed Olefin components. The raw material for polypropylene is monomeric C3H6, an entire hydrocarbon compound [5]. PPF microfibers are shorter than 30 mm and do not serve a load-bearing function, but they do overcome plastic shrinkage and prevent the creation of concrete fractures. As a result, they strengthen the element's durability and extend its life [6]. Yew et al. [7] examined the performance of concrete reinforced with different polypropylene fibers. Concrete's tensile and flexural strength and its modulus of elasticity improved using polypropylene fibers. Moreover, adding a 0.5 % volume fraction of polypropylene fibers reduced the slump by 95.8 %. Deb et al. [8] proved an improvement in the ductility of the concrete with the inclusion of the PPF. Cracks are detrimental to concrete's mechanical and durability properties because they propagate under the influence of loads and allow aggressive agents to enter the surrounding environment. Polypropylene fiber in concrete acts as a crack arrestor and alters the fresh and hardened properties due to improper packing and dispersion, negatively impacting concrete [9]. The addition of PPF enhances the mechanical property of the concrete as it bridges the macro and micro-cracks present in the concrete and inhibits the further propagation of stress-induced failure [10]. However, excessive PPF content in concrete mixtures increases abrasion and freeze-thaw resistance and reduces volume expansions caused by sulfate attack and alkaline silica reaction (ASR) [11].

Thus it becomes necessary to use the optimum amount of PPF in concrete. Using soft techniques like ANSYS and ABAQUS simulation and modeling has been a preferred approach over the conventional destructive testing by several researchers in recent times to determine the property enhancement and optimize the PPF content in the concrete [12–14]. Understanding the positive impact of PPF addition in concrete and using the ANSYS simulation and modeling techniques, the present study aims at determining the optimum PPF content in the concrete while improving its mechanical properties, viz., bending and uniaxial tensile strength.

2 Materials and Methods

Concrete variants with compressive strength classification B25 were examined. These concretes were designed in ANSYS workbench in line with ASTM regulations. Polypropylene microfiber was considered while modeling the fiber-reinforced concrete for discrete concrete reinforcement. The modeled variants were based on the quantities of microfibers, which were 0, 3, 5 and 7 kg/m^2. The concrete damage plasticity model was created to explain how concrete behaves mechanically when subjected to uniaxial, biaxial and volumetric stress conditions with negligible lateral compression [4, 15, 16]. To model irreversible deformations in concrete, the mechanical behavior of the material is based on isotropic elastic damage in conjunction with isotropic plastic behavior for bending and tension. The assumption that the orientation of the microfibers in concrete is chaotic makes this technique appropriate, and because the content is so huge, the models may be made to assume that the concrete hardens in the same way in all possible directions. The method mentioned above not only permits the use of the model under simple or cyclic static loads or dynamic loads but also considers concrete reinforcement with individual rods, meshes, or scattered reinforcement. The scattered concrete reinforcement in the model is chosen based on the energy needed for the formation and full opening of a crack.

Young's modulus, Poisson's ratio, ultimate uniaxial tension strength, ultimate uniaxial compression strength, diagram of concrete deformations in the axes "force versus CMOD" from bending test, Dilation angle measured in the p–q plane at high confining pressure, default values concerning the ratio of initial equibiaxial compressive yield stress to initial uniaxial compressive yield stress, flow potential eccentricity and coefficient of the shape of plastic surface flow were the variables used to configure the parameters of the accumulated damage concrete damage plasticity model. These parameters' values were chosen in accordance with tests, regulatory document specifications, numerical modeling, and recommendations made in scientific and technical documents [4, 17–20]. Based on the findings of a concrete test under bending, a method for creating a diagram of the severe deformation of concrete under uniaxial strain is used. It entails establishing the model parameters of concrete's plastic behavior on the findings of a numerical experiment. As a flow chart, Figure 1 depicts the order of parameter selection for the damaged concrete plasticity model.

The numerical model has dimensions of 400 × 100 × 150 mm for each model, with a notch 2 mm wide and 25 mm deep on the bottom side of the brick for the three-point bending test utilizing the crack mouth opening displacement (CMOD) method. The numerical model for concrete that is prone to bending is composed of a concrete beam, two supporting bars, and a loading bar. Figure 2(a), Figure 2(b), Figure 2(c) and Figure 2(d) represent the variants of B25 concretes modeled in the present study. Similarly, models of uniaxial test blocks made of B25 concrete variants with dimensions of 150 × 150 × 550 mm and a notch in the middle of the brick measuring 100 × 100 × 60 mm are created. The models created in this manner with ANSYS Workbench are shown in Figure 3(a), Figure 3(b), Figure 3(c), and Figure 3(d). The models are changed into FEM models by adding the mesh. The model's mesh thickness varies from 7mm to 15mm. These variances give the deformation values extra depth. Figure 4(a) and Figure 4(b) show examples of the meshing that was produced for the three-point bending and tensile model, respectively.

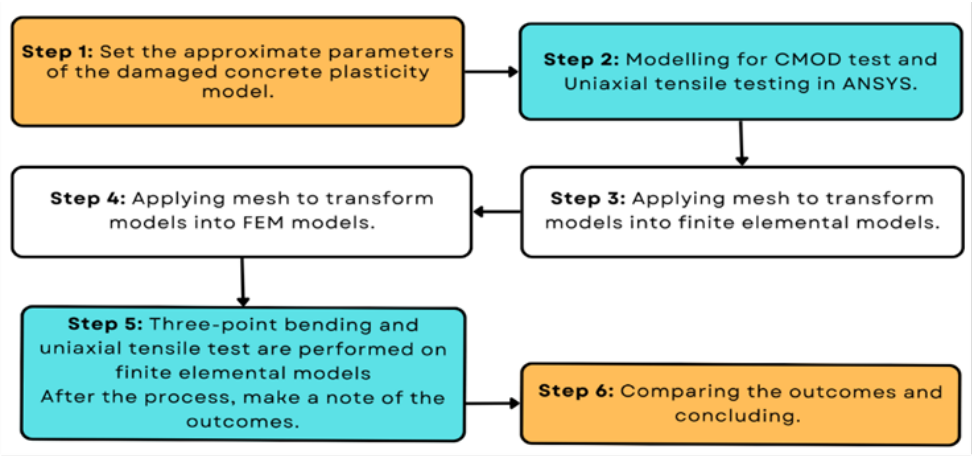

Figure 1: Flow chart of the selection sequence concerning damaged concrete plasticity model parameters

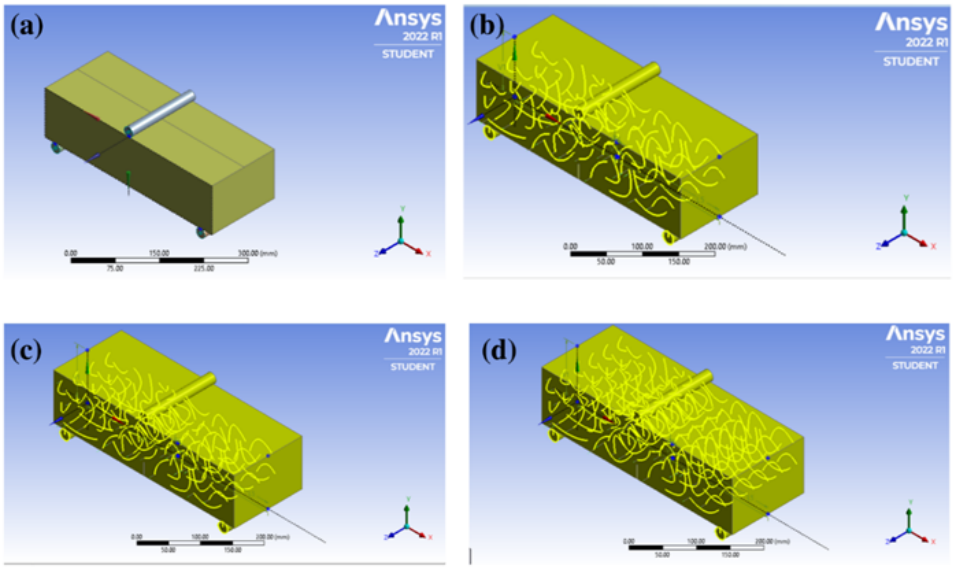

Figure 2: Models for three-point bending test utilizing crack mouth opening displacement (CMOD) method of B25 concrete with: **(a)** 0 % **(b)** 3 %, **(c)** 5 % and **(d)** 7 % by weight of polypropylene microfibers.

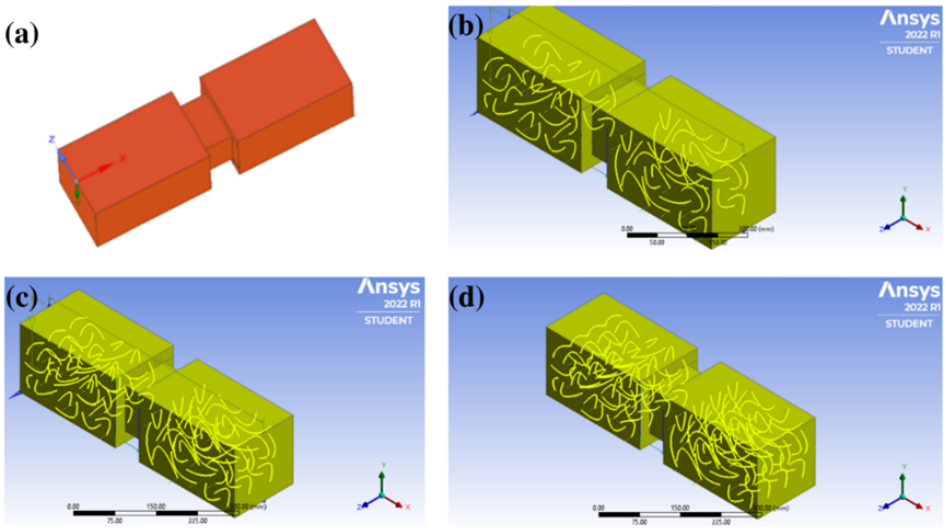

Figure 3: Models for uniaxial test utilizing crack mouth opening displacement (CMOD) method of B25 concrete with: **(a)** 0 % **(b)** 3 %, **(c)** 5 % and **(d)** 7 % by weight of polypropylene microfibers.

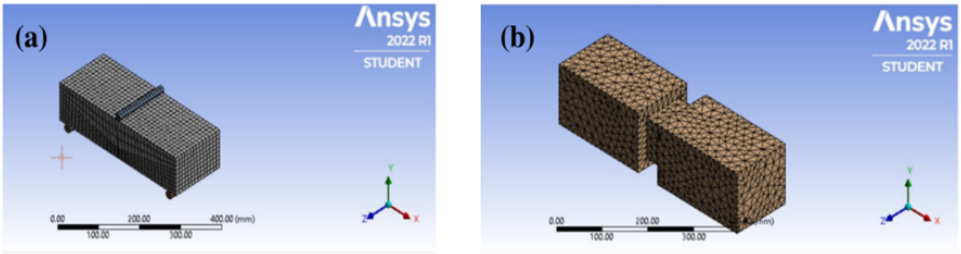

Figure 4: Meshed models sample for: **(a)** three-point bending and **(b)** uniaxial test using ANSYS workbench.

3 Results and Discussion

The results obtained through the FEM analysis for three-point bending after subjecting the designed variants of B25 concrete to 1 kN are represented in Figure 5(a), Figure 5(b), Figure 5(c) and Figure 5(d). The results obtained for the uniaxial tensile loading using FEM analysis after subjecting the designed variants of B25 concrete in Figure 6(a), Figure 6(b), Figure 6(c) and Figure 6(d).

Table 1 and Table 2 detail the result obtained from the three-point bending and uniaxial tensile loading test analysis. The findings above show that reinforced concrete has a stronger uniaxial tensile strength than non-reinforced concrete, which increases brick durability. The toughness and uniaxial tensile stress of the material also increase with increasing polypropylene microfiber content.

Table 1: Three-point bending deformation in B25 concrete variants.

Sl.	Force applied (N)	Three-point bending deformation (mm)			
		0% fiber	3% fiber	5% fiber	7% fiber
1	1000	0.029	0.026	0.025	0.024
2	2000	0.058	0.051	0.050	0.048
3	3000	0.083	0.075	0.071	0.067
4	4000	0.117	0.104	0.100	0.095
5	5000	0.145	0.130	0.125	0.117
6	6000	0.170	0.155	0.144	0.143
7	7000	0.194	0.176	0.172	0.158
8	8000	0.224	0.198	0.192	0.182
9	9000	0.240	0.213	.207	.202

Table 2: Tensile deformation in B25 concrete variants.

Sl.	Tensile rupture crack opening (mm)	Uniaxial tensile strength (MPa)			
		0% fiber	3% fiber	5% fiber	7% fiber
1	0.10	31.10	37.80	39.90	40.36
2	0.15	46.47	75.60	79.90	80.80
3	0.20	62.33	113.40	119.85	121.18
4	0.25	78.18	151.24	159.80	161.57

The results thus obtained are in direct agreement with similar work done earlier [21–23], wherein the researchers noticed a reduction in crack growth and an improvement in durability with the increased fiber reinforcement in concrete concerning tensile strength, impact strength and also the chloride binding. The three-point bending deformation was reduced by an average of 10, 14 and 18 % with the inclusion of 3, 5 and 7 % by weight of the microfibers in the B25 concrete. The uniaxial strength improved by an average of 65, 74 and 76 % with the inclusion of 3, 5 and 7n% by weight of microfibers in the B25 concretes.

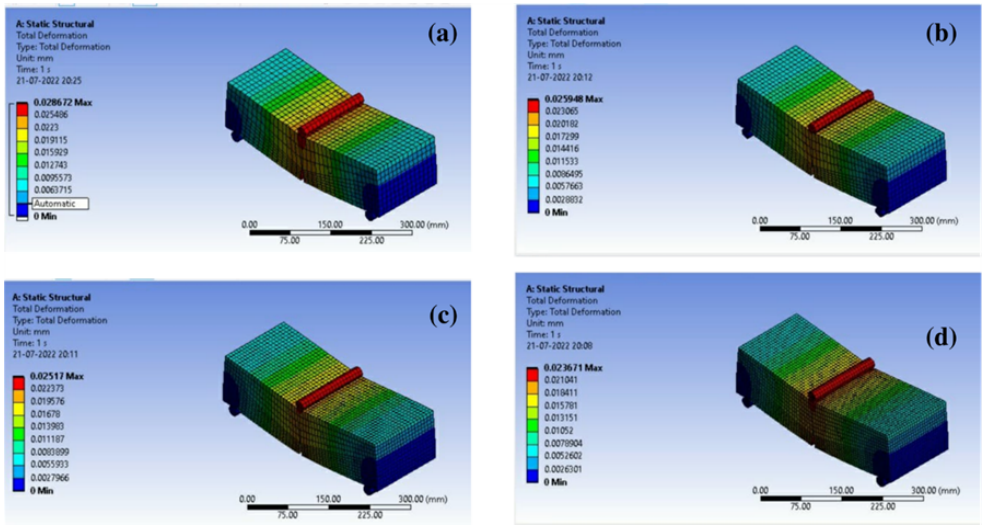

Figure 5: Three-point bending analysis models of B25 concrete with: (a) 0 % (b) 3 %, (c) 5 % and (d) 7 % by weight of polypropylene microfibers.

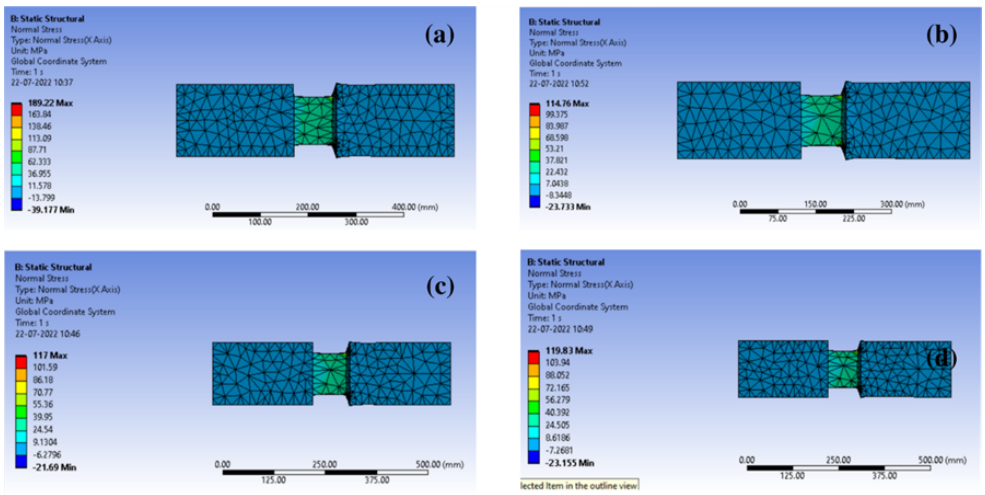

Figure 6: Uniaxial tensile test analysis models of B25 concrete with: (a) 0 % (b) 3 %, (c) 5 % and (d) 7 % by weight of polypropylene microfibers.

4 Conclusion

The work focused on developing and analyzing B25 concrete models using the ANSYS workbench. Four variants were analyzed having the variation of polypropylene content in the material. The study indicated increased durability concerning the reduction in the three-point bending deformation and increased uniaxial strength with the increased microfiber content in the B25 concretes.

Declaration of Competing Interests

The authors declare that they have no known competing financial interests or personal relationships that could have appeared to influence the work reported in this paper.

Funding Declaration

This research did not receive any grants from governmental, private, or nonprofit funding bodies.

Author Contribution

V. Srikanth: Data curation, Writing–Original draft preparation, Methodology, Investigation, Software, Validation; **Suhas Kowshik**: Conceptualization, Supervision, Validation, Writing- Reviewing and Editing; **Dhanraj Narasimha**: Conceptualization, Writing-Reviewing and Editing; **Santosh Patil**: Methodology; **Kaustubh Samanth**: Validation; Udit Rathee: Software.

References

[1] J. Blazy and R. Blazy, "Polypropylene fiber reinforced concrete and its application in creating architectural forms of public spaces," *Case Studies in Construction Materials*, vol. 14, p. e00549, jun 2021.

[2] R. F. Zollo, "Fiber-reinforced concrete: an overview after 30 years of development," *Cement and Concrete Composites*, vol. 19, pp. 107–122, jan 1997.

[3] S. V. Klyuev, A. V. Klyuev, and N. I. Vatin, "Fiber concrete for the construction industry," *Magazine of Civil Engineering*, vol. 84, no. 8, pp. 41–47, 2018.

[4] N. Belyakov, O. Smirnova, A. Alekseev, and H. Tan, "Numerical Simulation of the Mechanical Behavior of Fiber-Reinforced Cement Composites Subjected Dynamic Loading," *Applied Sciences*, vol. 11, p. 1112, jan 2021.

[5] T. C. Madhavi, L. S. Raju, and M. Deepak, "Polypropylene Fiber Reinforced Concrete- A Review," *International Journal of Applied Engineering Research*, vol. 4, no. 4, pp. 2250–2459, 2014.

[6] S. Antonov, M. Gravit, E. Meshalkin, I. Dmitriev, and A. Shchukin, "Study of the Compressive Strength of Concrete with Polypropylene Microfiber," in *Lecture Notes in Civil Engineering*, vol. 180, pp. 543–552, 2022.

[7] M. K. Yew, H. B. Mahmud, B. C. Ang, and M. C. Yew, "Influence of different types of polypropylene fibre on the mechanical properties of high-strength oil palm shell lightweight concrete," *Construction and Building Materials*, vol. 90, pp. 36–43, aug 2015.

[8] S. Deb, N. Mitra, S. B. Majumder, and S. Maitra, "Improvement in tensile and flexural ductility with the addition of different types of polypropylene fibers in cementitious composites," *Construction and Building Materials*, vol. 180, pp. 405–411, aug 2018.

[9] A. Lakshmi, P. Pandit, Y. Bhagwat, and G. Nayak, "A Review on Efficiency of Polypropylene Fiber-Reinforced Concrete," in *Lecture Notes in Civil Engineering* (L. Nandagiri, M. Narasimhan, S. Marathe, and S. Dinesh, eds.), vol. 162, pp. 799–812, Springer, Singapore, 2022.

[10] B. Li, Y. Chi, L. Xu, Y. Shi, and C. Li, "Experimental investigation on the flexural behavior of steel-polypropylene hybrid fiber reinforced concrete," *Construction and Building Materials*, vol. 191, pp. 80–94, dec 2018.

[11] M. R. Latifi, Ö. Biricik, and A. Mardani Aghabaglou, "Effect of the addition of polypropylene fiber on concrete properties," *Journal of Adhesion Science and Technology*, vol. 36, pp. 345–369, feb 2022.

[12] N. Hammad, A. M. ElNemr, and H. E.-D. Hassan, "Flexural performance of reinforced Alkali-activated concrete beams incorporating steel and structural Macro synthetic polypropylene fiber," *Construction and Building Materials*, vol. 324, p. 126634, mar 2022.

[13] P. Dhanabal, P. N. Reddy, and K. S. Sushmitha, "Analytical and Experimental Study on Flexural Behavior of Beam-column Joint with Addition of Polypropylene Fibers," *Journal of Modern Materials*, vol. 9, pp. 26–35, jun 2022.

[14] S. M. Mahmoud, M. E. El-Zoughiby, A. A. Mahmoud, and M. A. Abd Elrahman, "Nonlinear Finite Element Analysis of Polypropylene Lightweight RC Beams," *Engineering Research Journal*, vol. 173, pp. 1–15, mar 2022.

[15] M. Hafezolghorani, F. Hejazi, R. Vaghei, M. S. B. Jaafar, and K. Karimzade, "Simplified damage plasticity model for concrete," *Structural Engineering International*, vol. 27, pp. 68–78, feb 2017.

[16] J. M. Dulinska and I. J. Murzyn, "Dynamic behaviour of a concrete building under a mainshock–aftershock seismic sequence with a concrete damage plasticity material model," *Geomatics, Natural Hazards and Risk*, vol. 7, pp. 25–34, may 2016.

[17] A. Furtado, H. Rodrigues, A. Arêde, H. Varum, M. Grubišić, and T. K. Šipoš, "Prediction of the earthquake response of a three-storey infilled RC structure," *Engineering Structures*, vol. 171, pp. 214–235, sep 2018.

[18] S. Seok, G. Haikal, J. A. Ramirez, L. N. Lowes, and J. Lim, "Finite element simulation of bond-zone behavior of pullout test of reinforcement embedded in concrete using concrete damage-plasticity model 2 (CDPM2)," *Engineering Structures*, vol. 221, p. 110984, oct 2020.

[19] V. Popov, V. Morozov, Y. Pukharenko, and M. Plyusnin, "Consideration of Variability of Concrete Characteristics in Calculation of Reinforced Concrete Structures," *Materials Science Forum*, vol. 871, pp. 166–172, sep 2016.

[20] H. Cheng, C. M. Paz, B. C. Pinheiro, and S. F. Estefen, "Experimentally based parameters applied to concrete damage plasticity model for strain hardening cementitious composite in sandwich pipes," *Materials and Structures*, vol. 53, p. 78, aug 2020.

[21] V. Afroughsabet, L. Biolzi, and T. Ozbakkaloglu, "High-performance fiber-reinforced concrete: a review," *Journal of Materials Science*, vol. 51, pp. 6517–6551, jul 2016.

[22] S. Hamoush, T. Abu-Lebdeh, and T. Cummins, "Deflection behavior of concrete beams reinforced with PVA micro-fibers," *Construction and Building Materials*, vol. 24, pp. 2285–2293, nov 2010.

[23] W. Nana, H. Tran, T. Goubin, G. Kubisztal, A. Bennani, T. Bui, G. Cardia, and A. Limam, "Behaviour of macro-synthetic fibers reinforced concrete: Experimental, numerical and design code investigations," *Structures*, vol. 32, pp. 1271–1286, aug 2021.

Journal of Computers, Mechanical and Management

Journal homepage: www.jcmm.co.in

Volume 1 Issue 1

Astoundingly Smart System Furnishing Ranking of Big Data In Search Engines

Kakoli Banerjee*and Shishir Dua

Department of Computer Science and Engineering, JSS Academy of Technical Education, Noida, Uttar Pradesh, India 201301

Abstract

The abruptly escalating internet is sensational. It inculcates a humungous volume of big data, which is obsolete and tedious to manage, scrutinize, analyze and perform operations upon them in conventional ways. Big data has thus expedited the search and retrieval of information, necessitating the development of contemporary search algorithms to aid this process. However, the primary hindrance for the first and second generations of conventional search engines was the syntax of keywords devoid of semantic meaning and the lack of a knowledge base that linked disparate web material. This article presents a framework based on trendy technologies, specifically Extracting, Transforming and Integrating (ETI) processes, ontology graphs, and indexing Resource Description Framework (RDF) using the wide-column Not only Structured Query Language (NoSQL) method. The most significant contribution in this regard is developing a mathematical model to compute the similarity score between a query and stored RDF documents using semantic relations. Numerous operations were carried out to evaluate the effectiveness of the proposed methodology in installing data sources, such as DBpedia and YAGO dataset. Insofar as experimental results are concerned, the suggested model achieves greater precision than other comparable systems.

Keywords: YAGO Dataset; DBpedia; Ontology; Semantic Web; NoSQL

1 Introduction

Search engines underwent a decent frequency of generation versions. In the initial generation, it thoroughly relied on depicting information and corresponding data which matched the input query only. Contemporary second-generation search engines enable real-time query scrutiny and analysis by employing machine learning techniques, deep learning algorithms and complementary data models, subsequently deducing the worthwhile keywords of query analysis and ditching semantic stuff [1]. Nowadays, these are inculcating consideration of part of tremendous enterprises to endow with access to information. The internet is the most substantial syntax source of data, datasets and information ever initiated. Static web, including Hyper-Text Markup Language (HTML), elucidates the syntax structure of information. Henceforth, a traditional search engine can comprehend syntax but cannot infer the speculations and requirements. Figure 1 depicts the third generation of search engines that utilize semantic relations amongst immense things to evolve a knowledge graph [2]. Ontology validates the elements that exist or may have existed in any field or context and is continually applied to illustrate semantic relations. The ontology classes elucidate the verbs, word senses, or notion and association types. Efficacious tools for a semantic search engine employing ontology include Ontology Web Language (OWL) and Resource Description Framework (RDF), evolving decipherable information. RDF is a language for interpreting information about sources accessible on the internet [3–5]. In RDF, the predicate denotes relationships between the subject and the object. The object is rather the value. It includes another resource or a literal value comprising a number or word.

*Corresponding author: kakoli.banerjee@jssaten.ac.in
Received: 28 August 2022; **Accepted:** 17 September 2022; **Published:** 30 October 2022
© 2022 Journal of Computers, Mechanical and Management.
This is an open access article and is licensed under a Creative Commons Attribution-Non Commercial 4.0 International License.
DOI: 10.57159/gadl.jcmm.1.1.23018.

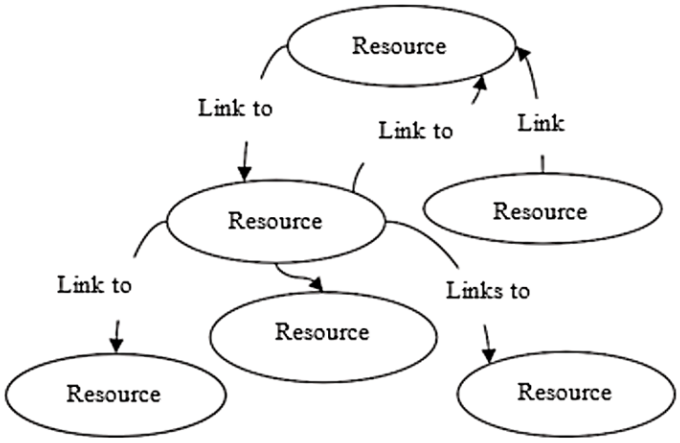

Figure 1: The general structure of the semantic web.

There are quite a few operational obstructions and research highlights related to search engines, which are enlisted in this paragraph. These incorporate [6–8]:

- The current well-scaled traditional or standard search engines that pivot on syntax relationships between keywords or topics, ditching semantic relations.
- The semantic search engines that do not scale decently and focus on the maiden field in the search area and context
- The big data possess predicament, namely time complexity, scalability, and availability required to enhance the knowledge base of any search engine

The contributions cited in this article are designated into three paramount categories. These are furnished further on (a) recommendation of semantic search system framework, (b)augmentation and enhancement of knowledge base through more than one source using proposed Extracting, Transforming and Integrating (ETI) processes, (c) proposal and evaluation of a novel mathematical representation for computing and determining semantic relations between distinct subjects, and (d) variety of testing factors, held for evaluating recommended framework.

2 Background

This section includes a concise review and summary of a simple survey of the most common forms of Information Retrieval (IR) models. Also, different conventional methods of measuring the degree of similarity at the level of characters or words are briefly reviewed.

2.1 Different models of information retrieval systems

An IR model governs how a document and a query are represented. There are two common main models: Boolean and vector space models, [6] of which the vector space model is employed in the present work.

Boolean model

This model is the simplest and oldest model used in search engines. The concept of exact match and the laws of Boolean algebra is used to match the search results with the query entered by the user [6]. The weight of keyword k_i in page p_j is calculated according to Eq. [1]

$$w_{ij} = \begin{cases} 1 & \text{if } k_i \text{ appears in } p_i \\ 0 & \text{otherwise} \end{cases} \tag{1}$$

Vector space model

In this model, a document is represented as a weight vector. The weight of keyword k_i in page p_j is no longer 0,1 as in the previous model but can be any number. We can use Keyword Frequency - Inverse Page Frequency (KF-IPF) scheme to assign a weight for each component.

Let M be the total number of pages in the system and pf_i be the number of pages in which keyword k_i appears at least once. Let f_{ij} be the frequency count of keyword k_i in page p_j [6]. Then keyword frequency kf_{ij} is given by Eq. 3. The inverse document frequency ipf_{ij} is given by the Eq. [2]. Finally, we can get the component's weight using Eq. 4.

$$kf_{ij} = \frac{f_{ij}}{\max(f_1, f_2, \ldots, f_m)} \tag{2}$$

$$ipf_{ij} = \log\left(\frac{M}{pf_i}\right) \tag{3}$$

$$w_{ij} = kf_{ij} \times ipf_{ij} \tag{4}$$

The Needleman-Wunsch method is a dynamic model commonly used in biology and bioinformatics to compare genome sequencing, as it has recently been used in some standard search engines. DNA consists of a large sequence of a specific set of string characters, where this method measures the degree of similarity by aligning two entire sequences. The usage of this method can be logical and correct if the two sequences are of the same length and share a high degree of similarity [8]. The Smith-Waterman method is another example of a dynamic programming model and is also used in bioinformatics, which can compare two sequences by aligning each character with the other to obtain the highest degree of similarity. This method does not require that the two sequences have the same length and have a high degree of similarity. However, the good thing about this method is that one can extract similar areas in any two sequences and do not necessarily have a complete similarity [9]. Longest Common SubString (LCS) method is a sequential comparison between two sequences, and the degree of similarity depends on the length of the similar contiguous chain of characters. That is, the longer the length of the string containing similar characters, the greater the proportion of similarity, even if the meaning is different. Unlike the last two methods, LCS calculates the similarity between the two sequences based on the number of operations that match them. The operations, such as deletions, substitutions, or insertions, are calculated on a sequence of characters. The degree of similarity here reflects the distance between the two sequences. This method is used in some search engines to fix errors in the user-submitted query following one of the terms in the utilized database [2, 3].

2.2 Term-based similarity measurement methods

The cosine method is a similarity score mathematical measurement between two vectors that calculates the cosine of the angle between them. The weight of each Wikipedia article is calculated by this method. The Euclidean distance (ED) method is the distance measurement between two strings or two vectors. The similarity score between two elements is one minus the distance of these two elements. Distance is calculated as the square root of the sum of squared differences between related elements. Dice's Coefficient is twice the amount of common terms in the associated strings divided by the total number of words in both strands [10–12].

2.3 Semantic-based similarity measurement methods

The Explicit Semantic Analysis (ESA) method is a measure used to estimate the semantic relatedness among two arbitrary subjects. The relatedness of pair documents in the same language is evaluated by this method. The latent Semantic Analysis (LSA) method is popular for estimating semantic-based similarity. LSA assumes that strings are close in meaning and will happen in similar parts of the text. LSA includes a matrix that holds word counts per paragraph. In the matrix, rows describe distinct words, and columns represent a specific paragraph. Second-order Occurrence Pointwise Mutual Information (SOC-PMI) is a semantic score measurement method using pointwise information to sort lists of significant neighbor terms of two strings. The relation score between two strings that do not occur regularly can be calculated.

3 Related Works

Standard search systems include search engines like Google, Yahoo, and Bing, directories like Deutsche Medizinische Online Zeitung (DMOZ), and Meta Search systems like Dogpile and Mamma. The vast majority of common search techniques are extremely popular, yet their results are occasionally erroneous, with low precision and high recall. Modern and intelligent search systems, such as Swoogle, Semantic Web Search Engine (SWSE), and Falcons Object Search [12], are created with the semantic approach in mind. Swoogle is a system that crawls and indexes web documents based on their semantic content. It includes four major components: data finding, metadata development, data analysis, and data retrieval. It permits the classification of metadata using the rational surfer model. However, these systems had problems, such as insufficient indexing of enormously big data and slow query response [13]. Moreover, Swoogle lacks a technique for sorting relevant results by relevance. Hogan et al. [14] have referred to the semantic approach as SWSE. Based on RDF and link-related data, it is a comprehensive search system that offers comparable services to conventional search engines. It includes the crawling, indexing, ranking, argumentation, and retrieval phases.

However, SWSE has some flaws, such as

- The system does not scale well.
- The system does not appear resistant in the face of varied, noisy, inconsistent, and possibly contradicting data obtained.

Hakia is an additional system that functions as a comprehensive semantic engine for particular applications. This system is a different form of search engine that produces more accurate and trustworthy results than standard search engines.

It includes a query processor, ontology analyzer, QDex store, and ranking methodology. This system, like others, relies on correlating outcomes in terms of meaning as opposed to statistical methodologies, which lends strength and credibility to the results. Fatima et al. [15] developed a system reliant on the semantic web. For sorting and retrieving data, the suggested search engine in this system depended on a robust query language processor and an intuitive user interface. This system lacks novel algorithms that increase system performance, regardless of the technical methods employed.

4 Method

4.1 Proposed framework

The suggested framework, Semantic Engine based on Enhancing Knowledge (SEEK), is designed modularly and reasonably composed of two separate stages. Firstly, the offline stage is a back end where the server runs solely away from users. The offline phase involves ETI and indexing based on semantic relation processes. Secondly, the knowledge source phase converts JavaScript Object Notation (JSON) format into RDF schema and stores related subjects into a cache table for faster retrieval. Thirdly, the online phase is a front-end stage where a user can operate directly with the knowledge source in real time. As presented in Figure 2, Each bold box focuses on the contributions of the present work.

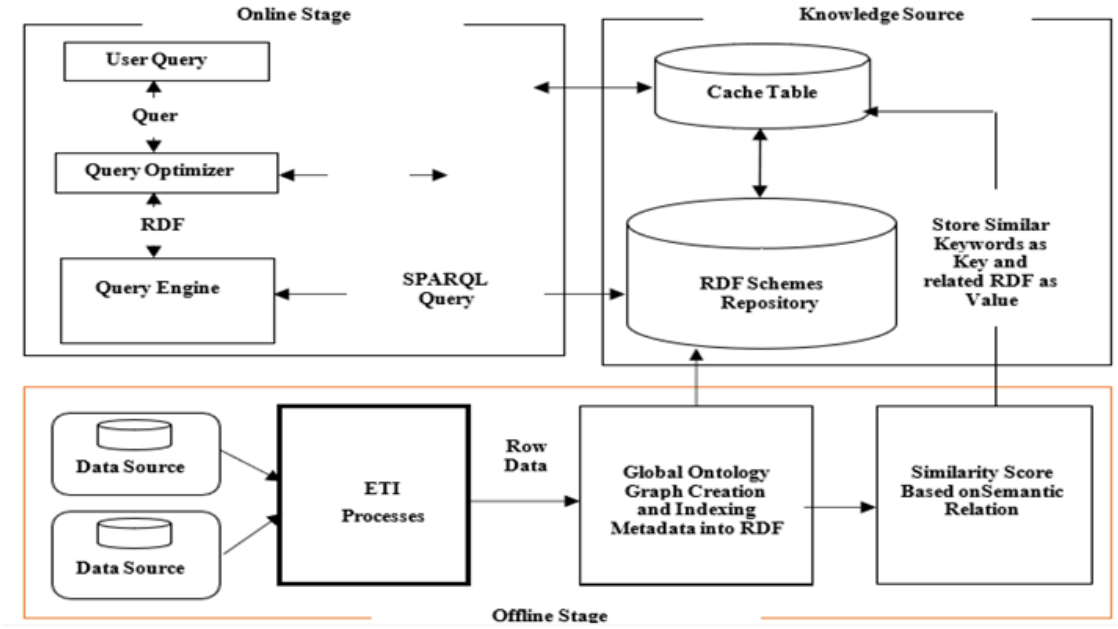

Figure 2: Proposed SEEK architecture.

Offline phase

This phase consists of three integrated stages: ETI (Extracting, Transforming, and Integrating) processes, indexing process, and similarity score calculation process based on semantic relation, of which the present study deals with the ETI and the similarity score calculation processes.

ETI Processes: This stage is responsible for ETI processes that extract data from different data sources and convert it into uniform JSON format. The ETI job manager on a master thread invokes a schema analyzer to identify the schema of the API data sources (e.g., Facebook, Twitter, DBpedia APIs). This stage outputs a uniformly integrated schema in JSON format. ETI processes are initiated on the master thread and distributed on several slave threads using the MapReduce technique for parallel processing. The extracting process involves fetching data from the source, which should be correct and accurate. The transforming process performs a series of complicated data cleaning and converts it into JSON format. The integrating process is used to bind extracted data into another JSON format. Algorithm 1 represents the overall steps of how the schema is being created. In the schema creator procedure, the master thread parallelly assigns collections of different data sources (input) to slave threads for creating the schema (output).

Algorithm 1 Schema Creator Procedure

```
procedure SCHEMA CREATOR
    Input: Data Source (DS_i)
    Output: Schema
    Begin
    dataset ← DS_i.open connection
    count ← dataset.collection.Names()
    Schema ← null
    for i ← 0 to count do
        for record ∈ dataset.collection(i) do
            for column_name ∈ record do
                Schema ← schema ∪ column_name
            end for
        end for
    end for
    Return Schema
end procedure
```

After that, Algorithm 2 shows how data can be extracted. In the extraction procedure, the inputs are the data source, the number of threads assigned to this data source (thread counter) and the schema design from the previous method. The output of this procedure is Row data in batches.

Algorithm 2 Extraction Procedure

```
procedure EXTRACTION
    Input: Data Source (DS_i), thread counter (TC), Schema
    Output: Row Data
    Begin
    dataset ← DS_i.open connection
    count ← dataset.collection.Names()
    Limit ← Count
    for i ← 0 to count do
        Start ← limit ∗ i
        Batch ← Read data (batch size)
        Row Data ← Extract (process id, Batch, DS_i, start, limit, schema)
    end for
    Return Row Data
end procedure
```

Finally, the transformation procedure can record all the distinctions in the data source and compile the schema into a JSON format, as shown in Algorithm 3. In the transformation procedure, the inputs are the data source, extracted row data, and schema design. The output of this procedure is integrated data in JSON format.

Algorithm 3 Transformation Procedure

```
procedure TRANSFORMATION
    Input: Data Source (DS_i), Row Data, Schema
    Output: Data in JSON format
    Begin
    Initialize schema ()
    Data Collection ← Row Data.Length
    Limit ← Data Collection.Count
    Start ← 1
    while Start < Limit do
        Clean (Row Data)
        Remove Duplicates (Row Data)
        Schema ← Bind Row Data
        Start++
    end while
    JSON ← Schema
    Return JSON
end procedure
```

Similarity score calculation processes: A basic structure of the semantic ontology graph is depicted in Figure 3.

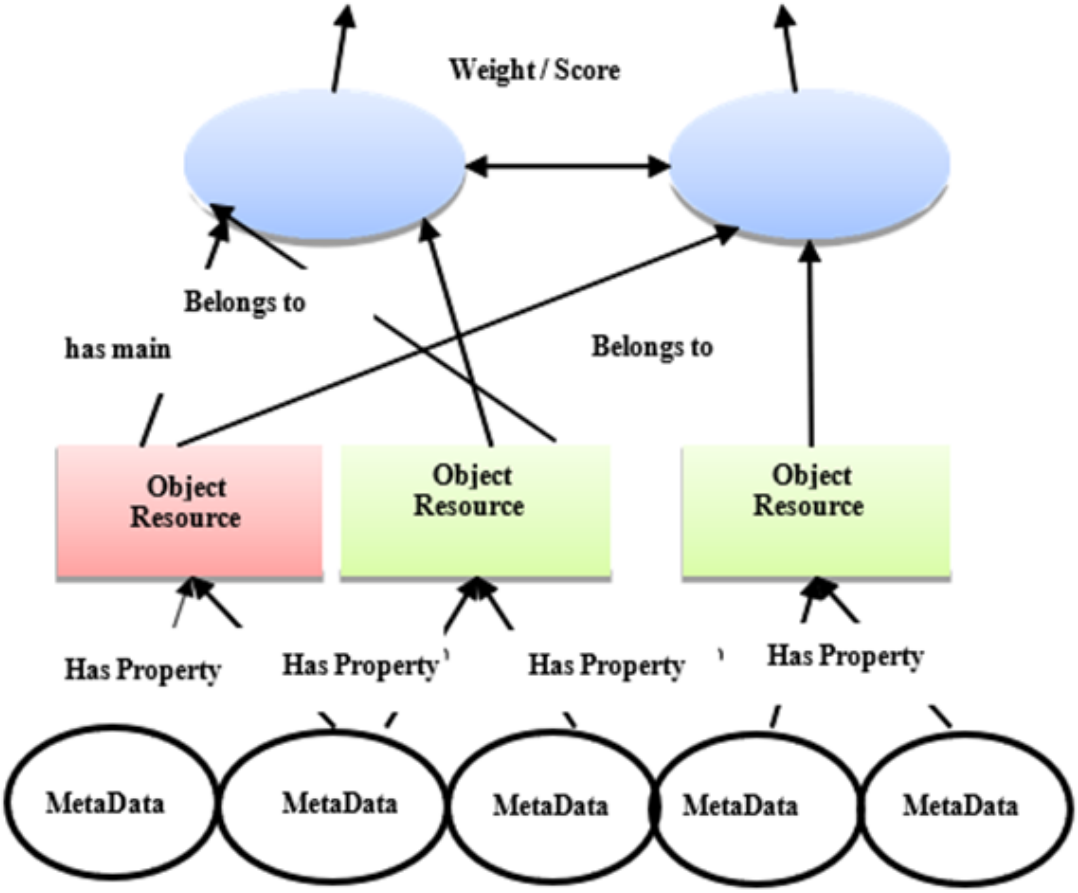

Figure 3: Structure of the Semantic Ontology Graph [8].

Semantic Score (SS) equation, represented by Eqs. [5] and [6], is used to measure the weighting score between two subjects (I and J) in the ontology graph [8], where:

- S_i is the count of input relations of the subject I from different objects.
- S_j is the count of input relations of subject J from different objects.
- T is the total number of subjects in the graph.

$$SS_{in}(S_i, S_j) = 1 - \frac{\max(\log S_i, \log S_j) - \log(S_i \cap S_j)}{\log T - \min(\log S_i, \log S_j)} \tag{5}$$

$$SS_{in}(S_i, S_j) = \begin{cases} 0 & S_i \neq S_j \\ 1 & S_i = S_j \\ \text{otherwise} & S_i \text{ related to } S_j \end{cases} \tag{6}$$

Figure 4 illustrates an example of calculating semantic scores between two subjects (I and J). If the subject (I) has four incoming links from different objects (A, D, E, and F). Then the semantic relation of the subject (I) would be four. Considering that the subject (J) has five incoming links from different objects (A, B, C, F, and G), then the semantic relation of the subject (J) would be five. However, two objects (A and F) belonged to both subjects. So, the semantic relation of both subjects (I and J) is two. If the ontology graph has 1000 subjects, then the semantic score by applying Eq. [5] equals 0.83, which means there exists high semantic relation between two subjects (I and J) as per Eq. [6].

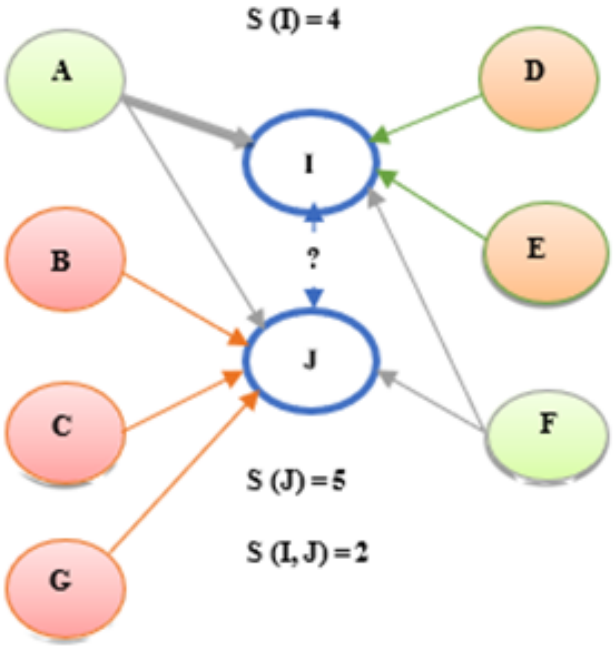

Figure 4: Example of calculating Semantic Score between two subjects (I and J).

Knowledge source phase

The present work employs HBase integrated with Hadoop for knowledge sourcing. It consists of one master and six slave machines. The integration of HBase with Hadoop archives has many advantages as (a) Hadoop runs batch jobs using the MAP - Reduce technique on distributed machines to achieve maximum throughput and overall performance [16, 17], (b) HBase provides good latency, scalability and fault tolerance wherein the replication process handles fault tolerance. Scalability is handled by splitting each table horizontally into regions, and (c) The integration is done successfully because they use the same underlying HDFS file systems [18].

Online phase

This phase incorporates two crucial stages. The initial stage instills optimizing input query, and the consequent stage is the actual retrieving process by the query engine. The query optimizer phase is implemented wherein the stop words removal, stemming and keyword expansion processes are applied to the input query from the user. Wordnet tool is used to expand keywords to extend search domains. The semantic score between extended keywords and actual query keywords is computed to generate a key of the input subject. Subsequently, the value of the corresponding key is returned from caching table. Then the query engine is implemented. At this stage, the actual retrieval process is applied using the Simple Protocol and RDF Query Language (SPARQL) query to return the objects of the corresponding subject value. The query engine is used to generate a SPARQL query to retrieve related information from RDF and the corresponding source.

4.2 Experimental setup

The proposed framework is evaluated using a cluster of, one head machine node and six slave machines. The head machine had Intel core i7 processor @2.6GHz with 16GB RAM. The slave machines possessed Intel core i3 processor@ 2.2GHz with 4GB RAM for each. Hadoop version 2.9.2 was used as an open-source tool. Hadoop was assisted with three workers per MAP operation and two workers per REDUCE operation. Also, Apache HBase version 2.2.0 was utilized. Multiple parallel slave workers were considered for the execution of ETI jobs.

4.3 Datasets description

The proposed framework was evaluated using two real-world datasets. Table 1 depicts some statistical information from these datasets. The two real-world datasets are:

- DBpedia, a pre-eminent real-world dataset utilized in the semantic web research community. The DBpedia version used to compute and augment the acuteness of cited framework is 2016-04.
- YAGO, yet another great real-world dataset developed at Max Planck institute. The YAGO version used to evaluate our framework is 2015-03.

Table 1: Brief statistical information of DBpedia and YAGO datasets.

Parameters	DBpedia	YAGO
# Entities in person Domain	1.5 M	1.3 M
# Entities in work Domain	490 K	510 K
# Entities in the organization Domain	275 K	350 K
# Entities in places Domain	810 K	1.2 M
# Entities in the biology Domain	301 K	150 K
# N-Quads used	150 M	120 M

5 Results and Discussion

5.1 ETI execution results

Figure 5 depicts the average ETI execution time recorded for different workers. According to this figure, seven threads were utilized owing to the reason that they stipulated pretty slightest of the execution time.

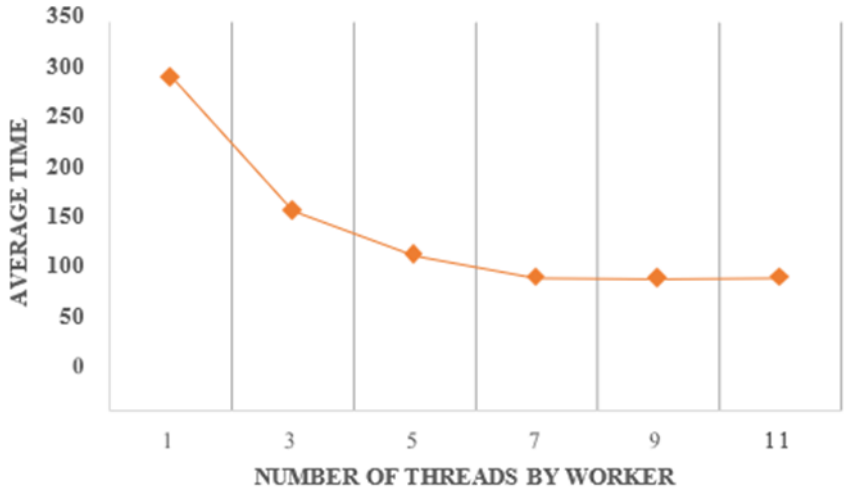

Figure 5: Average execution time of ETI job from a different source to JSON format.

5.2 Offline phase performance measurements

The proposed framework was evaluated using numerous nodes per cluster, as depicted in Figure 6 According to the figure, the greater the nodes per cluster, the slackened is loading time for each dataset. So, six nodes per cluster and one master node for that cluster were used in the evaluation and assessment process.

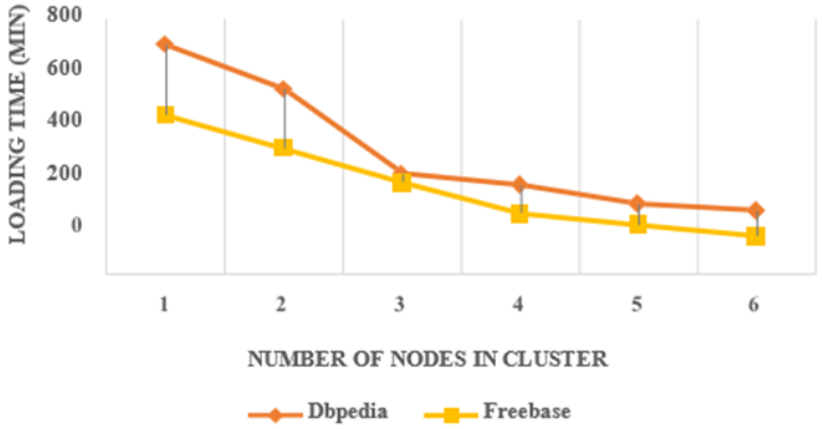

Figure 6: Loading time per cluster.

5.3 Online phase and query performance measurements

To scrutinize whether the proposed methods ameliorate the consequences and results, humans use different technologies to analyze humongous frequency queries in length. The effectuated four queries were cited under:

- **Query I**: In this test case, the system is triggered by a straightforward abstruse single word as query (e.g., network).
- **Query II**: In this query, the system is triggered by the same query as in query I (e.g., networks), but this query is expanded using the word net to extend the search area.
- **Query III**: In this query, the system is triggered by complex multiple words as a query (e.g., computer networks and protocols). Also, in this test case, all different proposed techniques are implemented.
- **Query IV**: In this query, the system is triggered by the same query as in query III (e.g., computer networks and protocols), but this query is expanded using the word net to extend the search area.

Table 2 provides the results of different online queries, and Table 3 details the compassion between the proposed system and other related systems.

Table 2: Result of different online queries.

Parameters	Query I	Query II	Query III	Query IV
Input Keywords	1	1	1	1
Extended Keywords	8	0	8	0
True Positive	8690	6481	8630	4991
False Positive	302	430	362	1120
Precision	0.966	0.937	0.959	0.889
Recall	0.938	0.943	0.921	0.957
F-score	0.952	0.935	0.94	0.921
Response Time at online phase (sec)	2.570	1.220	3.490	.400

Table 3: Compassion between the proposed system and other related systems.

Parameters	Swoogle	Falcon	Proposed
Support Ontology	✓	✓	✓
Semantic Relations	✓	✓	✓
Support Ranking	×	✓	✓
Handle Big Data	×	×	✓
High Precision	✓	×	✓
High Recall	×	✓	×
Response Time	Sluggish	Sluggish	Medium

6 Conclusion

As a matter of conjecture, this manuscript postulated a semantic retrieval framework for augmenting and enhancing knowledge and search area using the integration of more than one semantic source. The proposed framework is effectuated by deploying some modern technologies, including ontology graph, RDF, MAP-REDUCE technique implemented in Hadoop, Not only Structured Query Language (NoSQL) model using Hbase and proposed mathematical model for calculating semantic relations between subjects. Six slave nodes with one master node were utilized to scrutinize the framework. Two datasets (e.g., DBpedia and YAGO) were implemented to inculcate knowledge. Four queries were used in experiments that worked well to compute and test the proposed framework. Experimental results manifested a spectacular degree of precision and profound acuteness of cited tested queries in decent response time compared to related systems.

Declaration of Competing Interests

The authors declare that they have no known competing financial interests or personal relationships that could have appeared to influence the work reported in this paper.

Funding Declaration

This research did not receive any grants from governmental, private, or nonprofit funding bodies.

Author Contribution

Shishir Dua: Data curation, Writing–Original draft preparation, Methodology, Investigation, Software, Validation; **Kakoli Banerjee**: Conceptualization, Supervision, Validation, Writing- Reviewing and Editing

References

[1] C. Gavankar, T. Bhosale, D. Gunda, A. Chavan, and S. Hassan, "A Comparative Study of Semantic Search Systems," in *2020 International Conference on Computer Communication and Informatics (ICCCI)*, pp. 1–7, IEEE, jan 2020.

[2] Z. Pan, "Optimization of Information Retrieval Algorithm for Digital Library Based on Semantic Search Engine," in *2020 International Conference on Computer Engineering and Application (ICCEA)*, pp. 364–367, IEEE, mar 2020.

[3] A. Dramilio, C. Faustine, S. Sanjaya, and B. Soewito, "The Effect and Technique in Search Engine Optimization," in *2020 International Conference on Information Management and Technology (ICIMTech)*, pp. 348–353, IEEE, aug 2020.

[4] M. N. Asim, M. Wasim, M. U. Ghani Khan, N. Mahmood, and W. Mahmood, "The Use of Ontology in Retrieval: A Study on Textual, Multilingual, and Multimedia Retrieval," *IEEE Access*, vol. 7, pp. 21662–21686, 2019.

[5] A. Begdouri, O. Chergui, and D. Leclet-Groux, "A knowledge-based approach for keywords modeling into a semantic graph," *International Journal of Information Science & Technology, iJIST*, vol. 2, no. 1, pp. 2550–5114, 2018.

[6] M. M. El-Gayar, N. E. Mekky, A. Atwan, and H. Soliman, "Enhanced Search Engine Using Proposed Framework and Ranking Algorithm Based on Semantic Relations," *IEEE Access*, vol. 7, pp. 139337–139349, 2019.

[7] A. Nadeem, M. Hussain, and A. Iftikhar, "New Technique to Rank Without Off Page Search Engine Optimization," in *2020 IEEE 23rd International Multitopic Conference (INMIC)*, pp. 1–6, IEEE, nov 2020.

[8] M. Elgayar, "A Novel Knowledge-based Semantic Search Engine," *International journal of simulation: systems, science & technology*, vol. 20, pp. 9.1–9.9, oct 2019.

[9] Y. S. Negi and S. Kumar, "A Comparative Analysis of Keyword- and Semantic-Based Search Engines," in *Advances in Intelligent Systems and Computing*, vol. 243, pp. 727–736, 2014.

[10] B. R. Prasad and S. Agarwal, "Comparative Study of Big Data Computing and Storage Tools: A Review," *International Journal of Database Theory and Application*, vol. 9, pp. 45–66, jan 2016.

[11] D. Singh and C. K. Reddy, "A survey on platforms for big data analytics," *Journal of Big Data*, vol. 2, p. 8, dec 2015.

[12] Y. Qu and G. Cheng, "Falcons Concept Search: A Practical Search Engine for Web Ontologies," *IEEE Transactions on Systems, Man, and Cybernetics - Part A: Systems and Humans*, vol. 41, pp. 810–816, jul 2011.

[13] L. Ding, T. Finin, A. Joshi, R. Pan, R. S. Cost, Y. Peng, P. Reddivari, V. Doshi, and J. Sachs, "Swoogle Bibliographic Search," *Proceedings of the Thirteenth ACM conference on Information and knowledge management - CIKM '04*, p. 652, 2004.

[14] A. Hogan, A. Harth, J. Umbrich, S. Kinsella, A. Polleres, and S. Decker, "Searching and Browsing Linked Data with SWSE: The Semantic Web Search Engine," *SSRN Electronic Journal*, 2011.

[15] A. Fatima, C. Luca, and G. Wilson, "New Framework for Semantic Search Engine," in *2014 UKSim-AMSS 16th International Conference on Computer Modelling and Simulation*, pp. 446–451, IEEE, mar 2014.

[16] A. Oussous, F.-Z. Benjelloun, A. Ait Lahcen, and S. Belfkih, "Big Data technologies: A survey," *Journal of King Saud University - Computer and Information Sciences*, vol. 30, pp. 431–448, oct 2018.

[17] K. Shvachko, H. Kuang, S. Radia, and R. Chansler, "The Hadoop Distributed File System," in *2010 IEEE 26th Symposium on Mass Storage Systems and Technologies (MSST)*, pp. 1–10, IEEE, may 2010.

[18] D. Vohra, "Using Apache HBase," in *Pro Docker*, pp. 141–150, Berkeley, CA: Apress, 2016.

Journal of Computers, Mechanical and Management

Journal homepage: www.jcmm.co.in

Volume 1 Issue 1

Friction Stir Welding of Different Aluminum-Silicon Alloy Compositions Utilizing Conventional Vertical Milling Machine

K. J. Santosh Kumar[a], Ganesh Arjun Bhargav[a], Yuvaraja Naik[b], and K. Bommanna[*c]

[a]Department of Mechanical Engineering, K.S. School of Engineering and Management, Bangalore, Karnataka, India 560109

[b]Department of Mechanical Engineering, Presidency University Bangalore, Karnataka, India, 560064

[c]Department of Mechanical Engineering, A P S College of Engineering, Bangalore, Karnataka, India 560082

Abstract

Friction-Stir Welding (FSW) is a solid-state procedure for welding two plates in which there is relative motion between the tool and workpiece, which creates the heat required for the material of the two edges to join by atomic diffusion. The present research article focuses on friction stir welding of dissimilar aluminum-silicon alloys utilizing a vertical milling machine and altering process parameters. Moreover, testing is done on the weld joints for the best process parameter. The process parameters considered in the present work for joining dissimilar aluminum alloys primarily were a constant tool feed rate of 63 mm/min and three varied tool rotational speed rates of 710, 1000 and 1400 rpm. Mechanical characterization of weld joints, such as tensile, hardness, microstructural studies and surface roughness tests, were used to identify the most optimal parameter. The results indicated that Al-Si alloys having Al-5 %Si with Al-12 %Si FSW joints welded using 1000 rpm tool rotational speed proved to have better hardness and lesser surface roughness while, Al-Si alloys having Al-12 %Si with Al-17 %Si FSW joints, had better hardness and roughness properties when welded using 1400 rpm tool rotational speed. Concerning the ultimate tensile strength, Al-Si alloys having Al-5 %Si with Al-12 %Si and Al-12 %Si with Al-17 %Si FSW joints welded using 1400 rpm tool rotational speed offered better results.

Keywords: Friction Stir Welding; Weld Joints; Aluminum Alloys; Silicon; Mechanical Properties

1 Introduction

Friction-Stir Welding (FSW) is a solid-state procedure for welding two plates in which there is relative motion between the tool and workpiece, which creates the heat required for the material of the two edges to join by atomic diffusion [1] and was developed by The Welding Institute (TWI), in 1991 [2]. TWI successfully obtained patents for FSW in Europe, the United States, Japan and Australia while completing a development study demonstrating FSW as a realistic and viable technology for welding aluminum alloys from the 2XXX, 5XXX, and 6XXX series [3, 4]. Figure 1 depicts a diagrammatic representation of friction stir welding. Unlike traditional fusion welding processes employed for dissimilar materials, the FSW process consumes less time and is cost-effective [5]. Moreover, FSW does not require the melting of material as the temperature involved in this process is significantly lower than the melting temperature of the base materials, and the secondary phase development does not occur during this process [6–10]. Previous studies reveal that of all the process parameters, tool rotational speed and feed rate play a major role in the quality of FSW processed parts [11–13]. The literature reviewed indicated that the wear rate reduces as the tool feed rate increases. However, beyond a certain value, the wear rate begins to increase. The highest resistance to wear was obtained at a tool feed rate of 65 mm/min [6]. The studies also indicated that a tool rotational speed of 1300 rpm showed better quality weld and strength [14].

*Corresponding author: bommannak_cta@rediffmail.com

Received: 13 September 2022; **Accepted:** 29 September 2022; **Published:** 30 October 2022

© 2022 Journal of Computers, Mechanical and Management.

This is an open access article and is licensed under a Creative Commons Attribution-Non Commercial 4.0 International License.

DOI: 10.57159/gadl.jcmm.1.1.23012.

The present work is unique as it investigates the microstructure, hardness and tensile strength of FSW joints in order to determine the value of process parameters to achieve the best mechanical properties and minimum surface roughness of Al-Si alloy FSW joints, as the investigated properties affect the corrosion behavior, fatigue strength and life cycle of FSW joints.

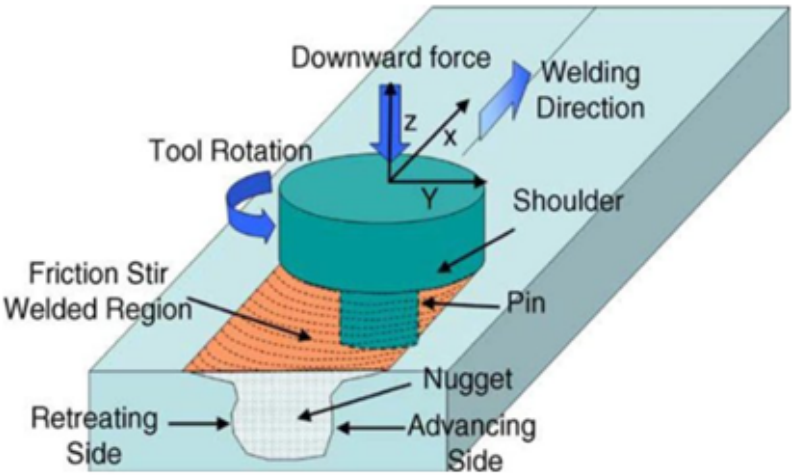

Figure 1: Schematic representation of a friction stir welding process [15].

2 Materials and Method

Conventional milling machines have proved to be used to undertake friction stir welding of aluminum alloys [16]. Therefore, the present work utilizes the laboratory-installed conventional turret mill-based milling machine, as shown in Figure 2(a), for the friction stir welding process. Figure 2(b) depicts an overview of the FSW plate for the shoulder tool-contacting side. This surface was distinguished by the so-called wake effect and the presence of semicircular features similar to those produced by conventional milling [17, 18].

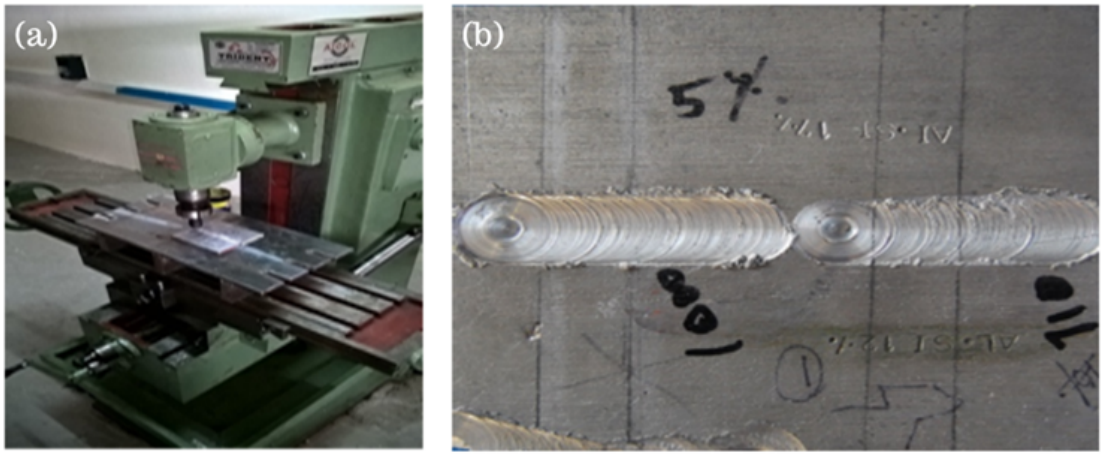

Figure 2: **(a)** Vertical milling machine setup; **(b)** friction-welded Al-Si specimen.

Silicon is the principal alloying ingredient in the Al-Si alloys, as its addition results in good castability and weldability because of its high fluidity and minimal shrinkage properties. Thus, the friction stir welding was performed on two different combinations of three different Al-Si compositions (Al-5 %Si with Al-12 %Si and Al-12 %Si with Al-17 %Si). Tool rotational speed, the most significant process parameter, was varied, and the tool feed rate was maintained constant. The rotational speeds used were 710, 1000 and 1400 rpm, and the feed rate was maintained at 63 mm/min.

2.1 Tensile test

Tensile strength is the ability of a material to withstand fracture when a pulling force is applied. The material with good tensile strength resists higher loads; therefore, it is necessary to check the tensile strength of the joint. The specimens are prepared as per the ASTM standard E08. The dimensions of the tensile test specimens are as shown in Figure 3(a). Tensile test was performed using a universal testing machine, suitable for small loads (less than 2000 kg).

A tensile specimen of Al-Si alloy prepared according to the ASTM standard is shown in Figure 3(b). A few fractured specimens comprising Al-5 %Si with Al-12 %Si and Al-12 %Si with Al-17 %Si FSW joints welded using 710, 1000 and 1400 rpm are shown in Fig. 3(c) from left to right.

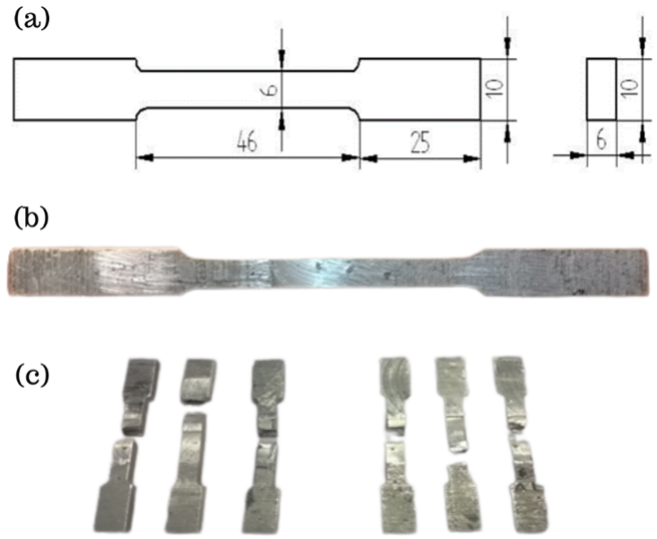

Figure 3: Tensile test specimen: **(a)** standard dimensions used for specimen preparation; **(b)** sample tensile specimen; **(c)** fractured tensile specimen.

2.2 Hardness test

Hardness, a mechanical property of the material, is its resistance to deformation and is assessed by a standard test that measures the material's surface resistance to indentation. It impacts the tribological performance of a material and is also an essential aspect to consider during machining [19]. In simple words, hardness is the property of a material that enables it to resist plastic deformation, penetration, indentation, and scratching. Figure 4(a) shows the laboratory-installed Rockwell hardness testing machine used in the present work, which was used to determine the hardness by comparing the depth of an indenter's penetration under a large force (100 Kgf is the load chosen for the test) to the pre-load penetration.

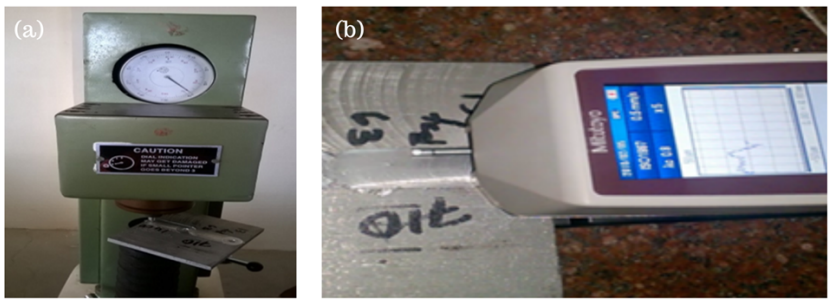

Figure 4: Laboratory equipment used for testing of FSW specimen: **(a)** Rockwell hardness testing machine; **(b)** surface profilometer.

2.3 Surface roughness test

Surface roughness affects working on a surface. Under variable loading conditions, the fracture of welded joints initiates at the component's surface. Consequently, surface roughness has a substantial impact on the fatigue of the welded joint [20]. As depicted in Figure 4(b), a diamond indent stylus profilometer was used to assess the change in longitudinal surface roughness (Ra) caused by the FSW process on the side in contact with the shoulder.

3 Results and Discussion

3.1 Tensile strength

The average experimental values of ultimate tensile strength obtained for Al-5 %Si with Al-12 %Si and Al-12 %Si with Al-17 %Si FSW joints are shown in Table 1. The bar chart in Figure 5 compares the two dissimilar joints at various tool rotational speeds.

Table 1: Ultimate tensile strength of welded joints values of the FSW joints.

Welding condition	Average ultimate tensile strength (MPa)	
	Al-5%Si with Al-12%Si	Al-12%Si with Al-17%Si
710 rpm at 63 mm/min	59.5	88.6
1000 rpm at 63 mm/min	83.0	134.7
1400 rpm at 63 mm/min	89.0	112.7

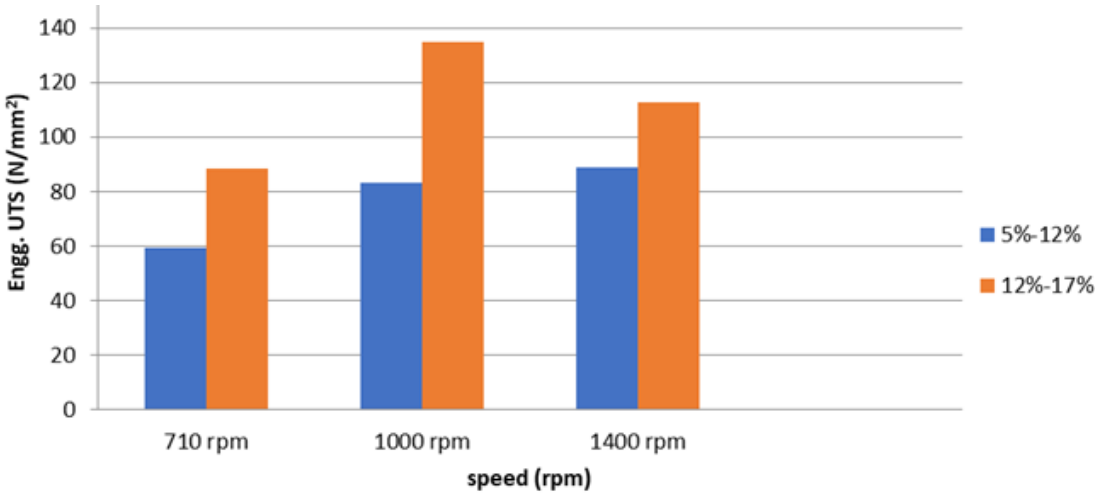

Figure 5: Ultimate tensile strength of various tested FSW joints.

From Figure 5, the comparison between the two dissimilar welded joints at various tool rotational speeds could be observed. The obtained tensile behavior results indicated increased tensile strength with the tool rotational speed in the case of Al-5 %Si with Al-12 %Si FSW joint. The higher speeds resulted in poor heat generation and plastic flow of the material, which might have resulted in a weak interface at the joint. The higher the welding speeds, the lower the heat produced, which speeded up the cooling of the welded seams. It can also be inferred that when welding rates were higher, there was a lower metallurgical transformation and higher strengths. In the case of Al-5 %Si with Al-12 %Si FSW joint, the tensile strength initially increased with speed but later started reducing.

3.2 Rockwell hardness

The average hardness values obtained for Al-5 %Si with Al-12 %Si and Al-12 %Si with Al-17 %Si FSW joints after the experimentation are given in Table 2. These hardness results are compared for the two dissimilar FSW joints welded at different tool rotational speeds. At a tool rotational speed of 1000 rpm, the hardness increased in both the Al-Si variants. However, the Al-12 %Si with Al-17 %Si dissimilar joint contained a higher percentage of silicon, which led to exceptional hardness and strength.

Table 2: Hardness of FSW joints.

Welding condition	Average Rockwell hardness (RHN)	
	Al-5%Si with Al-12%Si	Al-12%Si with Al-17%Si
710 rpm at 63 mm/min	67.5	62
1000 rpm at 63 mm/min	70.72	78.5
1400 rpm at 63 mm/min	60.5	63.5

3.3 Surface roughness

The results indicated that surface roughness depends on the tool rotational speed and the hardness of the material. Concerning Al-5 %Si with Al-12 %Si FSW joint, it was observed that the surface roughness initially decreased but then increased with the increase in the tool rotational speed. However, in the case of Al-12 %Si with Al-17 %Si FSW joint, the surface roughness decreased with the increase in the tool rotational speed. Table 3 shows the average values obtained for the surface roughness test. The test results with standard deviation bars are represented in Figure 6.

Table 3: Surface roughness values of the FSW joints.

Welding condition	Surface Roughness, Ra (μm)	
	Al-5%Si with Al-12%Si	Al-12%Si with Al-17%Si
710 rpm at 63 mm/min	5.946	4.683
1000 rpm at 63 mm/min	4.404	5.540
1400 rpm at 63 mm/min	7.276	2.870

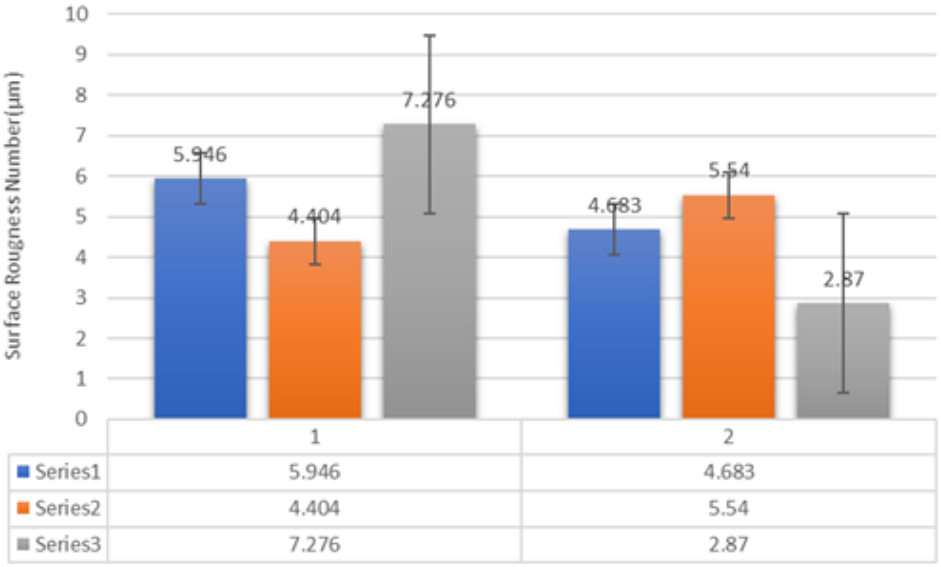

Figure 6: Surface roughness of FSW joints: Series 1 - 710 rpm at 63 mm/min; Series 2 - 1000 rpm at 63 mm/min; Series 3 - 1400 rpm at 63 mm/min.

3.4 Microstructure analysis

A microstructure study was done using Scanning Electron Microscope (SEM) on the weld joints of the friction stir welded specimens. The SEM images were magnified to 200 microns, concentrating on 5 different points (locations) of the weld joints: top, bottom, right, left and the middle region (nugget region). During welding, the plunging force required to drill the Al-5 %Si -Al-12 %Si FSW joint was 12 KN, and for Al-12 %Si -Al-17 %Si FSW joint was more than 20KN. Figure 7, Figure 8 and Figure 9 represent the SEM images for Al-5 %Si -Al-12 %Si FSW joint, while Figure 10, Figure 11 and Figure 12 Al-12 %Si -Al-17 %Si FSW joint.

Figure 7(a) depicts the dispersion of Si particles over the weld joint, where Si needle-like formations can be seen. As seen in the figure, the dynamic recrystallization of this welded connection was minimal. As friction stir welding commences, the tooltip drilled and penetrated the plate stirs the region, as shown in Figure 7(b). As a result of the fact that only a small area is churned in this place, the silicon particles are spread more uniformly. As depicted in Figure 7(c), fewer silicon particles are intermixed on the left side of the weld, which contains 5 % silicon and 95 % aluminum. Consequently, there are fewer silicon particles visible in this view. Due to the low tool rotational speed, it becomes hard to combine the silicon particles. Since it is a known fact that low tool rotating speeds produce lower frictional temperatures, this leads to less mixing of silicon particles during welding. As shown in Figure 7(d), the right side of the weld part is comprised of a 12 % silicon plate, representing a higher silicon content than the region on the advancing side. Therefore, the resultant image contains a large proportion of silicon. The region in Figure 7(e) illustrates that the welding speed is relatively sluggish for perfectly blending silicon particles compared to the other two weld speeds. Evident in this section are features resembling needles.

Figure 8(a) shows the dispersion of silicon particles in fine grains. A few silicon particles have been burned and can be seen as flakes. There are no needle-like structures or cluster formations, which contribute to the absence of crack propagation or defects. The structure in Figure 8(b) differs from that in the top region. Silicon particles form needle-like structures that exist. These needles could be the cause of crack initiation and propagation. When the bottom region is compared to the top region, it is clear that the stirring operation in this area was insufficient. Figure 8(c) shows that the retreating side of the weld zone has fewer silicon particles and needle-like structures. This indicates that a percentage of the silicon was moved from the upper to the lower region during welding. There are also flaws in this area. Figure 8(d) shows tiny silicon grains, indicating that the area was well-welded. It also shows that this region's percentage of silicon particles is lower than in the other. The silicon percentage is the same as in the top region. Figure 8(e) shows similar results to the top and advancing side portions. It is clear that the percentage of silicon is lower. Fine grain-like structures can be seen, indicating a good weld joint in the area.

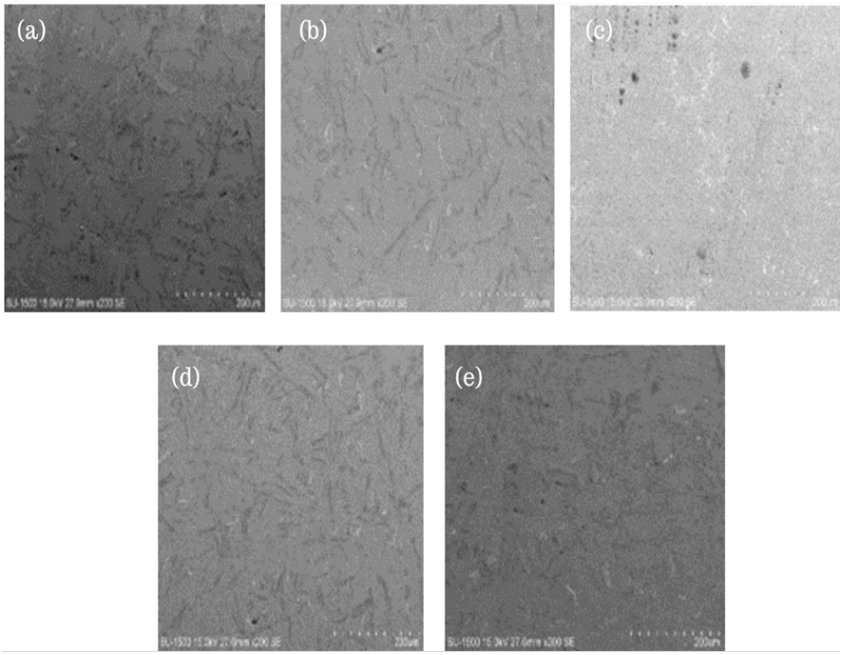

Figure 7: SEM images of Al-5 %Si -Al-12 %Si FSW joint welded using 710 rpm speed at various locations of cross-section: **(a)** top; **(b)** bottom **(c)** Retreating side (left); **(d)** Advancing side (right); **(e)** Nugget zone (middle) portion.

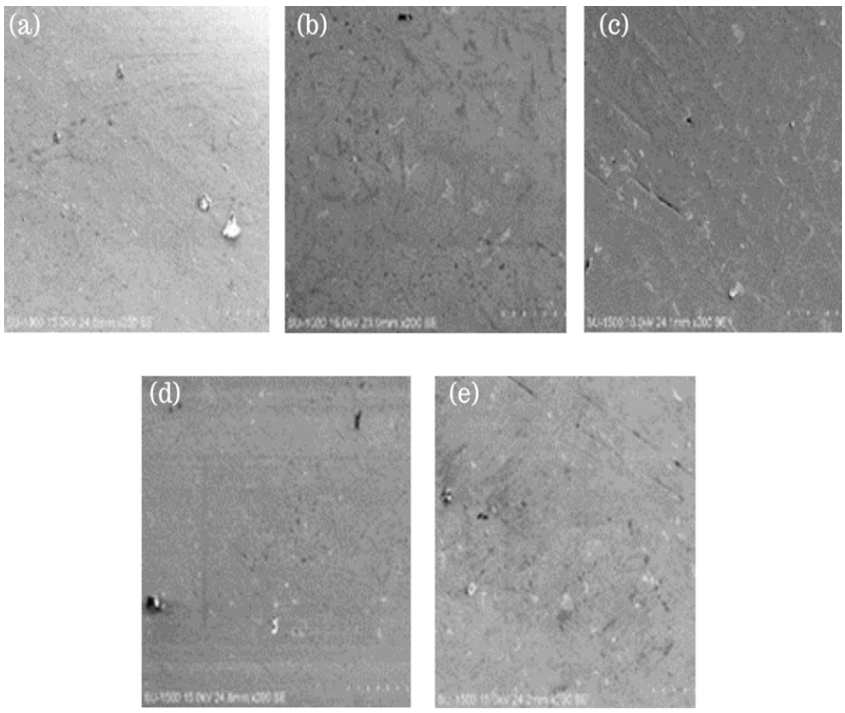

Figure 8: SEM images of Al-5 %Si -Al-12 %Si FSW joint welded using 1000 rpm speed at various locations of cross-section: **(a)** top; **(b)** bottom **(c)** Retreating side (left); **(d)** Advancing side (right); **(e)** Nugget zone (middle) portion.

Figure 9(a) depicts the cross section's top region. The grains in this area have a high silicon content and form tiny, needle-like structures. This is due to the high rotational speed of the tool. Figure 9(b) shows needle-like structures of silicon particles, similar to the weld joint's upper section. This indicates that the particles are properly mixed during welding. Figure 9(c), the retreating side, depicts needle-like structures of silicon particles. It also has a higher percentage of silicon particles. Because of the faster tool rotational speed, silicon can be seen moving from the upper to lower region. However, the region's grain structure is not refined. Silicon is abundant in small grain particles in the region depicted in Figure 9(d). Compared to the other regions of the welded joint, the silicon in this region has been refined. The tool's stirring action in this region improves the distribution of silicon particles. Figure 9(e) depicts the region where silicon can be found in fine grains and needle-like formations. Also visible is the diffusion of silicon particles, similar to that seen in other regions except for the advancing side of the welded region.

Figure 10(a) shows that the welded zone has undergone greater plastic deformation, dispersing the silicon particles into smaller grains. It has gone through less dynamic recrystallization. It also shows that the area has a sound weld from welding. Figure 10(b) shows that silicon particles are present throughout the region as needle structures.

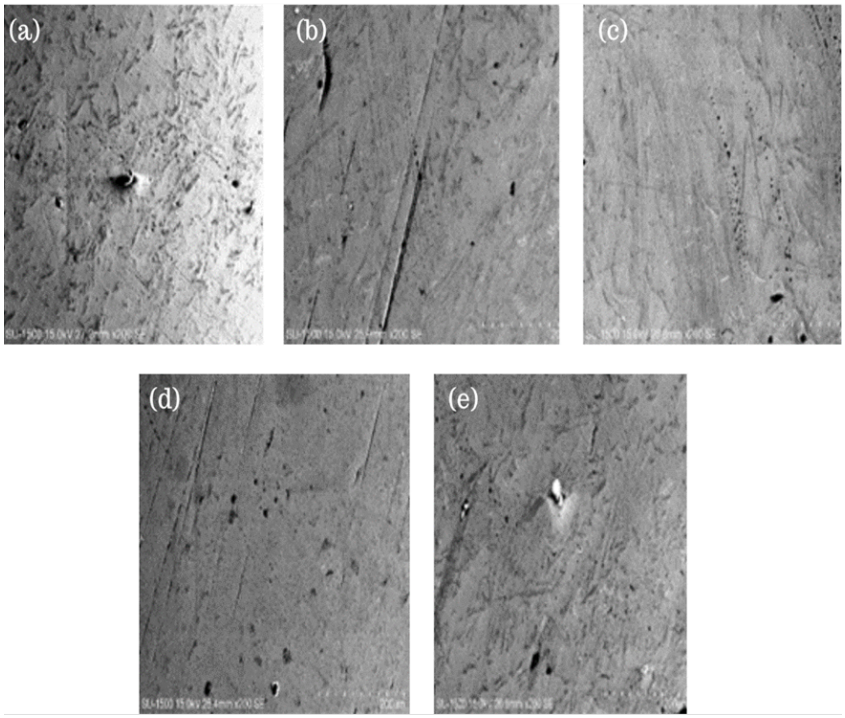

Figure 9: SEM images of Al-5 %Si -Al-12 %Si FSW joint welded using 1400 rpm speed at various locations of cross-section: **(a)** top; **(b)** bottom **(c)** Retreating side (left); **(d)** Advancing side (right); **(e)** Nugget zone (middle) portion.

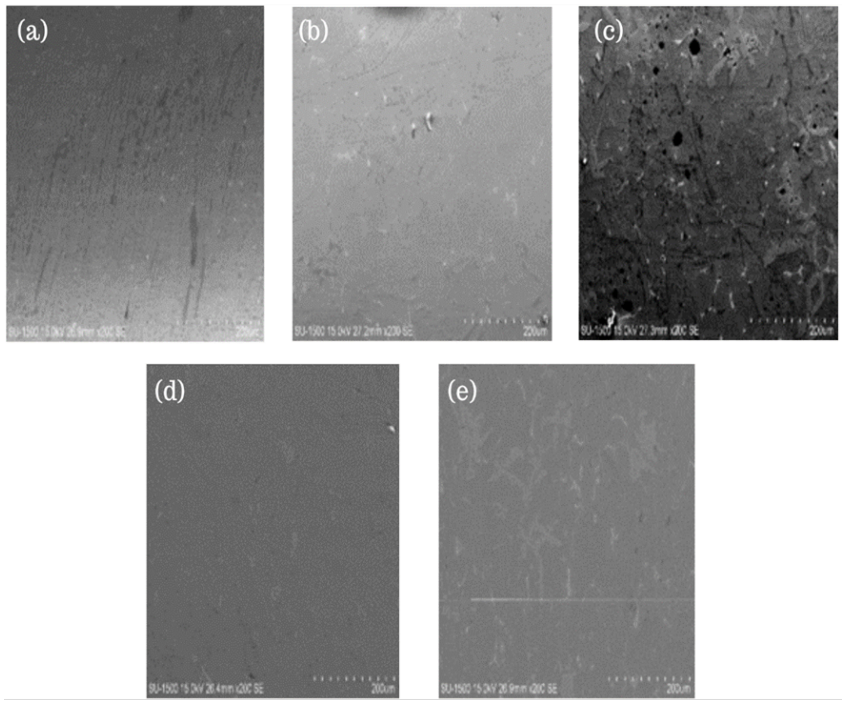

Figure 10: SEM images of Al-12 %Si -Al-17 %Si FSW joint welded using 710 rpm speed at various locations of cross-section: **(a)** top; **(b)** bottom **(c)** Retreating side (left); **(d)** Advancing side (right); **(e)** Nugget zone (middle) portion.

The refinement of the composition did not go well at 710 rpm. Dendrite shapes can also be found in the area. These silicon particles are not distributed evenly throughout the region. Figure 10(c) depicts the formation of clusters of silicon particles throughout the region, as well as the increased hardness and force required to move this silicon due to its higher composition. Defects such as porosity are also visible in the region. The distribution of silicon has not been very good in this region. Figure 10(d) depicts the region containing silicon refined into fine grains. Despite being refined, the silicon is in the form of needle-like structures. Because of the material's higher hardness and a higher silicon percentage, the load required to penetrate this region is high. Figure 10(e) shows that silicon in this region is present in cluster formation due to increased silicon diffusion from the higher region. These cluster formations are more likely to cause crack initiation and propagation. Dendrite shapes can also be found in this region. Most energy has been used to move the silicon from the higher to the lower region.

Compared to the other welded joints, the region shown in Figure 11(a) indicates that most of the silicon has already diffused and is not well refined. However, because silicon diffusion is greater and more evenly distributed, the tensile strength and hardness values obtained at this weld joint are higher than those obtained at the other welded joints. There are also web-like structures in the region. Figure 11(b) shows that silicon is more common and can be found in cluster formation, dendrite formations, and needle-like structures. Fine particles are insignificant in this region. The energy required for material displacement is also higher when compared to the Al-5 %Si with Al-12 %Si FSW joint. Because of the higher percentage of silicon in this region, the hardness and tensile strength are higher. Figure 11(c) shows this region's higher silicon percentage. It can be found in cluster formations but in smaller shapes that are compacted. In this region, the web or dendrite shapes are less visible. Because of the increased hardness, the weld joint has developed a few flaws.

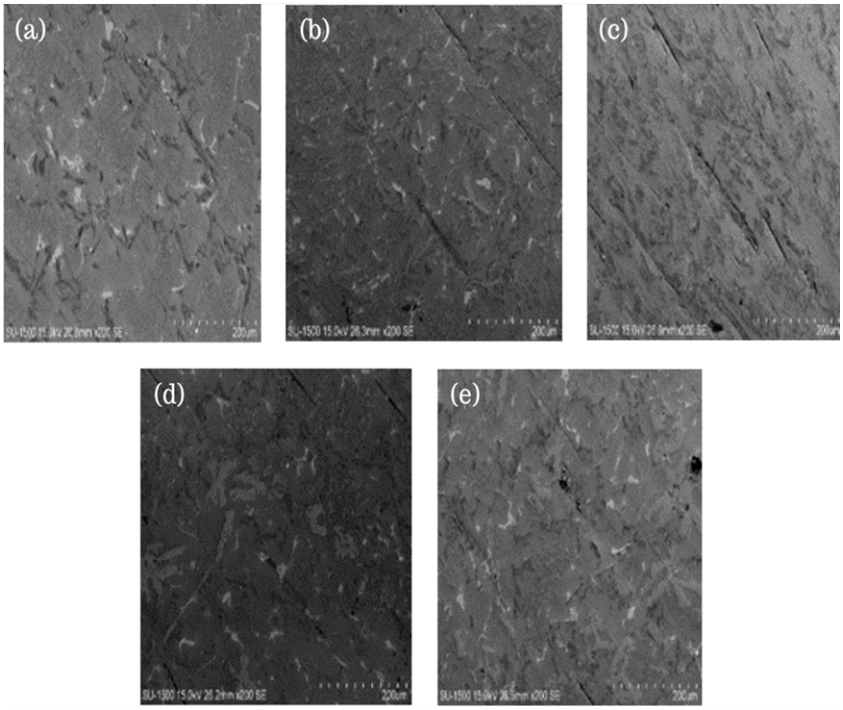

Figure 11: SEM images of Al-12 %Si -Al-17 %Si FSW joint welded using 1000 rpm speed at various locations of cross-section: **(a)** top; **(b)** bottom **(c)** Retreating side (left); **(d)** Advancing side (right); **(e)** Nugget zone (middle) portion.

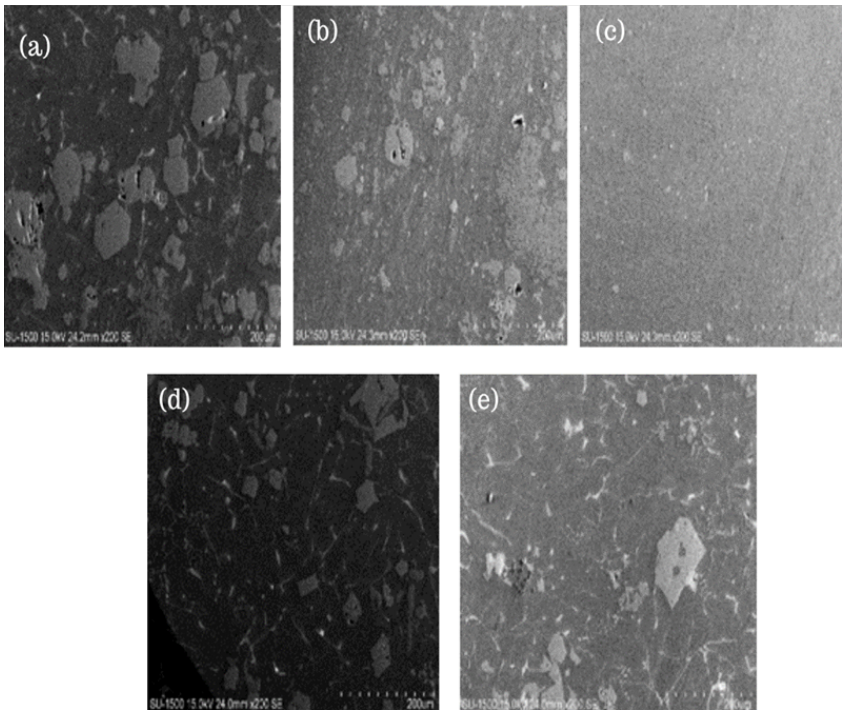

Figure 12: SEM images of Al-12 %Si -Al-17 %Si FSW joint welded using 1400 rpm speed at various locations of cross-section: **(a)** top; **(b)** bottom **(c)** Retreating side (left); **(d)** Advancing side (right); **(e)** Nugget zone (middle) portion.

The presence of silicon in cluster formation and web-like structures indicates that the silicon in the area depicted in Figure 11(d) has not been effectively refined. This region also has a porosity defect. The presence of silicon in cluster formation and web shapes can be seen in the region depicted in Fig. 11(e). There has been no silicon refinement, and its distribution is also not uniform throughout the region. Figure 12(a) shows that silicon is present in cluster and hexagonal shapes. The increased tool rotational speed contributed to less heat generation, resulting in less plastic deformation. The silicon particles have diffused from the higher percentage region to the lower percentage region. The load distribution is also uneven due to the large cluster and hexagonal shapes, resulting in the material failure in the region. Figure 12(b) depicts the presence of silicon in this region in the cluster and hexagonal shapes. However, the silicon is not evenly distributed and is not in the form of fine grains. The composition is completely refined into fine grains in the region depicted in Figure 12(c). However, weld joint diffusion from the higher region is negligible. The material's stirring action only refined the particles in the region, but the displacement of other particles from other regions is not visible. The silicon is present in hexagonal clusters in the area depicted in Figure 12(d). It demonstrates that there is much silicon in the area and that stirring has no effect. The tool rotational speed of 1400 rpm has not been as effective in welding the zone as required for the sound weld. Figure 12(e) shows that silicon diffusion has not been very well in the nugget zone, and the results of hardness and tensile strength indicate a decrease in the same when compared to the welded joint using 1000 rpm speed for Al-12 %Si-Al-17 %Si FSW joint. The silicon distribution in the region is not uniform, making it prone to failure. The variable silicon content of the materials affects most of their mechanical properties. Silicon is diffused from both base materials when they are semi-solid due to heat produced by friction between the surface of the base materials and the tool during welding. By varying the rotational speed of the tool, the variation in the silicon particle distribution can be seen in Figure 12.

4 Conclusion

This research was done to identify the properties of FSW joints made from 6 mm thick plates with Al-Si 5 %, Al-Si 12 %, and Al-Si 17 %. The welding process was carried out at a constant tool feed rate of 63 mm/min. The samples were evaluated for hardness, ultimate tensile strength, surface roughness and microstructure. From the experimental results, it has been observed that Al-12 %Si -Al-17 %Si FSW joints welded using 1000 rpm offered a proper distribution of grains in the weldment, and the same weldment gave well results in hardness number of 78.5 RHN with ultimate tensile strength of 70.12 N/mm^2 for Al-5 %-12 %Si and highest UTS of 78.5 N/mm^2 in Al-12 %Si -Al-17 %Si FSW welded using 1000 rpm. By inspecting the microstructure of the Al-5 %Si -Al-12 %Si FSW joints welded using 1000 rpm; the silicon has been distributed uniformly. Compared to the other two weld joints, this one has less porosity and other defects. At 1400 rpm, the silicon in the Al-12 %Si -Al-17 %Si combination is evenly distributed and has a lower porosity.

Declaration of Competing Interests

The authors declare that they have no known competing financial interests or personal relationships that could have appeared to influence the work reported in this paper.

Funding Declaration

This research did not receive any grants from governmental, private, or nonprofit funding bodies.

Author Contribution

K. J. Santosh Kumar: Conceptualization, Methodology; **Ganesh Arjun Bhargav**: Data curation, Writing- Original draft preparation; **Yuvaraja Naik**: Visualization, Investigation; **K. Bommanna**: Writing- Reviewing and Editing.

References

[1] B. Vijaya Ramnath, C. Elanchezhian, S. Rajesh, S. Jaya Prakash, B. M. Kumaar, and K. Rajeshkannan, "Design and Development of Milling Fixture for Friction Stir Welding," *Materials Today: Proceedings*, vol. 5, no. 1, pp. 1832–1838, 2018.

[2] Q. Chu, W. Y. Li, D. Wu, X. C. Liu, S. J. Hao, Y. F. Zou, X. W. Yang, and A. Vairis, "In-depth understanding of material flow behavior and refinement mechanism during bobbin tool friction stir welding," *International Journal of Machine Tools and Manufacture*, vol. 171, p. 103816, dec 2021.

[3] Z. Y. Ma, A. H. Feng, D. L. Chen, and J. Shen, "Recent Advances in Friction Stir Welding/Processing of Aluminum Alloys: Microstructural Evolution and Mechanical Properties," *Critical Reviews in Solid State and Materials Sciences*, vol. 43, pp. 269–333, jul 2018.

[4] P. L. Threadgill, A. J. Leonard, H. R. Shercliff, and P. J. Withers, "Friction stir welding of aluminium alloys," *International Materials Reviews*, vol. 54, pp. 49–93, mar 2009.

[5] R. P. Singh, S. Dubey, A. Singh, and S. Kumar, "A review paper on friction stir welding process," *Materials Today: Proceedings*, vol. 38, pp. 6–11, 2020.

[6] N. Saini, D. K. Dwivedi, P. K. Jain, and H. Singh, "Surface modification of cast Al-17Engineering, vol. 100, no. January, pp. 1522–1531, 2015.

[7] S. L. Rajaseelan and S. Kumarasamy, "Mechanical properties and microstructural characterization of dissimilar friction stir welded AA5083 and AA6061 aluminium alloys," *Mechanika*, vol. 26, pp. 545–552, dec 2020.

[8] P. Sadeesh, K. M. Venkatesh, V. Rajkumar, P. Avinash, N. Arivazhagan, R. K. Devendranath, and S. Narayanan, "Studies on friction stir welding of aa 2024 and aa 6061 dissimilar metals," *Procedia Engineering*, vol. 75, pp. 145–149, 2014.

[9] M. P. Reddy, A. A. S. William, M. M. Prashanth, S. S. Kumar, K. D. Ramkumar, N. Arivazhagan, and S. Narayanan, "Assessment of Mechanical Properties of AISI 4140 and AISI 316 Dissimilar Weldments," *Procedia Engineering*, vol. 75, no. 2, pp. 29–33, 2014.

[10] M. M. Abd Elnabi, A. B. Elshalakany, M. M. Abdel-Mottaleb, T. A. Osman, and A. El Mokadem, "Influence of friction stir welding parameters on metallurgical and mechanical properties of dissimilar AA5454-AA7075 aluminum alloys," *Journal of Materials Research and Technology*, vol. 8, pp. 1684–1693, apr 2019.

[11] S. Delijaicov, P. A. de Oliveira Silva, H. B. Resende, and M. H. F. Batalha, "Effect of weld parameters on residual stress, hardness and microstructure of dissimilar AA2024-T3 and AA7475-T761 friction stir welded joints," *Materials Research*, vol. 21, aug 2018.

[12] M. Sindhuja, S. Neelakrishnan, and B. S. Davidson, "Effect of Welding Parameters on Mechanical Properties of Friction Stir Welding of Dissimilar Metals- A Review," *IOP Conference Series: Materials Science and Engineering*, vol. 1185, p. 012019, sep 2021.

[13] I. Kalemba-Rec, M. Kopyściański, D. Miara, and K. Krasnowski, "Effect of process parameters on mechanical properties of friction stir welded dissimilar 7075-T651 and 5083-H111 aluminum alloys," *International Journal of Advanced Manufacturing Technology*, vol. 97, pp. 2767–2779, jul 2018.

[14] V. Saravanan, S. Rajakumar, and A. Muruganandam, "Influence of Tool Rotation Speed on Macrostructure, Microstructure and Mechanical behaviour of Dissimilar Friction Stir Welded AA2014-T6 and AA7075-T6 Aluminum Alloys," *Journal of Advances in Mechanical Engineering and Science*, vol. 2, pp. 19–24, aug 2016.

[15] R. Mishra and Z. Ma, "Friction stir welding and processing," *Materials Science and Engineering: R: Reports*, vol. 50, pp. 1–78, aug 2005.

[16] T. Minton and D. J. Mynors, "Utilisation of engineering workshop equipment for friction stir welding," *Journal of Materials Processing Technology*, vol. 177, pp. 336–339, jul 2006.

[17] K. Krishnan, "On the formation of onion rings in friction stir welds," *Materials Science and Engineering: A*, vol. 327, pp. 246–251, apr 2002.

[18] L. Ceschini, I. Boromei, G. Minak, A. Morri, and F. Tarterini, "Effect of friction stir welding on microstructure, tensile and fatigue properties of the AA7005/10 vol.Technology, vol. 67, pp. 605–615, mar 2007.

[19] R. Bhat, N. Mohan, S. Sharma, and S. Rao, "Influence of Seawater Absorption on the Hardness of Glass Fiber/Polyester Composite," *Journal of Computers, Mechanical and Management*, vol. 1, pp. 1–11, oct 2022.

[20] R. K. Bhushan and D. Sharma, "Investigation of mechanical properties and surface roughness of friction stir welded AA6061-T651," *International Journal of Mechanical and Materials Engineering*, vol. 15, p. 7, dec 2020.

Journal of Computers, Mechanical and Management

Journal homepage: www.jcmm.co.in

Volume 1 Issue 1

Metaheuristics for Multi Criteria Test Case Prioritization for Regression Testing

Deepa Shivakumar*

Department of Information Science and Engineering, RV College of Engineering, Bengaluru, Karnataka, India 560026

Abstract

Regression testing plays a major role in software maintenance. The occurrence of any new fault during the retesting or modification process needs to be analyzed effectively. Regression testing needs enormous effort to produce a higher fault detection rate. Test case prioritization is an efficient way to predict the fault detection rate. Under the constraints of project deliveries, it is too costly to run a large number of test cases frequently. Test case prioritization is needed to rank the test cases. The prioritization must be done to detect the maximum number of faults in the available time. Though many test case prioritization techniques have been proposed, they have not considered the risk of skipping the test cases. The present work proposes a method to solve the test case prioritization or test case subset selection as a multi-criteria optimization problem. A metaheuristics algorithm is proposed in this work combining particle swarm optimization (PSO) with the bat algorithm (BA) is proposed to solve the problem of finding the best subset of regression test cases with multi-objectives of reducing risk in skipping test cases, maximizing the number of faults within the constraints of time. The proposed approach provided a significant increase in Average Percentage of Faults Detected (APFD) and coverage while ensuring lower execution time and resource cost compared to existing works.

Keywords: Software Testing; Regression Testing; Test Case Prioritization; Particle Swarm Optimization; Bat Algorithm

1 Introduction

Software engineering is not just programming and software development but the implementation of engineering procedures for the development of any software systematically. Regression testing is usually a time-consuming and expensive activity. It is typically performed before releasing the product to the customer to ensure that any changes in the code base, such as bug fixing, new requirements, or code restructuring, do not introduce side effects [1]. As software evolves, regression testing needs to be done frequently. Running the entire regression test suite is complex in terms of time and resources, often accounting for 80

Many different techniques have been proposed to address this problem, which can be grouped into four major categories: test case selection, test case reduction, test case prioritization, and test suite augmentation. Methods under the category of test case selection aim to select a subset of test cases that cover the modified or newly added code [3]. Methods in the category of test case reduction attempt to remove redundant or irrelevant test cases from the test suite [4]. Methods in the category of test case prioritization reschedule the execution order of test cases based on certain goals. Methods in the category of test suite augmentation generate new test cases to cover newly added or modified code elements.

Test case managers use any of these methods alone or in combination, but test case prioritization is the most widely adopted method. Test case prioritization aims to find a subset of test cases and their scheduling order in a way that speeds up fault detection. Test case subset selection for prioritization can be based on multiple cues such as structural coverage, fault historical data, error

*Corresponding author: deepaskumar.sse20@rvce.edu.in
Received: 15 September 2022; **Accepted:** 03 October 2022; **Published:** 30 October 2022
© 2022 Journal of Computers, Mechanical and Management.
This is an open access article and is licensed under a Creative Commons Attribution-Non Commercial 4.0 International License.
DOI: 10.57159/gadl.jcmm.1.1.23015.

probability, and similarity between test cases and severity. Most test case prioritization schemes aim to maximize coverage to identify more faults with less effort. However, they often neglect other optimization criteria such as resources and deadline times. Several researchers have conducted various works in this selected area of research.

For example, Rothermel et al. [5] analyzed several techniques to prioritize test cases based on total coverage of code components, code components not earlier covered, and the ability to reveal faults in code components. The authors measured the fault detection rate among these three techniques and compared them to randomly and optimally ordered test suites. Harrold and Orso [6] analyzed the problems in the selection and prioritization of test cases and identified the issues in prioritization. They provided guidelines for designing test case prioritization.

Tonella et al. [7] applied a machine learning (ML) algorithm called case-based ranking to prioritize test cases. They collected and evaluated user inputs across multiple cases using multiple prioritized indexes to iteratively order the test cases. User input played a key role in prioritizing the test cases in this work. Jiang et al. [8] proposed an adaptive random testing strategy based on maximizing coverage and increasing the likelihood of detecting faults. This method demonstrated lower execution time compared to other coverage-based schemes. Zhang et al. [9] proposed a test case prioritization technique based on the unified modeling language (UML) design model coverage, deviating from existing works on code coverage. They estimated error probability and severity for the classes and prioritized test cases based on the selected metrics. However, this method only considered dependencies at a near level and did not consider far-off dependencies.

Li et al. [10] evaluated the effectiveness of greedy, evolutionary, and metaheuristic algorithms for test case prioritization. The effectiveness of the algorithms was measured in terms of code coverage metrics, without considering other critical parameters such as fault detection probability and resource cost. Zhang et al. [11] proposed adaptive random test case prioritization techniques based on maximizing code coverage. The proposed techniques were effective compared to random testing. However, the approach considered code coverage as the only parameter in evaluating the effectiveness of random test case prioritization techniques. Zhang et al. [12] proposed an adaptive random sequence-based black box test case prioritization technique. This technique evaluated group test cases against category partition-based distance measures and performed well compared to random prioritization. The prioritization aimed to maximize coverage.

Eghbali et al. [13] improved the performance of coverage-based prioritization techniques using the lexicographic ordering strategy. They proposed a new heuristic to break ties in the selection of test cases, which improved coverage but did not consider other parameters such as fault detection probability and resource cost minimization. Chen et al. [14] used a genetic algorithm to reorder the test case prioritization technique to increase the number of faults detected. The method considered block-level coverage instead of method-level coverage. They experimented with 0/1 knapsack solvers for test suite reordering to maximize coverage. The algorithms were evaluated in terms of space/time costs and test case coverage, but they demonstrated lower fault detection probability.

Zhang [15] proposed a time-aware test case prioritization technique applying integer linear programming. The technique aimed to maximize coverage, but the fault detection probability was still lower due to function-level coverage. Chen et al. [14] proposed an adaptive random sequence-based prioritization based on clustering. They clustered the test cases based on several objectives and methods invocation sequence using K-means and K-medoids clustering algorithms. By clustering, the test suite was formed with diverse test cases, designed to maximize coverage. Wang et al. [16] proposed a test case prioritization technique based on a fixed-size candidate set adaptive random testing algorithm to increase fault detection probabilities. They proposed a greedy prioritization technique with reduced randomness and increased fault detection effectiveness.

Debroy et al. [17] estimated test case size based on failure rate and constructed a predictive model with the failure rate of different parts of the code and the number of test cases needed to test it. However, the suitability of this model for large-size software is untested. Palma et al. [18] used a logistic regression model to predict the priority of test cases. They found a correlation between the coverage of methods and the priority of test cases. However, resource cost was not considered a factor in test case prioritization.

Overall, various test case prioritization techniques have been proposed to improve regression testing efficiency and effectiveness. However, there is still room for improvement in considering multiple optimization criteria such as fault detection probability, resource cost, and deadline times in the prioritization process.

From the survey summary (Table **??**), most test case prioritization techniques are observed to be focused only on maximizing the coverage in terms of code function and block level. As a result, test case fault prediction probability would be relatively lower. In addition, most approaches considered few parameters like coverage and failure detection and did not consider parameters like deadline and resource cost. Thus, the present work attempts to solve this problem and fill the research gap.

The present work views test case prioritization as a multi-criteria optimization problem and proposes a metaheuristics solution based on combining particle swarm optimization with the bat algorithm. Metaheuristics are approximation methods that tackle difficult optimization problems by proffering good solutions within practical computational time in place of a guaranteed best solution [19]. The majority of metaheuristics are based on biological evolution principles. In particular, they are concerned with simulating various biological metaphors that differ in the nature of the representation schemes [20]. There are three main paradigms: evolutionary, swarm, and immune systems. Evolutionary algorithms (EAs) simulate the biological progression of evolution at the cellular level employing selection, crossover, mutation, and reproduction operators to generate increasingly better candidate solutions (chromosomes). For evolutionary computation, there are four historical paradigms: evolutionary programming, evolutionary strategies, genetic algorithms, and genetic programming [21]. Swarm intelligence (SI) mimics the collective behavior of agents in a community, such as birds and insects. SI mainly depends on the decentralization principle, i.e., the candidate solutions are updated through

local interaction with each other and their environment [22]. The most popular SI algorithms are particle swarm optimization (PSO) and ant colony optimization (ACO) [23]. PSO is a more referred metaheuristics algorithm due to its simplicity and flexibility. In many works, it is observed that Metaheuristics algorithms get into local minima problems. Metaheuristics combining two different optimization algorithms are used to solve the local minima problem in a single optimization algorithm. The initial solution to the problem is found using PSO, and this initial solution is further refined by the bat algorithm to provide the final solution. The test case subset is selected based on multiple criteria of coverage, minimizing redundant and irrelevant test cases, reducing the time difference between test execution time and deadline, and maximizing the fault prediction probability.

The novel contributions of this work are:

1. Modeling the test case prioritization as a multi-criteria optimization problem and proposing a metaheuristics solution to the optimization problem, and
2. Providing a novel object-oriented coverage analysis with a higher probability of fault detection.

Table 1: Previous similar studies

Author	**Review**
Rothermel et al. [5]	Considered only rate of fault detection as the parameter for test case prioritization
Tonella et al. [7]	User guide ranking based on coverage information. Prioritization based only on coverage
Jiang et al. [8]	Considered maximizing coverage and increasing fault detection ability
Zhang et al. [9]	Based only on code coverage maximization
Li et al. [10]	Considered maximizing code coverage as the only test case prioritization criteria
Zhang et al. [11]	Adaptive random testing to maximize the coverage
Zhang et al. [12]	Grouping test cases based on coverage and selecting test cases to maximize the coverage
Eghbali et al. [13]	Considered maximizing code coverage as the only test case prioritization criteria
Chen et al. [14]	Applied clustering to select test cases to maximize the coverage
Wang et al. [16]	Applied adaptive random testing to maximize fault detection probability
Debroy et al. [17]	Considered only coverage and fault detection probability in test case selection
Palma et al. [18]	Considered only fault detection probability in test case selection

2 Method

This study employs a metaheuristic test case prioritizing strategy. The proposed metaheuristic test case prioritization views the problem of test case subset selection as a multi-criteria optimization problem. The test cases must be selected from the regression test suite in such a way as to maximally cover the impact due to code changes, maximize the fault detection probability, minimize the deviation to a deadline, and minimize the deviation to the budget allocated.

Let us assume that the regression test suite R has n test cases $\{t_1, t_2, t_3, \ldots, t_n\}$, and the objective of the proposed solution is to select any m test cases such that the code change impact (CCI) is covered maximally by the m test cases. The fault detection probability (FP) must be higher with the subset of m test cases. The timeline to execute m test cases must be less than the deadline d. Mathematically, the said condition is represented by Eq. [1], where E represents the test case execution time:

$$\sum_{i=1}^{m} E(t_i) < d \tag{1}$$

Moreover, the total cost of executing m test cases must be less than or equal to the test budget B. Mathematically, the condition is represented by Eq. [2], where C is the resource cost of execution of the test case:

$$\sum_{i=1}^{m} C(t_i) \leq B \tag{2}$$

CCI is measured in terms of impact within the class (CCIw) and across class (CCIa) and determined using Eq. [3]. The impact within the class is determined by Eq. [4], where b_i is the number of lines that are impacted in each of the functions, which are called by the function where code changes are made:

$$CCI = CCI_w + CCI_a \tag{3}$$

$$CCI_w = \alpha \sum_{i=0}^{\infty} \beta^i b_i \tag{4}$$

The value for α and β is set as 1 and 0.90, respectively, as per the observations made in [14]. CCIa is calculated similarly for all the classes related to the class where the change is made. FP is measured as the cyclomatic complexity of the code section where the changes are made. A control flow graph is constructed based on the code, as depicted in Figure 1.

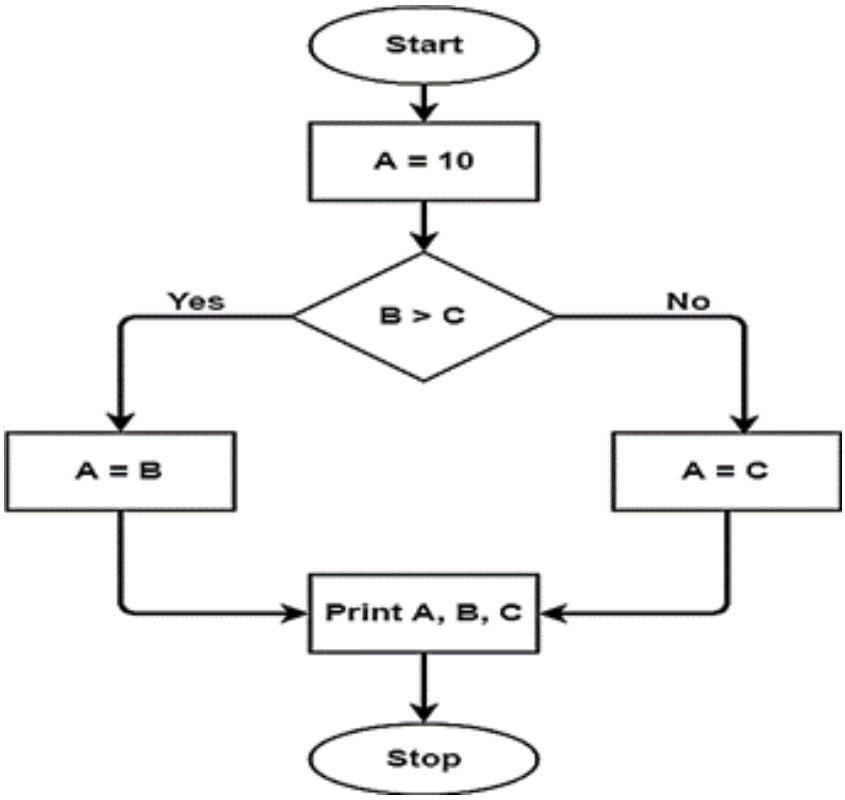

Figure 1: Control flow graph representing the code section

From the control flow, FP is calculated using Eq. [5], where E is the number of edges in the control flow, N is the number of nodes in the control flow, and P is the number of connected components. The time for execution of the test case and the resource cost for the execution of the test case is found based on the historical average of observations over past runs. For each of the n test cases, the values of (CCI, FP, $E(t_i)$, $C(t_i)$) are calculated. After calculation, the best subset of m test cases is found using metaheuristics combining PSO and BA. The metaheuristic approach adopted in this work to solve the local minima problem is using a single optimization algorithm.

$$FP = E - N + 2P \tag{5}$$

PSO is a swarm intelligence algorithm simulating the social behavior of a swarm of organisms. This method is popular for solving optimization problems due to its simplicity, flexibility, and versatility. It is believed that organisms tend to move randomly with different velocities and use them to update their position. Each candidate solution is termed a particle. Each particle tries to attain its best velocity based on its local best (p_{best}) value and its neighbor's global best (g_{best}). Each particle's next position depends on the current position, current velocity, distance from the current position to p_{best}, and distance from the current position to g_{best}. The movement of the particle in its search space depends on its velocity. For a particle X, its current position $X_i(t+1)$ and current velocity $V_i(t+1)$ are updated as shown by Eq. [6] and Eq. [7], respectively:

$$X_i(t+1) = X_i(t) + V_i(t+1) \tag{6}$$

$$V_i(t+1) = wV_i(t) + c_1 r_1(p^i_{\text{best}}(t) - X_i(t)) + c_2 r_2(g^i_{\text{best}}(t) - X_i(t)) \tag{7}$$

In Eq. 6 and Eq. 7, t is the iterative value, c_1 and c_2 are acceleration coefficients, r_1 and r_2 are random numbers, and w is the inertia weight. The iteration is repeated until the termination condition is met. BA is a bio-inspired search optimization algorithm based on the bio-sonar characteristics of bats. Bats use a type of sonar called echolocation to detect prey. They fly from a position X_i with a random velocity V_i with frequency f and loudness A_0 in search of prey. They adjust the wavelength of their emitted pulses and pulse emission rate depending on their proximity to their prey. A bat's location, velocity, and pulse frequency are updated over successive iterations t. Mathematically, all three discussed parameters can be determined using Eq. 8, Eq. [9], and Eq. [10]:

$$f_i = f_{\text{min}} + (f_{\text{max}} - f_{\text{min}})\beta \tag{8}$$

$$FV_i^t = FV_i^{t-1} + (FX_i^{t-1} - Fx_*)f_i \tag{9}$$

$$x_i^t = X_i^{t-1} + V_i^t \tag{10}$$

This work uses PSO to find the initial solution and BA to refine the obtained solution. PSO starts k particles. Each particle is a random group of m test cases. For each particle, the fitness function F is calculated using Eq. [11], where abs is the absolute value:

$$F = \sum_{i=1}^{m} CCI_i + \sum_{i=1}^{m} FP_i + \frac{1}{1 + |d - \sum_{i=1}^{m} E(t_i)|} + \frac{1}{1 + |B - \sum_{i=1}^{m} C(t_i)|} \tag{11}$$

The particle with the best value of F is taken as the best particle (p_{best}) in all rounds, and new particles (k) are created with p_{best} as the seed. The iteration is repeated either until the maximum iteration is configured or until there is no further movement in particles. The best solution (m test cases) found by PSO is input to the BA. The BA starts with m test cases found by PSO and does a bat search by selectively replacing one or more test cases in m and assigning them to it. The fitness function is evaluated for the bats. BA is stopped when there is no further change in the fitness value of the bat. At the end of bat convergence, an optimal solution of m test cases with the highest value of F is obtained. The overall algorithmic flow of the proposed solution is given in Figure 2.

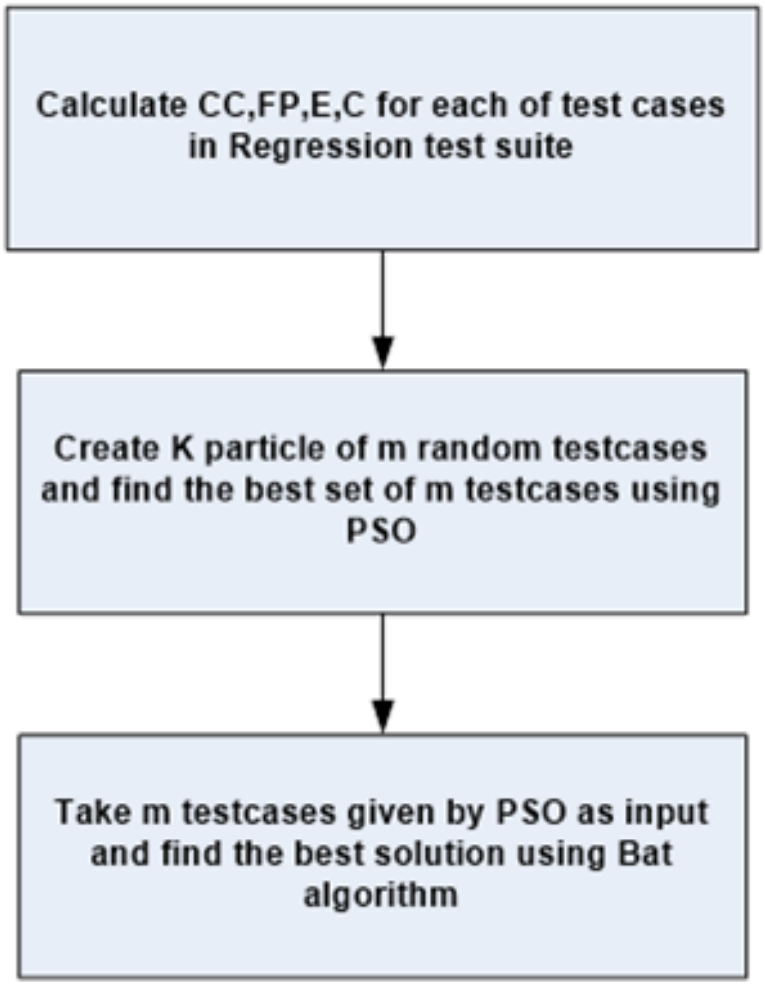

Figure 2: Overall algorithmic flow of the proposed solution

3 Results and Discussion

The performance of the proposed solution is evaluated against a dataset of four medium-sized programs: Flex, Grep, gzip, and Sed. The performance is measured regarding the average percentage of faults detected (APFD), whose value ranges from 0 to 1. The higher the value of APFD, the higher the faults are detected by the test suite. In addition to APFD, the performance is also measured in terms of coverage lines, execution time, and resource budget. The performance of the proposed solution is compared against the fixed-size-candidate-set adaptive random testing (FSCS-ART) technique proposed by Eghbali and Tahvildari [13] and the adaptive random sequence (ARS) approach proposed by Palma et al. [18]. The APFD is measured for all four medium-sized programs, and the result for the same is shown in Table 2 and Figure 3. The average APFD in the proposed solution is 3.45% higher compared to [13] and 7.14% higher compared to [18]. APFD has increased in the proposed solution due to increased coverage and measuring the cyclomatic complexity of each covered class. While works [18] and [13] made fault estimation only based on lines of code, the proposed solution estimated it in terms of the complexity of the code covered. More complex is the code; there are more chances of fault. This was exploited well in the proposed solution, and as a result, APFD increased.

Table 2: Comparison of APFD%

Programs	Proposed	FSCS-ART [13]	ARS [18]
Flex	0.900	0.880	0.840
Grep	0.890	0.860	0.830
gzip	0.912	0.890	0.840
Sed	0.900	0.880	0.850
Average	0.900	0.870	0.840

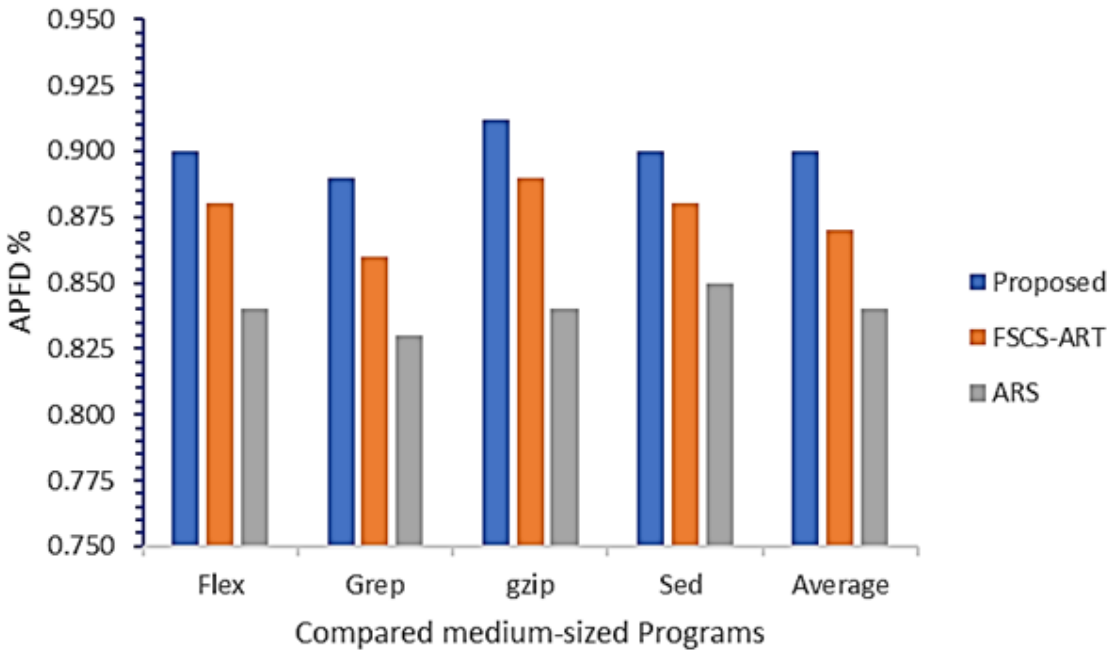

Figure 3: Comparison of average APFD

The coverage line was measured in terms of the percentage of total lines covered by the optimal test cases, and the result is given in Table 3 and Figure 4. The coverage percentage is marginally higher in the proposed solution. It is, on average, 19% higher than results obtained by Eghbali et al. [13] and 25% higher than that of Palma et al. [18]. The increased coverage in the proposed solution is due to the maximization of coverage as an important parameter in multi-objective optimization and coverage based on impact within and across classes or functions.

Table 3: Comparison of coverage%

Programs	Proposed	FSCS-ART [13]	ARS [18]
Flex	2.9	2.11	1.94
Grep	2.7	2.16	1.97
gzip	2.6	2.2	2.0
Sed	2.5	2.1	2.04
Average	2.67	2.14	1.98

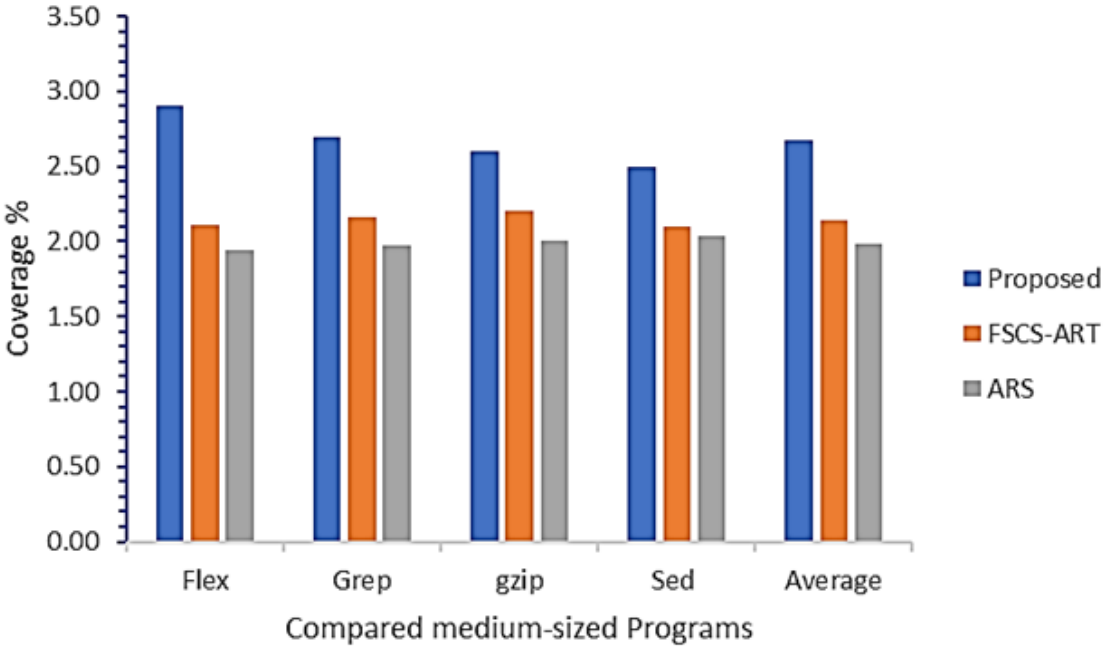

Figure 4: Comparison of average coverage percentage

The execution time of test cases was measured, and the result is given in Table 4 and Figure 5. The average execution time in the proposed solution is 23.81% lower compared to Eghbali et al. [13] and 42.86% lower compared to Palma et al. work [18]. The execution time has been reduced in the proposed solution due to considering reducing variance to the deadline as an important optimization parameter, but both works[13] and [18] did not consider time optimization.

Table 4: Comparison of execution time in minutes

Programs	**Proposed**	**FSCS-ART [13]]**	**ARS [18]**
Flex	10.0	12.0	14.0
Grep	9.0	13.0	15.0
gzip	11.0	13.0	15.0
Sed	12.0	14.0	16.0
Average	10.5	13.0	15.0

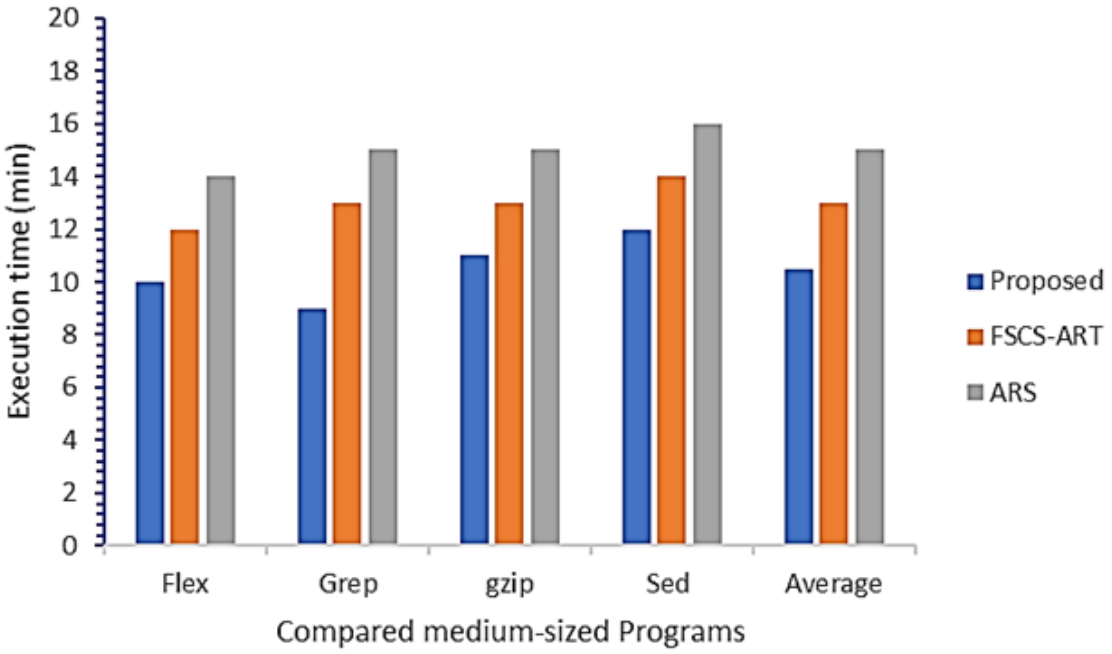

Figure 5: Comparison of average execution time.

The total resource cost for the execution of test cases is measured, and the result is given in Table 5 and Figure 6. The average resource cost in the proposed solution has been reduced by 12.73% compared to [13] and 81.81% compared to [18]. Resource cost minimization was one of the goals in the proposed solution and was considered a parameter in multi-objective optimization. Solution [13] tried to reduce resources heuristically, but it was ineffective for the multi-objective optimization used in the proposed solution.

Table 5: Comparison of resource cost

Programs	**Proposed**	**FSCS-ART [13]**	**ARS [18]**
Flex	1.61	1.72	1.96
Grep	2.10	2.22	4.06
gzip	0.96	1.34	1.52
Sed	1.95	2.16	4.46
Average	1.65	1.86	3.00

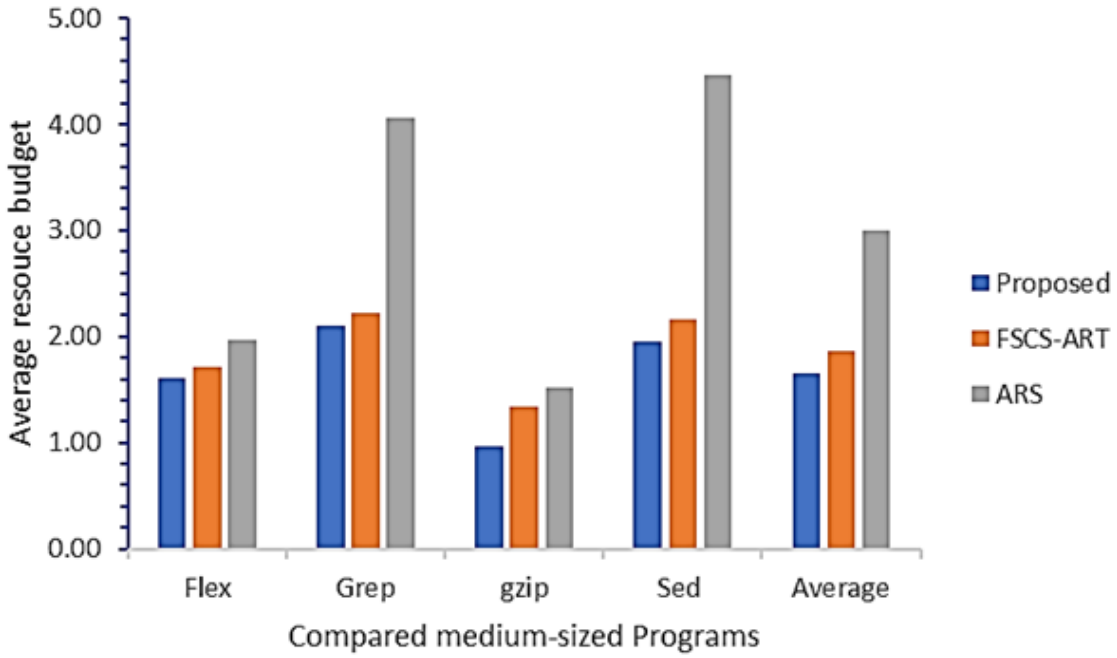

Figure 6: Comparison of average resource cost

Commercial software has more than a million lines of code (LOC), and test cases needed for checking the defects or failures are also huge. Regression testing the entire software for a small patch is resource-intensive, but the leakage of defects is also not desirable. Thus, effective test case prioritization techniques have been researched, and many works have been proposed.

Chen et al. [14] clustered the test cases based on their code coverage information and selected random test cases. Wang et al. [16] grouped the test cases using pairwise distance measurements and selected random test cases. Both methods addressed coverage and fault detection probability in test suite reduction, but they did not consider the execution time and resource cost minimization. The proposed solution viewed test case prioritization as an optimization problem based on multiple coverage factors, fault detection probability, resource cost, and execution. The coverage, resource cost, fault detection probability, and execution time in the proposed solution are far better than Chen et al. [14] and Wang et al. [16].

4 Conclusion

This work proposed a metaheuristics test case prioritization technique for regression testing. The proposed solution selected test cases based on multiple objectives of maximizing the coverage, maximizing the fault detection probability, minimizing the execution time to meet the deadline and minimizing the resource cost to meet the test budget. Through performance, the proposed solution provided a significant increase in APFD and coverage, while ensured lower execution time and resource cost compared to existing works. Evaluating the performance of the proposed solution against large-size software systems is within the scope of future work.

Declaration of Competing Interests

The author declares that she has no known competing financial interests or personal relationships that could have appeared to influence the work reported in this paper.

Funding Declaration

This research did not receive any grants from governmental, private, or nonprofit funding bodies.

Author Contribution

Deepa Shivakumar: Conceptualization, Methodology, Data curation, Investigation, Software, Validation; Writing–Original draft preparation, Writing- Reviewing and Editing.

References

[1] T. K. Akila and M. Arunachalam, Test case prioritization using modified genetic algorithm and ant colony optimization for regression testing, "International Journal of Advanced Technology and Engineering Exploration," 9 (88), pp. 384–400, 2022.

[2] U. Dash and A. A. Acharya, A systematic review of test case prioritization approaches, 2022, pp. 653–666.

[3] Z. C. Demir and Ş. Emrah Amrahov, Dominating set-based test prioritization algorithms for regression testing, "Soft Computing," 26 (17), pp. 8203–8220, 2022.

[4] M. Qasim, A. Bibi, S. J. Hussain, N. Z. Jhanjhi, M. Humayun, N. U.Sama, Test case prioritization techniques in software regression testing: An overview, "International Journal of Advanced and Applied Sciences," 8 (5), pp. 107–121, 2021.

[5] G. Rothermel and M. J. Harrold, A safe, efficient regression test selection technique, "ACM Transactions on Software Engineering and Methodology," 6 (2), pp. 173–210, 1997.

[6] M. J. Harrold and A. Orso, Retesting software during development and maintenance, "Proceedings of the 2008 Frontiers of Software Maintenance, FoSM 2008," pp. 99–108, 2008.

[7] P. Tonella, P. Avesani, and A. Susi, Using the case-based ranking methodology for test case prioritization, "IEEE International Conference on Software Maintenance, ICSM," pp. 123–132, 2006.

[8] B. Jiang, Z. Zhang, W. K. Chan, and T. H. Tse, Adaptive random test case prioritization, in 2009 IEEE/ACM International Conference on Automated Software Engineering, 2009, pp. 233–244.

[9] T. Zhang, X. Wang, D. Wei, and J. Fang, Test case prioritization technique based on error probability and severity of uml models, "International Journal of Software Engineering and Knowledge Engineering," 28 (06), pp. 831–844, 2018.

[10] Z. Li, M. Harman, and R. M. Hierons, Search algorithms for regression test case prioritization, "IEEE Transactions on Software Engineering," 33 (4), pp. 225–237, 2007.

[11] X. Zhang, T. Y. Chen, and H. Liu, An application of adaptive random sequence in test case prioritization, in Proceedings of the International Conference on Software Engineering and Knowledge Engineering, SEKE, 2014, pp. 126–131.

[12] X. Zhang, X. Xie, and T. Y. Chen, Test case prioritization using adaptive random sequence with category-partition-based distance, in 2016 IEEE International Conference on Software Quality, Reliability and Security (QRS), 2016, pp. 374–385.

[13] S. Eghbali and L. Tahvildari, Test case prioritization using lexicographical ordering, "IEEE Transactions on Software Engineering," 42 (12), pp. 1178–1195, 2016.

[14] J. Chen et al., Test case prioritization for object-oriented software: An adaptive random sequence approach based on clustering, "Journal of Systems and Software," 135, pp. 107–125, 2018.

[15] L. Zhang, S.-S. S. Hou, C. Guo, T. Xie, and H. Mei, Time-aware test-case prioritization using integer linear programming, "Proceedings of the 18th International Symposium on Software Testing and Analysis - ISSTA '09," pp. 213–223, 2009.

[16] R. Wang, Z. Li, S. Jiang, and C. Tao, Regression test case prioritization based on fixed size candidate set ART algorithm, "International Journal of Software Engineering and Knowledge Engineering," 30 (3), pp. 291–320, 2020.

[17] V. Debroy and W. E. Wong, On the estimation of adequate test set size using fault failure rates, "Journal of Systems and Software," 84 (4), pp. 587–602, 2011.

[18] F. Palma, T. Abdou, A. Bener, J. Maidens, and S. Liu, An improvement to test case failure prediction in the context of test case prioritization, in Proceedings of the 14th International Conference on Predictive Models and Data Analytics in Software Engineering, Oct. 2018, pp. 80–89.

[19] O. I. Oduntan and P. Thulasiraman, Hybrid metaheuristic algorithm for clustering, "Proceedings of the 2018 IEEE Symposium Series on Computational Intelligence, SSCI 2018," pp. 1–9, 2019.

[20] M. Abdel-Basset, L. Abdel-Fatah, and A. K. Sangaiah, Metaheuristic algorithms: a comprehensive review, in Computational Intelligence for Multimedia Big Data on the Cloud with Engineering Applications, Elsevier, 2018, pp. 185–231.

[21] P. A. Vikhar, Evolutionary algorithms: A critical review and its future prospects, in 2016 International Conference on Global Trends in Signal Processing, Information Computing and Communication (ICGTSPICC), Dec. 2016, pp. 261–265.

[22] R. E. Neapolitan and X. Jiang, Swarm intelligence, in artificial intelligence, Chapman and Hall/CRC, 2018, pp. 377–385.

[23] T. Herlambang, D. Rahmalia, and T. Yulianto, Particle swarm optimization (PSO) and ant colony optimization (ACO) for optimizing PID parameters on autonomous underwater vehicle (AUV) control system, "Journal of Physics: Conference Series," 1211 (1), 2019.

Journal of Computers, Mechanical and Management

Journal homepage: www.jcmm.co.in

Volume 1 Issue 1

Impact Analysis of Work Culture and Transformation During COVID-19: A Structural Equation Modeling Approach

Sneh Bhiwaniwala[a], Vishwanath Bansal[*b], Babita Singla[c], Namesh Malarout[d], Sonia Vaz[e], Prithvi Hegde[f], Nisha S Tatkar[†g], and Anshika Sharma[h]

[a]Department of Mechanical and Industrial Engineering, Manipal Institute of Technology, Manipal Academy of Higher Education, Manipal, Karnataka, India 576104

[b]Department of Mechatronics Engineering, Manipal Institute of Technology, Manipal Academy of Higher Education, Manipal, Karnataka, India 576104

[c]Chitkara Business School, Chitkara University, Chandigarh, Punjab, India 140401

[d]Materials, Yanfeng Automotive Interiors, Mississauga, Canada L5R 4J6

[e]Department of Economics, Rosary College of Commerce and Arts, Navelim, Goa, India 403707

[f]Jagdish Sheth School of Management, Electronic City, Bengaluru, Karnataka, India 560100

[g]Department of Postgraduate Diploma in Management, Institute of PGDM, Mumbai Education Trust, Mumbai, Maharashtra, India 400050

[h]Department of Psychology, Amity University, Noida, Uttar Pradesh, India 201313

Abstract

Staff members use tried-and-true procedures when completing workplace visits, delivering services, and completing client tasks. However, the COVID-19 pandemic compelled employers to change the work styles of individual employees to ensure good communication, work-life balance, and flexibility for employees while maintaining optimal work productivity levels. In addition, the World Health Organization established social separation guidelines to combat COVID-19. Thus, the pandemic challenged the work culture and resulted in employees being quarantined in their homes. As a result of this transformation, employees were encouraged to use digital tools to facilitate work-from-home opportunities. The current study analyzes employees' psychological and productive effects of work-from-home culture. It also looks for coworker bonding threatened by this transformation and suggests a way to keep it intact. Through a thorough literature review, the authors developed a comprehensive model to assess the pandemic's impact on employees' lifestyles. The conceptual model was empirically tested by applying the model to data collected from 233 employees from various backgrounds. The model result was validated using Partial Least Squares Methods-Structural Equation Modeling. The inferences highlight the factors influencing employee morale and work culture and the parameters closely related to employee functioning in the organization that should not be affected.

Keywords: COVID 19; Employees; Organization; Work Culture; Pandemic

1 Introduction

Notably, COVID-19, as a significant threat to all organizations worldwide, has caused a change in the working environment of these organizations and the communication between employees. The pandemic outbreak compelled the government to implement preventive and controllable measures, such as guidelines for staying at home [1].

*Corresponding author: vishwanath.bansal@learner.manipal.edu

†Corresponding author: nishat_pgdm@met.edu

Received: 14 September 2022; **Accepted:** 31 October 2022; **Published:** 31 October 2022

© 2022 Journal of Computers, Mechanical and Management.

This is an open access article and is licensed under a Creative Commons Attribution-Non Commercial 4.0 International License.

DOI: 10.57159/gadl.jcmm.1.1.23020.

Online communication technologies have thrived to a large extent during this pandemic. Most studies have suggested that COVID-19 could pave the way for a teleworking revolution [2, 3]. Over the last decade, scientists have used work-from-home as a topic of debate and a regional study trend. As a result, work-from-home (WFH) has emerged as the new hot topic. This pandemic is unique in many ways, as the sudden shift to work-from-home and its viability was not anticipated. The pandemic compelled several organizations to turn telework into a requirement. Thus, the effects of teleworking's rapid and widespread adoption on workplace health following the COVID-19 pandemic have been assessed and discussed. Corporations were the essential players throughout pandemic management and played a part in mitigating the unforeseen safety effects of disease prevention initiatives. The effects of flexibility, work-life balance, lack of trust, etc., on the employee's teleworking efficiency, has been studied to increase work productivity in organizations. Thus the study would undoubtedly help develop the WFH model [4]. It is known that the implementation of the WFH strategy has both advantages and disadvantages, highlighted as follows:

1.1 Benefits of Telework

Several scientific studies and research conducted have cited the advantages of teleworking, and most of them contribute to practical advantages [5–7].

1. Work-life balance - Employees working from home save the strategic time they probably have spent commuting to their workplace with their family or babies.
2. Flexibility - The flexible working hours allowed employees to critically utilize and manage the work as per their comfort [6]. Moreover, it offers the versatility to telework with more than one company or works even though it is impossible to get to the workplace due to illness, remote home areas or care duties.
3. Commuting time reduced - Reducing commuting can have a beneficial impact on costs, time, and tension. This could be the primary factor why staff opted for telework.
4. Reduced work overheads - Organizations targeted the reductions by removing the need for costly workplace facilities and overheads like heating, power, etc. The new telework trial at the British Broadcasting Corporation (BBC) reduced costs by about 25% [8].
5. Expanded skills available for the employer - Teleworking companies have taken advantage of the labor market with skilled employees who are not generally willing to work full-time in a traditional workplace setting, such as people with disabilities or childcare duties.
6. A rise in productivity - Popular literature [7] shows high productivity in teleworkers than other employees, and this high level of performance is attributed to fewer interruptions, long working hours, and flexibility in scheduling work schedules. It should be noted that reports for increased telework productivity are typically derived from self-reporting results, with a few notable exceptions [9].

1.2 Problems with telework

Telework has become the solution for working with social distancing norms due to the COVID-19 pandemic. But with every new thing, there exist pros and cons. The various problems concerning teleworking include:

1. Social seclusion is the most commonly noted prime delinquent in teleworking; a study conducted in the United Kingdom (UK) in 1983 revealed that 60% of teleworkers referred to it as the most significant drawback [10]. It has been linked to an increased risk of heart disease, stroke, and even death, according to the Centers for Disease Control and Prevention (CDC).
2. Presentism – It is not just about working long hours but also about working while sick. According to publicly available statistics, teleworkers are less likely to be absent from work when they can. In contrast, they return to work while recovering from illness instead of taking a full day off [11]. Moreover, a further disadvantage for teleworkers is that their illness remains a secret. Some employees even continue to work while they are sick to ease their managers' worries about telework. People who work while ill are likely to suffer the consequences due to their level of employment [12].
3. Lack of support - Teleworkers place a high value on technological support, and providing the required technical support in a controlled office environment is difficult. Thus, a mobile teleworker's lack of technical support is more devastating [13].
4. Career progression - Job marginalization is a problem for home-based employees because "visibility and workplace communication networks are the main factors in employment opportunities" [14]. Since teleworkers are "out of the movement" of political events, such as the delivery, evaluation, reward, and promotion of services provided by organizations, the teleworkers inevitably become "politically disadvantaged" [6].
5. Blurring of boundaries - A survey found that 60% of their sample staff thought a convenient split between home and work. Even though many teleworkers attempt to establish a physical and temporal border between work and home life, such as by having a workspace exclusively for work, working from home blurs the lines between roles, not just for the teleworker but also for the family [15].

6. Telework and gender - According to Bibby [16], teleworking integrates work and home obligations better than the standard working culture and is practiced worldwide. However, sexuality determines how the work environment affects the employee. Women might be very concerned that working remotely would be a substitute strategy for keeping them out of the workforce when there is an additional complexity that others might assume that women who follow flexible work schedules do not work [6].

2 Related Work and Research Objective

According to the study by Mann et al. [6], teleworkers experience feelings they would not have experienced otherwise while working in the office. The negative feelings they experience while working in the office almost double. The study indicated that teleworkers' mental health problems increased compared to office employees' mental health problems. It also revealed that females have higher rates of mental illness than males. Conferring to work documented by Mustajab et al. [17], workplace flexibility causes massive changes in corporate culture and work performance. Women are especially affected by the new work environment, which requires them to do both office work and homework simultaneously. High workloads resulted in emotional vulnerability between husbands and wives, which triggered disagreement. WFH can be effectively extended to organizations that have excellent work facilities, but it cannot be applied to all areas of work .[18]

Bouziri et al. [19] concluded in their paper that the introduction of wireless and broadband internet aided the growth of home telecommuting since 2000. As of late March 2020, nearly all of us were confined to our homes and thus resulting in millions of employees being exposed to telecommuting. The article by Baert et al. [20] provided insights into how the study of Flemish employees viewed telework as a result of the COVID-19 crisis, in general, and in its broad form. According to most respondents (two-thirds), teleworking will become more popular. Employees with resident children surrounding them, on the other hand, are dissatisfied with the increase in teleworking. Long-term teleworking has a greater positive impact on employees with migration in certain areas. Working mental health is becoming increasingly important in management and workplace research. Academicians, clinicians and policymakers are particularly interested in learning more about how structural changes affect mental health. A few organizations use the findings of existing workplace mental health studies to guide job design. The presented work thus aims to investigate the factors that influence work culture and assist employers in understanding what this pandemic has resulted in and adapting to changes as needed. Thus, this research aims to determine the changes people have experienced from working from home, identify whether time flexibility has led to increased productivity at work and investigate areas such as coworker bonding and work-life balance during WFH.

3 Methods

This study's research philosophy is a positivist paradigm based on empirical observation and measurement. A questionnaire survey method was used to collect data. Structural Equation Modelling (SEM) used the Partial Least Square Technique, and Covariance Based Structural Equation (CB-SEM) modeling was used to test the hypotheses. The hypotheses are developed through previous studies linked to the study's variables. The empirical approach to research was chosen because it can provide quantitative evidence for the existence or absence of statistically significant relationships between the study variables. As the study aims to draw implications of the COVID-19 pandemic on the global working model, testing relationships between research variables becomes inevitable.

3.1 Hypothetical models

The relation between communication and work culture

COVID-19 has become a major challenge to all organizations worldwide, leading to the requirements concerning improvements in the methods of operation and even human contact within the organization [18, 19]. The WFH typically provides benefits, but the employees most widely experience a disruption of contact with peers and managers. Poor correspondence is also caused by technological issues such as network interruption, making it impossible to deliver reports and job-related information and creating a difference from the social contexts they frequently encountered in the workplace just before the COVID-19 outbreak [17]. In jobs, those employees who rely more on others experience more negative effects from prolonged telework. In particular, during this prolonged telework phase, they experience more disagreements with colleagues and family and struggle to balance the multiple means of contact accessible to them. Less satisfaction with prolonged telework is also the situation with employees who are used to receiving much feedback, interacting outside their organization, and experiencing high levels of job autonomy [21, 22]. A study found that using information and communication technology at home harms the quality and uniformity of sleep, resulting in a 'psychological disconnect' from work, but it happens only to those who do not set limits concerning the use of job-related technology at home [23]. Examination and analysis have indicated that the digital workplace mental health interventions can enhance psychological well-being and job performance among employees trying to find solutions to problems [24].

The relation between coworker bonding and work culture

The COVID-19 pandemic has resulted in managers increasing their subordinate's schedule and scope of work, which resulted in managers knowing more about their subordinates concerning values, strengths, motivations and interests [25]. Technology has easily made coworker connections during this pandemic, and employers tend to encourage employees to stay connected while respecting their organization's time and liberty. Limited communication, primarily due to internet issues, has resulted in a decrease in work output. It has disrupted the flow of work and caused psychological differences because employees are used to talking face-to-face and sorting things out rather than communicating via email [17].

The relation between infrastructure and work culture

Employees are experiencing a variety of issues because they do not fully comprehend the concept of WFH. Home is where most employees unwind after a long day at the office [26]. Several home-employed employees lose concentration because they are unsure whether to work or spend time with their families to appreciate the quarantine imposed to prevent COVID-19 from spreading. Many challenges, such as requests to chat via social networks and enjoyment, such as watching movies, karaoke singing, and playing with children, frequently result in lower motivation at work [18, 27]. WFH does not require employees to commute between the office and their homes, significantly reducing non-working time. The employees can spend this extra time either for their office work or household work, particularly in the case of married female employees [17]. Also, many employees feel confident about their jobs with WFH as they do not feel directly supervised by their managers as in the case of the normal workplace. Working under direct supervision sometimes makes employees uncomfortable because they must keep decorum in front of managers. Supervision, however, is no longer a barrier to work concerning WFH, as they are free to work without needing to maintain decorum, as they have to do in the office [20].

The relation between flexibility in timing and work culture

Employees prefer working without the manager's supervision because it gives them the freedom to work when they want [28]. Studies also have shown that the time consumed while commuting to the office is saved, which helps the employees save much productive time and also facilitates in saving much money in terms of transportation costs, which makes the employee more content with their job and thus more productive. The employee's wage is also not affected by the WFH policy as this is a force majeure, and employees can do nothing about it. Previously, there were clear distinctions between work and personal life; however, the pervasiveness of mobile technology devices has blurred these distinctions.

Employment is no longer specified with time and location, as over 64% of adults own a mobile phone. Work is done outside the office and working hours are not typical. A study conducted in 2012 [17] found that employees used mobile phones for holidays (40%), social events (27%), practice (14%), on a date (17%) and even in a toilet (12%).

The relation between work-life balance and work culture

In an attempt to avert the spread of COVID-19, an outbreak of public health that took thousands of lives and caused fears of the worst global crisis since the 'Great Depression,' almost half of the world's population was on lockdown. This has deeply influenced the business world and our mental and physical well-being [29]. Moreover, work-life balance has become one of the most crucial aspects of everyone's life during this economic downturn. During WFH, employees have found a balance between work and social life. Several employees have agreed that they have more leisure time and can spend more quality time with their families without leaving work with the implementation of the WFH policy [17]. In contrast, often, employees have to split the priority between communicating with the family and concentrating on the job to be completed; however, most of them claim that dividing the emphasis does not decrease the quality of time spent with the family during WFH [26]. However, female employees, particularly those with children, face few problems sharing household work with their partners, such as childcare, cooking, and other duties, because husbands cannot perform such duties efficiently and effectively, and household servants who perform the duties are coerced to leave because of quarantine. Moreover, this dual function and mission don't apply to partners who split activities with their partners, rendering the mood at home more harmonious and full of collaboration [18, 27].

The relation between policies of work-from-home, travel and work culture

After the outbreak, the World Health Organization (WHO) recommended that every country impose a lockdown to stop the spread of the virus, but this resulted in organizations having to change their working methodology to WFH [30]. Swift and coordinated policy changes were required to tackle the threat of recession looming over the whole world economy and look after the world's citizens [31]. During the pandemic, maintaining customer relationships and ensuring business continuity were the top priorities for every employer, but they were also considering the impact of the pandemic on their employees and the employee culture. The employees also tried to stay connected to their employers and other employees through technology. The ability of the executive team to adapt, encourage teamwork and provide mental support became of paramount importance. Travel bans resulted in work being slowed down but also resulted in wasting less time commuting to the office and time commuting to the client site [29]. International Labor Organization (ILO) laid out several rules to ensure the safety of the employees and their families, to re-stabilize the economy, and to protect the employees and their incomes [31].

3.2 Conceptual Modeling and Questionnaire Development

Based on the investigated literature a conceptual model was developed to illustrate the relationships between the variables in our study, which is shown in Figure 1

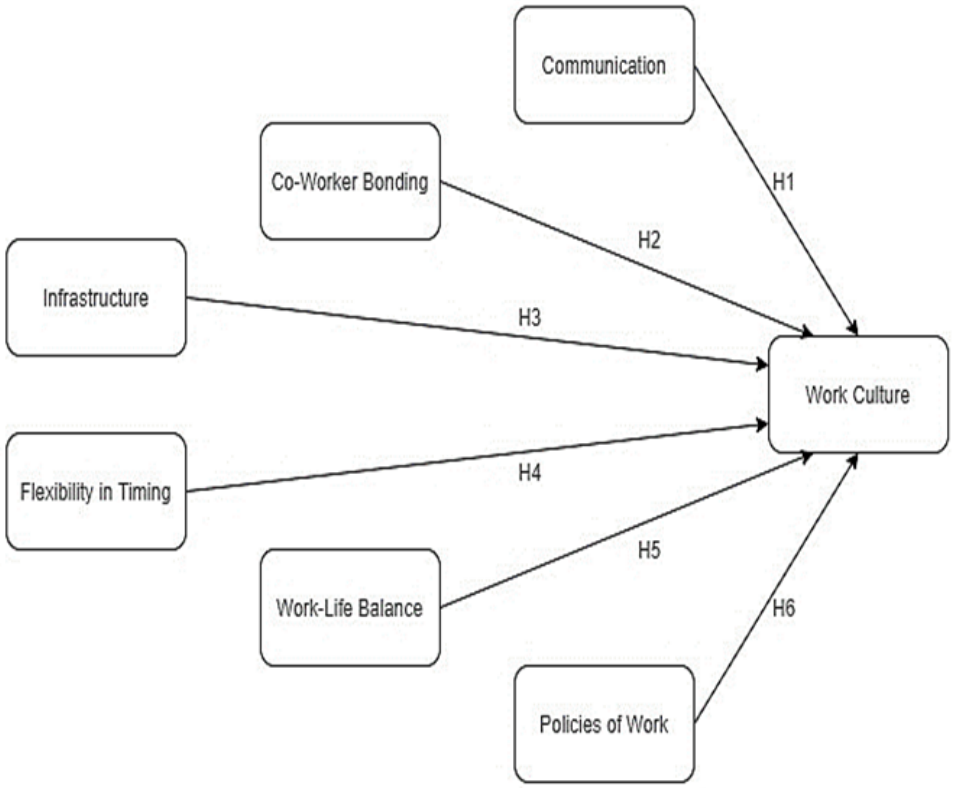

Figure 1: Conceptual model developed in the present study.

The questionnaire was developed based on the standard methodology of skimming through the accessible scales and measurements, collecting expert comments through the specialists in the field, pretesting the questionnaire, and subjecting it to the validation and reliability test through the pilot study [32]. The self-administered questionnaire developed in this research had two sections: the initial segment was designed to elicit the demographic details of the respondents (gender, age, the annual income of the family and zone in which their organization lie), and the second part elicits quantitative information through the Likert 5-point scale (1-Strongly disagree; 5-Strongly agree). The dimension of the study, meaning, contributing authors and the sample item from the questionnaire are shown in Table 1.

Table 1: The questionnaire's dimension, meaning, contributing authors and sample item.

Dimension	Meaning	Contributing articles	Sample item
Communication	Refers to the means of communication between the employees of the organization.	[6, 17, 29**?** , 31, 33]	I feel that telecommunications are hampering my work output.
Coworker Bonding	Refers to how coworkers become a team and how their team spirit is affected.	[6, 17, 29]	I feel that having emotional involvement plays an important role in productivity.
Infrastructure	Refers to the setup on which they work and the environment in which they work.	[17, 26, 29]	I feel an office setup is an aid to my work output.
Flexibility in Timing	Refers to the flexible working hours due to work-from-home.	[6, 17, 26]	I feel shift timings should always be flexible.
Work-Life Balance	Refers to the balance between the employee's work and personal life.	[17, 26, 29, 33]	I feel I have more time to look after myself
The policy of Working from Home and Travel	Refers to the various steps employers take to help improve their work productivity.	[30, 32, 33]	I think traveling for work when I can teleconference is unnecessary.

3.3 Sample design

Samples were drawn from all over India. Convenience sampling was used as the method of sampling owing to the limited resources available and the time constraint. The data was collected electronically through Google Form - questionnaire. The link for the questionnaire was communicated to many people through social sites, and 250 responses were received, out of which 233 were selected, as the rest were erroneous. This questionnaire was used for collecting primary data and information from the sample size of 233. The data thus collected was then analyzed using the structural equation modeling (SEM) package Smart PLS® version 3.0 and CB-SEM.

4 Results and Discussion

4.1 Descriptive statistics

The sample demographic characteristics are shown in Table 2. It can be observed that the number of male responses has been higher than that of female responses. In terms of age, the majority of the responses were from the age of 24 and more, followed by the age group of 21 to 24 years of age. According to the study, most organizations lie in the red zone. In terms of the annual income of the families, the majority were from the middle-class income group, and the least belonged to the elite group.

4.2 Negative impact of WFH

The proliferation of the COVID-19 outbreak affected the business, financial, social, political and cultural facets of every country in a greater scope. All organizations must have a policy and capacity to handle unexpected developments that could not be forecasted. COVID-19 has transformed the organization's attitude and the morale of its employees. WFH has become a trend that has both positive and negative implications for the company [6]. While many employees profit from WFH, they also recognize hazards and losses, such as exhaustion, that tend to decrease labor productivity induced by the syndication of jobs. In this situation, several employees are forced to perform different tasks simultaneously, like domestic and official duties, leading to losing concentration [34]. Using tablets, computers and networking resources also disrupts the quality of work, as one has to work and, along with that, contact supervisors and employees [35]. The job-syndication often induces reduced enthusiasm and efficiency in employees [36].

Table 2: Result of different online queries

Variable	Frequency	Percentage
Total	233.00	100.00
Gender		
Male	153.00	65.70
Female	80.00	34.30
Age		
<18	1.00	0.40
19-21	17.00	7.30
21-24	96.00	41.20
>24	119.00	51.10
Zone in which your organization lies		
Green zone	47.00	20.20
Yellow zone	37.00	15.90
Orange zone	49.00	21.00
Red zone	100.00	42.90
Annual income		
Lower (Less than 50,000)	26.00	11.20
Low (50,000–5,00,000)	51.00	21.80
Middle (5,00,000-25,00,000)	124.00	53.20
Upper Middle (25,00,000-50,00,000)	20.00	8.60
Elite (>50,00,000)	12.00	5.20

4.3 Positive impact of WFH

WFH has seen numerous beneficial impacts on employees who achieve an equilibrium between work-life and social life, leading to increased workplace productivity. An organization with a WFH policy promotes the work-life arrangement of its staff [37]. WFH's effect often offers flexibility for employees to function in a manner that allows them to be more comfortable with when and where they function, thereby creating workplace security to improve employee satisfaction [38]. WFH gives employees more time to interact with their families by saving time by not commuting to the office. It is special since they will operate in the home, clearly not juggling time for job and families, but this is not entirely applicable to male employees and appears to be experienced by married women employees [39], while most men employees feel responsible for spending time with their families [40], they do so at the same time to shield them from the impact of COVID-19 spread.

4.4 Impacts of WFH on work productivity

WFH impacts productivity at work [6]. WFH has improved the working style of most companies and the morale of its employees throughout the spread of COVID-19. When pointing at each positive and negative impact, one always looks at the effectiveness of the employee's job when performing from home. The finding of the previous studies was very surprising as the work output of employees working from home declined because of the absence of support facilities for work such as computers, internet networks, and some other disruptions like feeling overwhelmed by the same environment for a relatively long time with social restrictions imposed due to the pandemic. WFH was not the work culture already introduced in many organizations, so many companies and employees could not perform WFH in this situation. Furthermore, several employees experienced certain psychological disruptions, such as the fear of the COVID-19 outbreak, which is the cause for the WFH; thus, they were more involved in seeking out about the current COVID-19 outbreak on television or browsing the internet to know as to what degree the government has resolved the problem. This sometimes took too much time and triggered a lot of delayed jobs. From a gender viewpoint, the lack of distraction experienced by male employees was very less compared to the female employees. This results in male employees having comparatively higher work productivity.

An explanation was the multitasking position that they are put in. In other words, men do not play dual roles in their households, while females have to be on top of the smaller distractions they experience. Even though they sometimes share duties among partners, it is not their primary responsibility. Also, male employees generally convey that if they work from home, their family values it and tries not to disturb them. What has been noted in a previous study is that WFH does not necessarily have an improvement in workplace efficiency, and this is a significant point for further research.

4.5 Measurement model

Table 3 shows the factor loadings of the statements. Factors identified that could influence their decision was analyzed to determine the relationship between the different dimensions of work culture. For this purpose, factor analysis was applied to the responses provided by respondents. Factor analysis was used for data reduction to reduce many variables into a few factors. Further, to examine sample adequacy, Smart PLS was used. Table 4 provides the Smart PLS output. Reliability tests were performed to verify the instrument's accuracy with identical performance using Cronbach's Alpha (α). The composite reliability and α for all the constructs should be greater than 0.7. However, it can be noted that the majority of them have more than 0.7, as provided in the table. Thus, the considered factors prove significant in starting a business enterprise. The average variance extracted (AVE) $>$ 0.5 confirms convergence validity. For all the variables, the AVE of constructs was higher than 0.5. It means more than half of the variances in constructs are explained by their corresponding measures. Therefore, the data set is valid.

4.6 Structural model

The structural model analyzes the correlation between endogenous and exogenous variables. PLS-SEM provides a structural model calculation of the path coefficients for evaluating the importance and validity of the relationship of the structural model, R2, to determine the statistical accurateness of the model and the relevant effect of the exogenous variable on the endogenous variable. The relationship between the influencing factors and the work culture path model was structured to determine the relationship between the influencing factors. The structural model specifies the relations between constructs allowing testing of the study's hypotheses. Figure 2 indicates the path coefficient for the correlation between the user interface measurements. The path model explains how the contingent and independent variables contribute favorably to the path function. Figure 2 shows the value of t-statistics analyzed using bootstrapping in the SmartPLS3 version to test the hypothesis. Table 5 shows the standard deviation error and the value of t statistics to determine the hypothesis's results. Figure 3 shows the value of t-statistics analyzed using bootstrapping in the Smart PLS3 version to test the hypothesis. Table 5 shows the standard deviation error and the value of t-statistics to find out the results regarding the supporting or not supporting the hypothesis. The path coefficient between the variables communication and work culture is -0.0261, which is not significant at 0.01 (t = 0.242 not significant at 0.01). Hence the hypothesis that communication has a significant impact on the work culture has been rejected. The coefficient between coworker bonding and work culture is -0.0517, which is significant at 0.01 (t = 0.574 significant at 0.01). Hence the hypothesis that coworker bonding has a significant impact on the work culture has been accepted. The path coefficient between the variables infrastructure and work culture is -0.0542, which is not significant at 0.01 (t = 0.461 not significant at 0.01). Hence, the hypothesis that infrastructure significantly impacts the work culture has been rejected.

Table 3: Table 3. Factor Loadings.

Questionnaire Components	Communication	Co-worker bonding	Flexibility in timing	Infrastructure	Policies of WFH and travel	Work culture	Work-life balance
COM1	0.7789	0.0000	0.0000	0.0000	0.0000	0.0000	0.0000
COM2	0.8869	0.0000	0.0000	0.0000	0.0000	0.0000	0.0000
COM3	0.4943	0.0000	0.0000	0.0000	0.0000	0.0000	0.0000
COW1	0.0000	0.4265	0.0000	0.0000	0.0000	0.0000	0.0000
COW2	0.0000	0.9978	0.0000	0.0000	0.0000	0.0000	0.000
SHI1	0.0000	0.0000	0.9083	0.0000	0.0000	0.0000	0.0000
SHI2	0.0000	0.0000	0.8315	0.0000	0.0000	0.0000	0.0000
INF2	0.0000	0.0000	0.0000	0.9483	0.0000	0.0000	0.0000
INF1	0.0000	0.0000	0.0000	0.7447	0.0000	0.0000	0.000
POL1	0.0000	0.0000	0.0000	0.0000	0.8134	0.0000	0.0000
POL2	0.0000	0.0000	0.0000	0.0000	0.7504	0.0000	0.0000
POL3	0.0000	0.0000	0.0000	0.0000	0.5776	0.0000	0.000
WC1	0.0000	0.0000	0.0000	0.0000	0.0000	0.7222	0.0000
WC2	0.0000	0.0000	0.0000	0.0000	0.0000	0.7692	0.0000
WC3	0.0000	0.0000	0.0000	0.0000	0.0000	0.6494	0.000
WC4	0.0000	0.0000	0.0000	0.0000	0.0000	0.8475	0.0000
WLB1	0.0000	0.0000	0.0000	0.0000	0.0000	0.0000	0.7272
WLB2	0.0000	0.0000	0.0000	0.0000	0.0000	0.000	0.6331
WLB3	0.0000	0.0000	0.0000	0.0000	0.0000	0.0000	0.9028

Table 4: Quality Criterion and Composite Model.

Factors	AVE	Composite Reliability	Cronbach's Alpha	Communality
Communication	0.5459	0.7740	0.6163	0.5459
Coworker bonding	0.5888	0.7115	0.5359	0.5888
Flexibility in timing	0.7582	0.8622	0.6867	0.7582
Infrastructure	0.7270	0.8400	0.6618	0.7270
Policies of work-from-home	0.5194	0.7608	0.5370	0.5194
Work culture	0.5633	0.8364	0.7413	0.5633
Work-life balance	0.5816	0.8032	0.6464	0.5816

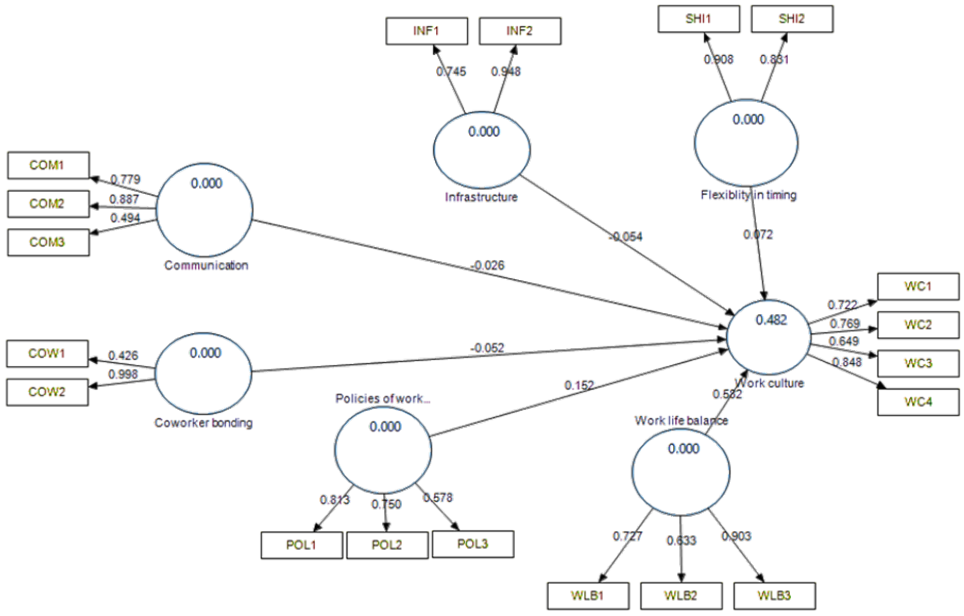

Figure 2: Path Model.

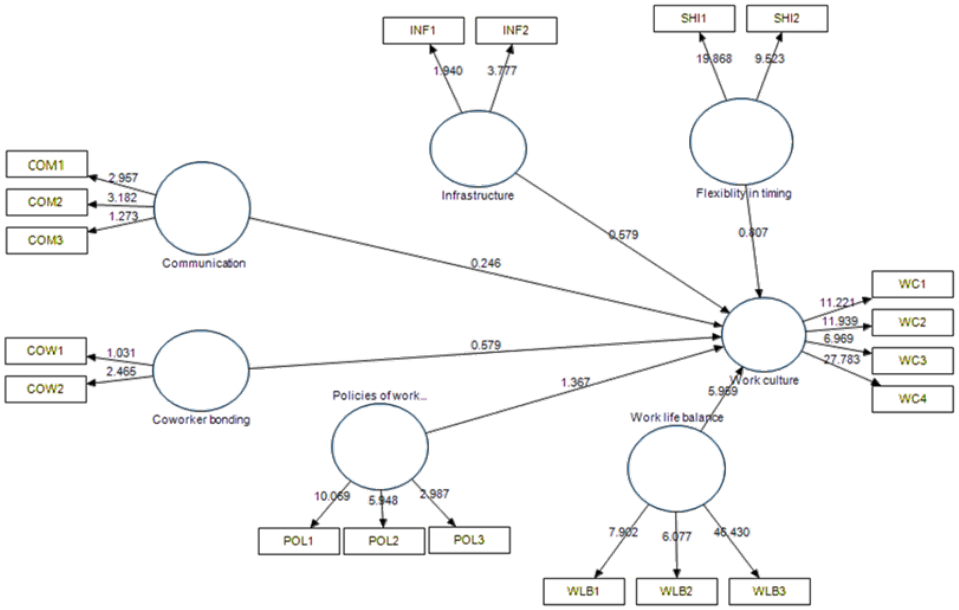

Figure 3: t-statistics model.

The path coefficient between the variable's flexibility in timings and work culture is 0.0723, which is not significant at 0.01 level (t = 0.727 not significant at 0.01 level). Hence, the hypothesis that flexibility in timings does not significantly impact the work culture has been rejected. The path coefficient between the variables work-life balance and work culture is 0.5822, which is significant at 0.01 level (t = 6.6003 is significant at 0.01 level). Hence the hypothesis that work-life balance has a significant impact on the work culture has not been accepted.

Table 5: Hypothesis testing.

H	Variables	Original Sample	Sample Mean	Standard Deviation	Standard Error	t-Statistics)	P Values	Support
H1	Communication & Work culture	-0.0261	-0.0466	0.1077	0.1077	0.2421	0.439	Not supported
H2	Coworker bonding & Work culture	-0.0517	-0.042	0.0898	0.0898	0.5753	0.004	Supported
H3	Infrastructure & Work culture	-0.0542	-0.0522	0.1173	0.1173	0.461	0.493	Not supported
H4	Flexibility in timing & Work culture	0.0723	0.0787	0.0994	0.0994	0.7273	0.857	Not supported
H5	Work-life balance & Work culture	0.5822	0.5763	0.0882	0.0882	6.6003	0.000	Supported
H6	Policies of work-from-home and travel & Work culture	0.1518	0.1535	0.1115	0.1115	1.3616	0.039	Supported

The path coefficient between work-from-home policies and travel and uncertainty avoidance is -0.0542, which is significant at 0.01 level (t = 1.361 significant at 0.01 level). Hence the hypothesis that policies of work-from-home and travel as a significant impact on the work culture has been accepted. Communication is an important factor influencing work culture, and organizations should pay attention to employers' mental well-being by maintaining regular communication and providing the necessary assistance. But the findings of the present work indicate that communication does not affect the organizational work culture. This finding contradicts many previous studies and research on the subject [17, 18, 21, 22, 24]. As stated in the study, coworker bonding is a deciding factor in determining whether the work culture has been affected by the COVID-19 pandemic. This finding is consistent with previous findings in similar contexts and situations [6, 17, 29]. Chainey [29] describes a company that gives each employee a virtual tour of their home office and then talks about various mementos they have at their homes, thereby creating a personal connection between the employees. Thus, employers should increase coworker bonding among employees by organizing various events or at the very least, some online bonding exercises. According to the findings, infrastructure does not affect organizational work culture. This finding contradicts many other studies on the subject [17, 20, 26, 41]. As a result, employers must understand the benefits of WFH and try to adapt. They should also know how to divide their time between household chores and work. According to the findings, timing flexibility does not affect organizational work culture. This finding contradicts the findings of several other studies for similar purposes [6, 17, 26]. Thus, employers should determine the optimal amount of flexibility to provide employees while WFH or even when working from the organization's office complexes. The study analysis supports the hypothesis that Work-Life Balance is a

deciding factor in determining whether or not the COVID-19 pandemic has affected work culture. This finding is consistent with many previous findings in a similar context and situation [17, 18, 26]. They concluded that employees who work-from-home could balance their personal and professional lives. They can also spend more time with their families without worrying about work. The study analysis supports the hypothesis that policies adopted by companies for WFH have a relationship with the organization's work culture. This result is consistent with previous studies in similar situations. [31, 33]. Employers should carefully consider their policies regarding working from home and travel for business as this will impact the company's overall productivity.

5 Conclusion

This study provides enlightening information on how employees have utilized telework during the COVID-19 pandemic and under typical working conditions. In addition, it highlights how employees' perspectives on teleworking and digital conferencing have shifted over time. The management and effectiveness of business operations have been significantly improved thanks to WFH. WFH can still be used by organizations even if their members do not require direct contact. It is impossible to use WFH for direct contact services such as those provided by health professionals, manufacturers, and transportation companies. According to the findings of the analysis, WFH is beneficial for female employees who need to multitask to maintain their careers and personal lives in a number of different ways from the point of view of gender difference. During COVID-19, the path model, t-statistics values, and independent variables coworkers show that a sense of community, work-life balance and policies allowing for work-from-home and travel all impacted the dependent variable work culture. The results of testing the hypothesis indicated that the values of significant factors, along with the path coefficient, t-statistics, and p-value, highlighted the work-life balance as an independent factor that significantly impacted work culture during COVID-19. It is possible to conclude that the new policies regarding travel, working from home, and relationships with coworkers have negatively affected the workplace culture during COVID-19.

Declaration of Competing Interests

The authors declare that they have no known competing financial interests or personal relationships that could have appeared to influence the work reported in this paper.

Funding Declaration

This research did not receive any grants from governmental, private, or nonprofit funding bodies.

Author Contribution

Sneh Bhiwaniwala: Conceptualization, Methodology; **Vishwanath Bansal**: Data curation, Writing- Original draft preparation; **Babita Singla**: Conceptualization, Methodology, Visualization; Investigation; **Namesh Malarout**: Conceptualization, investigation, writing—review and editing; **Sonia Vaz**: Conceptualization, Methodology, writing—review and editing; **Prithvi Hegde**: Software, writing—original draft preparation; **Nisha S Tatkar**: Conceptualization, Writing- Reviewing and Editing; **Anshika Sharma**: data curation, writing—original draft preparation.

References

[1] R. Bhat, V. K. Singh, N. Naik, C. R. Kamath, P. Mulimani, and N. Kulkarni, "COVID 2019 outbreak: The disappointment in Indian teachers," *Asian Journal of Psychiatry*, vol. 50, p. 102047, apr 2020.

[2] W. De Preter, "High demand for teleworking among employees," apr 2020.

[3] T. Knutson, "Telecommuting Surge Likely To Last Past COVID-19 Crisis, Predicts Brookings Report.," *Forbes*, apr 2020.

[4] N. Krasulja, M. Vasiljevic-Blagojevic, and I. Radojevic, "Working from home as alternative for acheving work-life balance," *Ekonomika*, vol. 61, no. 2, pp. 131–142, 2015.

[5] S. Lewis and C. L. Cooper, "Balancing the work/home interface: A European perspective," *Human Resource Management Review*, vol. 5, pp. 289–305, dec 1995.

[6] S. Mann, R. Varey, and W. Button, "An exploration of the emotional impact of tele-working via computer-mediated communication," *Journal of Managerial Psychology*, vol. 15, pp. 668–690, nov 2000.

[7] S. Montreuil and K. Lippel, "Telework and occupational health: A Quebec empirical study and regulatory implications," *Safety Science*, vol. 41, no. 4, pp. 339–358, 2003.

[8] R. Davis, "Home alone.," *Revolution (Oakland, Calif.)*, vol. 1, no. 6, pp. 22–7, 2000.

[9] J. D. Andrew, "Comparison of the job satisfaction and productivity of telecommuters versus in-house employees: A research note on work in progress," *Psychological Reports*, vol. 68, no. 3c, pp. 1223–1234, 1991.

[10] D. M. Vitorio and W. Linda, "Telework: A New Way of Working and Living," *International Labour Review*, vol. 129, no. 5, pp. 529–544, 1990.

[11] A. Nandi, D. Jahagirdar, M. C. Dimitris, J. A. Labrecque, E. C. Strumpf, J. S. Kaufman, I. Vincent, E. Atabay, S. Harper, A. Earle, and S. J. Heymann, "The Impact of Parental and Medical Leave Policies on Socioeconomic and Health Outcomes in OECD Countries: A Systematic Review of the Empirical Literature," *The Milbank Quarterly*, vol. 96, pp. 434–471, sep 2018.

[12] S. Clark, "Presentees: New Slaves of the Office Who Run on Fear," oct 1994.

[13] M. J. Gray, "Supporting teleworking with multimedia," *British Telecom technology journal*, vol. 13, no. 4, pp. 105–112, 1995.

[14] P. M. Leonardi, "Social Media, Knowledge Sharing, and Innovation: Toward a Theory of Communication Visibility," *Information Systems Research*, vol. 25, pp. 796–816, dec 2014.

[15] N. B. Ellison, "Social Impacts," *Social Science Computer Review*, vol. 17, pp. 338–356, aug 1999.

[16] A. Bibby, "Telework: Are Journalists Heading for Honeysuckle Cottage?," *The Journalist*, sep 1993.

[17] D. Mustajab, A. Bauw, A. Irawan, A. Rasyid, A. M. Aldrin, and H. M. Amin, "Covid-19 Pandemic: What are the Challenges and Opportunities for e-Leadership?," *Fiscaoeconomia*, vol. 4, no. 2, pp. 483–497, 2020.

[18] M. Groth, Y. Wu, H. Nguyen, and A. Johnson, "The Moment of Truth: A Review, Synthesis, and Research Agenda for the Customer Service Experience," *Annual Review of Organizational Psychology and Organizational Behavior*, vol. 6, pp. 89–113, jan 2019.

[19] H. Bouziri, D. R. M. Smith, A. Descatha, W. Dab, and K. Jean, "Working from home in the time of COVID-19: how to best preserve occupational health?," *Occupational and Environmental Medicine*, vol. 77, pp. 509–510, jul 2020.

[20] S. Baert, L. Lippens, E. Moens, P. Sterkens, and J. Weytjens, "How Do We Think the Covid-19 Crisis Will Affect Our Careers (If Any Remain)?," *GLO Discussion Paper*, 2020.

[21] B. B. Baltes, T. E. Briggs, J. W. Huff, J. A. Wright, and G. A. Neuman, "Flexible and compressed workweek schedules: A meta-analysis of their effects on work-related criteria.," *Journal of Applied Psychology*, vol. 84, pp. 496–513, aug 1999.

[22] T. D. Allen and K. M. Shockley, "Flexible Work Arrangements: Help or Hype?," in *Handbook of Families and Work: Interdisciplinary Perspectives*, p. 265, 2009.

[23] L. K. Barber and J. S. Jenkins, "Creating technological boundaries to protect bedtime: Examining work-home boundary management, psychological detachment and sleep," *Stress and Health*, vol. 30, pp. 259–264, aug 2014.

[24] S. Carolan, P. R. Harris, and K. Cavanagh, "Improving Employee Well-Being and Effectiveness: Systematic Review and Meta-Analysis of Web-Based Psychological Interventions Delivered in the Workplace," *Journal of Medical Internet Research*, vol. 19, p. e271, jul 2017.

[25] J. M. Berg, A. M. Grant, and V. Johnson, "When callings are calling: Crafting work and leisure in pursuit of unanswered occupational callings," *Organization Science*, vol. 21, no. 5, pp. 973–994, 2010.

[26] D. W. McCloskey, "An Examination of the Boundary Between Work and Home for Knowledge Workers," *International Journal of Human Capital and Information Technology Professionals*, vol. 9, pp. 25–41, jul 2018.

[27] S. Joyce, L. Tan, F. Shand, R. A. Bryant, and S. B. Harvey, "Can Resilience be Measured and Used to Predict Mental Health Symptomology Among First Responders Exposed to Repeated Trauma?," *Journal of Occupational & Environmental Medicine*, vol. 61, pp. 285–292, apr 2019.

[28] E. E. Kossek and R. J. Thompson, "Workplace Flexibility: Integrating Employer and Employee Perspectives to Close the Research-Practice Implementation Gap," in *The Oxford Handbook of Work and Family*, pp. 255–271, 2016.

[29] R. Chainey, "This is how COVID-19 could change the world of work for good," *World Economic Forum*, p. 1, 2020.

[30] A. D. Dubey and S. Tripathi, "Analysing the sentiments towards work-from-home experience during COVID-19 pandemic," *Journal of Innovation Management*, vol. 8, pp. 13–19, apr 2020.

[31] S. L. D. Restubog, A. C. G. Ocampo, and L. Wang, "Taking control amidst the chaos: Emotion regulation during the COVID-19 pandemic," *Journal of Vocational Behavior*, vol. 119, p. 103440, jun 2020.

[32] C. Hanson, "Indigenous Research Methodologies," vol. 5, no. 1, pp. 93–95, 2012.

[33] S. Chadha, M. Ennen, R. Parekh, and G. Pellumbi, "Reimagining medtech for a COVID-19 world," 2020.

[34] W. C. Clapp, M. T. Rubens, J. Sabharwal, and A. Gazzaley, "Deficit in switching between functional brain networks underlies the impact of multitasking on working memory in older adults," *Proceedings of the National Academy of Sciences of the United States of America*, vol. 108, pp. 7212–7217, apr 2011.

[35] M. İmren and H. G. Tekman, "the Relationship Between Media Multitasking, Working Memory and Sustained Attention," *Uludağ Üniversitesi Fen-Edebiyat Fakültesi Sosyal Bilimler Dergisi*, vol. 20, pp. 1075–1100, jul 2019.

[36] R. L. Jacobs, "Knowledge Work and Human Resource Development," *Human Resource Development Review*, vol. 16, no. 2, pp. 176–202, 2017.

[37] T. D. Weerasinghe and A. K. L. Jayawardana, "Flex-Work and Work-Life Balance: Effects of Role Conflicts and Work-Life Support Organizational Culture," *Sri Lankan Journal of Management*, pp. 49–76, dec 2019.

[38] X. Ma, "The effect mechanism of work flexibility on employee job satisfaction," *Journal of Physics: Conference Series*, vol. 1053, p. 012105, jul 2018.

[39] C. Magnusson, "Flexible time–but is the time owned? Family friendly and family unfriendly work arrangements, occupational gender composition and wages: a test of the mother-friendly job hypothesis in Sweden," *Community, Work and Family*, vol. 24, pp. 291–314, may 2021.

[40] D. J. Maume, "Can men make time for family? Paid work, care work, work-family reconciliation policies, and gender equality," *Social Currents*, vol. 3, pp. 43–63, mar 2016.

[41] J. Ferdous, "SWOT Analysis of CodersTrust Bangladesh," tech. rep., Dhaka, 2019.

Journal of Computers, Mechanical and Management

Journal homepage: www.jcmm.co.in

Volume 1 Issue 1

Sustainable Green Composites: A Review of Mechanical Characterization, Morphological Studies, Chemical Treatments, and Their Processing Methods

Nithesh Naik*[a], Nilakshman Sooriyaperakasam[b], Yashoda K. Abeykoon[c], Yomali S. Wijayarathna[d], G. Pranesh[a], Soumik Roy[a], Rovin Negi[e], Budnar Kunjibettu Aakif[f], Asela Kulatunga[g], and Jayakrishna Kandasamy[h]

[a]Department of Mechanical and Industrial Engineering, Manipal Institute of Technology, Manipal Academy of Higher Education, Manipal, Karnataka, India 576104

[b]Department of Mechanical Engineering, University of Moratuwa, Colombo, Sri Lanka 10400

[c]Department of Chemistry, Postgraduate Institute of Science, University of Peradeniya, Kandy, Sri Lanka 20400

[d]Department of Environmental and Industrial Sciences, Faculty of Science, University of Peradeniya, Kandy, Sri Lanka 20400

[e]Department of Aeronautics and Automobile Engineering, Manipal Institute of Technology, Manipal Academy of Higher Education, Manipal, Karnataka, India 576104

[f]Department of Chemical Enginering, Manipal Institute of Technology, Manipal Academy of Higher Education, Manipal, Karnataka, India 576104

[g]Department of Manufacturing and Industrial Engineering, University of Peradeniya, Kandy, Sri Lanka 20400

[h]School of Mechanical Engineering ,Vellore Institute of Technology, Vellore, Tamil Nadu, India 632014

Abstract

Composites have a wide application in the modern world and have successfully replaced traditional engineering materials. Dependencies on composites are extensively increased due to the desire for material durability, high modulus, chemical inertness, flame retardance and thermal isolation. The emergence of new bio-based materials and technologies has taken on new dimensions, bringing with it the profound promise of sustainable development through green composites. Next-generation materials, such as green composites, offer users a wide range of benefits. Although several scholarly articles are available on green composites, the most common ones are not covered in a single paper in the currently available literature. As a result, this article aims to give an overview of bioresin-based green composites so the reader can better understand the mechanical properties, chemical treatment methods, and associated processing techniques.

Keywords: Green Composites; Green Fibers; Bioplastics; Mechanical Properties; Chemical Treatment

1 Introduction

Composites are versatile groups of compounds that can be seen in unexpected applications. Dependencies of composites are extensively increased due to the desire for material durability, high modulus, chemical inertness, flame retardance and thermal isolation. The composite materials are broadly classified into three major categories: polymer matrix, metal matrix, and ceramic matrix [1].

*Corresponding author: nithesh.naik@manipal.edu

Received: 14 September 2022; **Accepted:** 31 October 2022; **Published:** 31 October 2022

© 2022 Journal of Computers, Mechanical and Management.
This is an open access article and is licensed under a Creative Commons Attribution-Non Commercial 4.0 International License.

DOI: 10.57159/gadl.jcmm.2.3.23014.

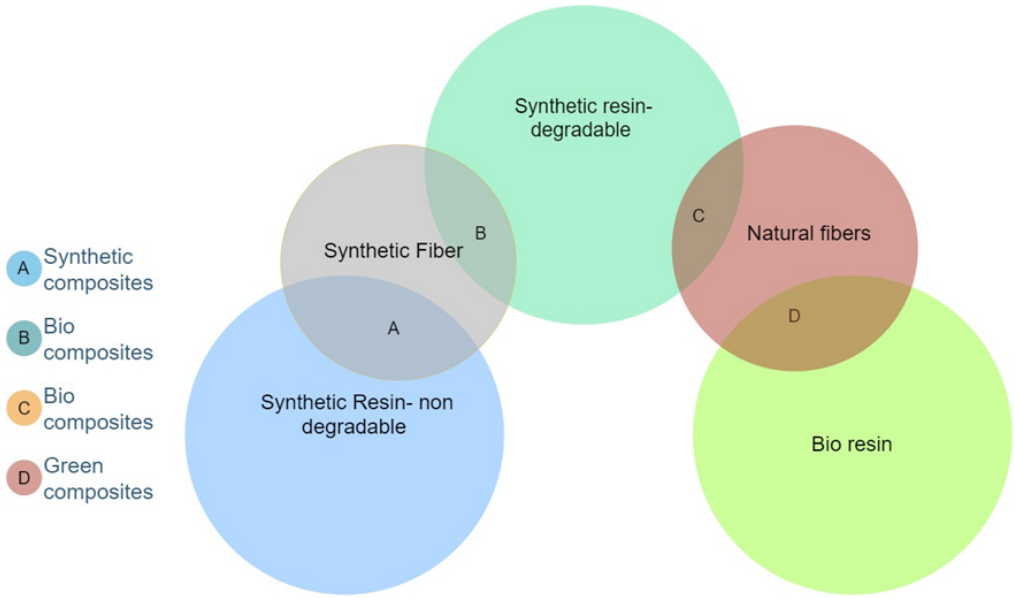

Figure 1: Classification of polymeric composites.

Among these composites, polymeric composites possess many benefits over the other two categories. Figure 1 depicts a broad classification of polymeric composites. These polymer matrices (both synthetic and biopolymers) are highly sought after due to their flexibility, lightweight and ease of production. Growing demand for sustainability has led to a surge for bio-based materials from non-renewable resources to replace synthetic materials. evolving decipherable information. Green composites (GC) show significant environmental friendliness and comparable attributes with synthetic polymers. GC prepared using natural fiber reinforcement demonstrates good mechanical properties such as tensile, compressive and flexural strengths and may be used for various applications [2–4]. Though the properties of GC predominantly depend on the properties of the matrix, fibers and reinforcement, the ultimate factor that dictates the properties of the composites is their intrinsic orientation of the constituents. Therefore, microscopic analyses are widely carried out to investigate the morphological properties of GC [5]. Finding new composite materials and improving the characteristic strength of composite materials remain the trend in the scientific community. Following that, the development of green materials is of serious interest soon after the realization of the environmental impacts caused by synthetic materials. Natural fiber production on the nanoscale is booming these days to incentivize the strength capacity of the reinforcement fibers in the composite elements [6, 7].

After all, the applications of biocomposites in automotive, building product applications, and aviation sectors, as well as biomedical, energy, and sports, have grown enormously [8, 9]. GC can either be formulated with natural fiber and biodegradable petroleum polymer matrices such as polycaprolactone (PCL), poly (butylene succinate) (PBS), co-polyester amide (PEA), poly butyrate adipate terephthalate (PBAT) and polyvinyl alcohol (PVA) or with natural fibers and bioresins [8, 10] such as cellulosic plastics, polylactides, soy-based plastics, starch plastics and microbially synthesized biopolymers. Several articles discuss green composites, but most often, they are only limited to a few fibers or resins or either limited to mechanical properties or chemical treatments of specific fiber/matrix combinations. In most cases, scholars overlook incorporating all aspects of green composites, including fiber and resin matrix processing methods. As a result, identifying gaps in all available relevant information and summarizing it in one place becomes an obvious requirement. Therefore, a potent researcher spends a great deal of time reading all the information from various sources, delaying the advancements that could contribute to creating a better world. Therefore, an effort has been made to synthesize all the relevant information related to the most common green fibers, bioresin & green composites in one place. Those interested in biofibers or bioresin can obtain most of the information from this article, as the authors have spent considerable time reviewing a vast body of literature and condensing it into a concise and informative paper. Composite manufacturers, young researchers, and those interested in GC can obtain as much information as possible from this single paper and expand their research, which may contribute to this field in the future.

In other words, the detailed study presented in this article aims to provide critical and clear insights into the commercially available/used bioresin-based green composites (BRGC), their biological classification, intrinsic properties, and surface preparation to achieve the optimal results desired for their respective applications. Through its various sections, this review discusses the biological classification of bioplastics and biofibers; the various mechanical characterization in terms of modulus, strength, flexibility, durability, micro macro-structural overviews; the chemical treatment methods; processing techniques of well-known GC; and challenges and future potentials of bioresin-based natural fiber reinforced green composites. Figure 2 provides a comprehensive overview of this review paper.

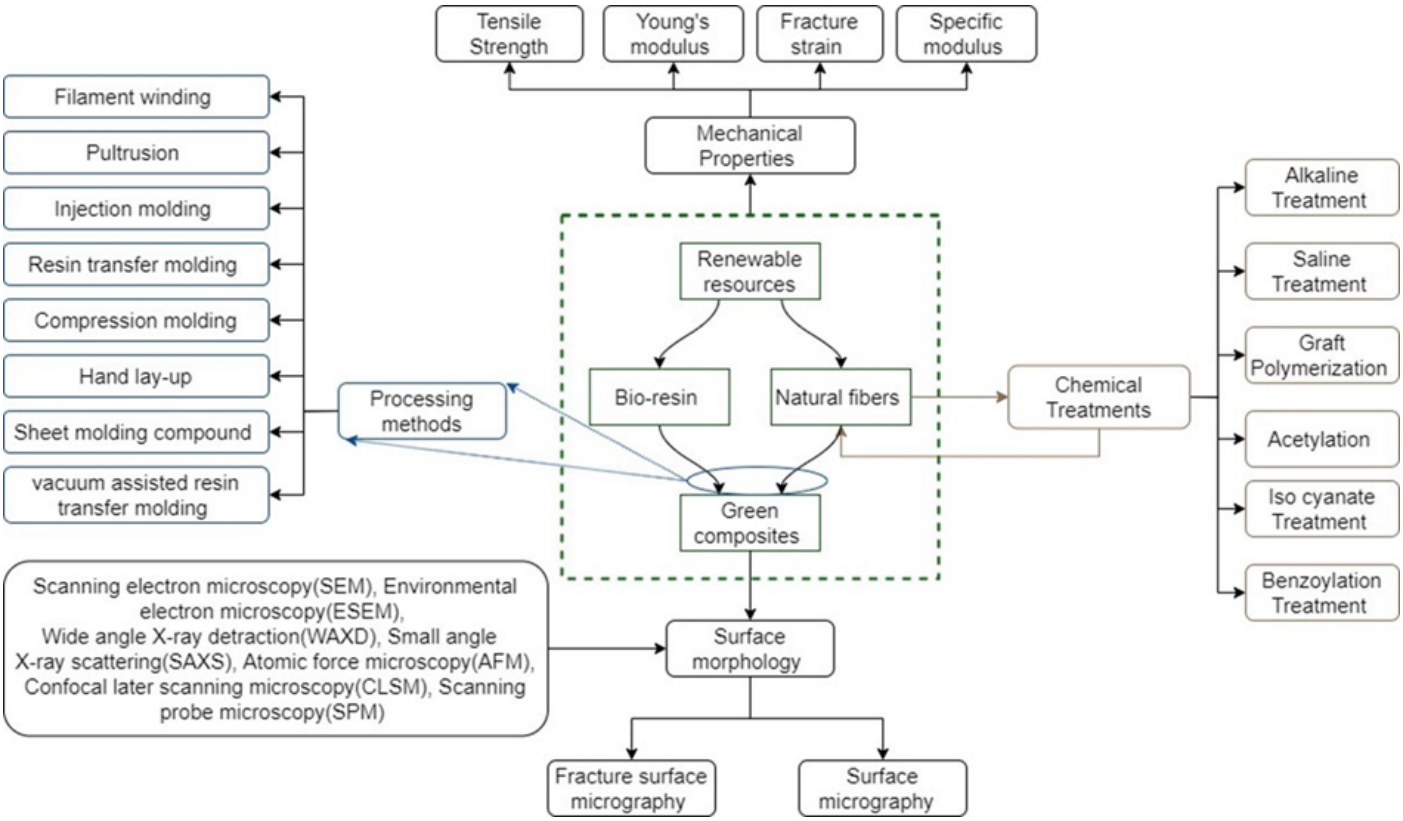

Figure 2: Overview.

2 Background

2.1 Search strategy

A non-systematic review of all published English-language material on green composites was done. The Google Scholar, SCOPUS, Research Gate, and Web of Science databases were scoured for academic articles for evaluation. The search was sequenced using numerous keyword combinations. The keywords employed were green composites, green fibers, bioplastics, mechanical properties, and chemical treatment. The permitted search terms included review articles, original research articles, case studies and data sets.

2.2 Selection strategy

The review includes all the articles that deal with the mechanical properties of green fiber/bioresin combinations, green fibers, chemical treatment of the green fibers, morphological analysis of fiber /matrix composites and green fibers. Apart from the inclusion and exclusion strategy, articles about all the relevant topics were manually searched to screen the work of interest and included if they matched the scope of the study.

2.3 Inclusion criteria

- Articles on green composites, green fibers and bioresin.
- Review articles and experimental studies on biocomposites.
- Full-text articles, experimental studies of different fibers/matrix combinations concerning the chemical treatment methods and morphological studies.

2.4 Exclusion criteria

- All the articles without full texts
- Studies that do not deal with the mechanical characterization, chemical treatment, and surface morphology of the green fibers, bioresins and their combinations

3 Biological Classification of Green Composites

The GC can be manufactured by combining natural fibers and biodegradable polymers, where biodegradable polymers can be derived from microbial synthesis, petrochemical synthesis, or natural resins. The constituents of green composites are summarized in Figure 3.

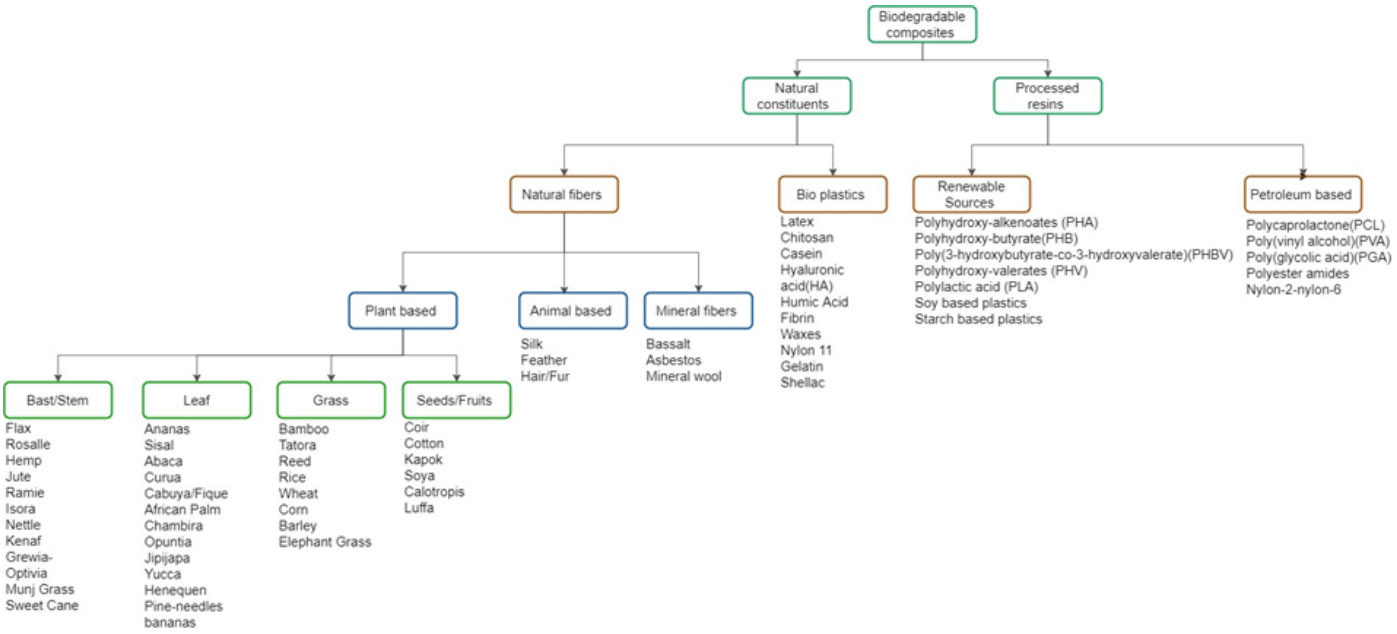

Figure 3: Classification of green composites.

3.1 Natural fibers

Almost all fibers are possible candidates for composite reinforcements. However, the cost, environmental requirements and performance standards are the factors that need to be satisfied before their deployment. Plant-based fibers, primarily lignocellulosic fibers, can meet these requirements. However, before employing fibers as a constituent for composites, they should be isolated from other constituents like lignin, hemicellulose, wax and proteins [8]. Natural fibers can be subdivided into fibers derived from plants, animals, and minerals. Plant-derived fibers can further be classified into wood feedstock or non-wood feedstock. Non-wood fibers are again subdivided into the grass, stem/bast, leaf or seed hair/fruit fibers, depending on their origin [11]. The reinforcement fibers' main objective is to improve the mechanical properties of the final composite. However, natural fibers extend the potential to deliver greater added value, sustainability, renewability and lower costs, especially in the automotive industry. Table 1 shows the annual production of commercially available natural fibers [11–13].

Fibers from agricultural residue

It is abundantly clear that the annual accumulation of agricultural residues, which ultimately leads to burning such biomass in open fields, will contribute to global warming [14]. As an alternative, researchers and environmental activists have started focusing on utilizing bio-waste while minimizing feedstock costs and negative environmental impacts [15]. The most abundant agro-residues are cereal straws, primarily utilized for energy generation and animal feed. According to the Cambridge University Press, the world's energy intake from cereal grains is around 60%. So, the opportunity to utilize the agricultural residue fibers is workable. Generally, the main fiber extracted from agricultural remaining is called cellulose fiber (CF). Bio-based residuals can be used as a reinforcement in many instances, such as bagasse, sunflower stalk, corn stalk, rice husk, soy stalk, wheat straw, corn husk [16–20]. Several studies deal with producing green composites from agricultural residues. Crop residues are excellent alternative substitute resources for natural fibers as they are bulkily available at low cost and widespread on a greater scale.

3.2 Bioplastics (Bioresins)

The matrix governs the composites' shapes, environmental tolerances, surface mien, and durability. Composite matrix/resin contributes the largest towards the environmental impact for most composite syntheses. Therefore, implementing a bioplastic (bioresin) would help achieve a positive impact on the sustainability of the outcome. Table 2 lists the commercially available/emerging bioplastics used in the different industrial arenas. Bioresins are generally derived as artificial or man-processed macromolecule constituents produced by biological sources. In other words, bioresins bind the fibrous material together and disperse the stress element throughout the composites, also known as the disperse phase. Crop-based bioplastics can either be thermosetting or thermoplastics. However, some studies reveal that non-biodegradable biopolymers can be seen in a few durability-demanding applications.

Table 1: Commercial natural fiber production [12, 13]

Fiber Source	World Production (10^3 tons)
Sugar cane Bagasse	102000
Bamboo	30000
Jute	2850
Kenaf	970
Flax	830
Grass	700
Sisal	378
Hemp	214
Coir	650
Ramie	100
Abaca	91
Banana	200
Cotton	19010
Kapok	123

These discoveries may contradict the paradigm that all natural polymers are biodegradable. Due to the desire for persistent polymers, which can be an alternative to synthetic polymers, non-degradable bioplastics were synthesized in a way that may degrade at very low rates / in the presence of specialized microorganisms. Polythioesters (PTE) [21] drop-in bioplastics such as bio-based polyethylene terephthalate (PET), bio-based Polyethylene Furanoate (Bio-PEF) [22], bio-based polyethylene (PE), bio-polycarbonate, bio-polyamide (PA 4,10/ PA 6,10) are few examples of biopolymers whose degradation rates are low. Biopolymers can either be hydrophilic or hydrophobic. Generally, bio-based polymers are the different constituent classes of hydrocolloids and lipids. These hydrocolloids are hydrophilic in nature. Lipids are hydrophobic in nature. Polysaccharides are hydrocolloids. Usually, they are carbohydrates formulated with carbon, hydrogen and oxygen in a 1:2:1 ratio. Polypeptides are generally proteins, a formation of long-chain amino acids. Figure 4 illustrates how conventional bioplastics fall under polysaccharides and polypeptides.

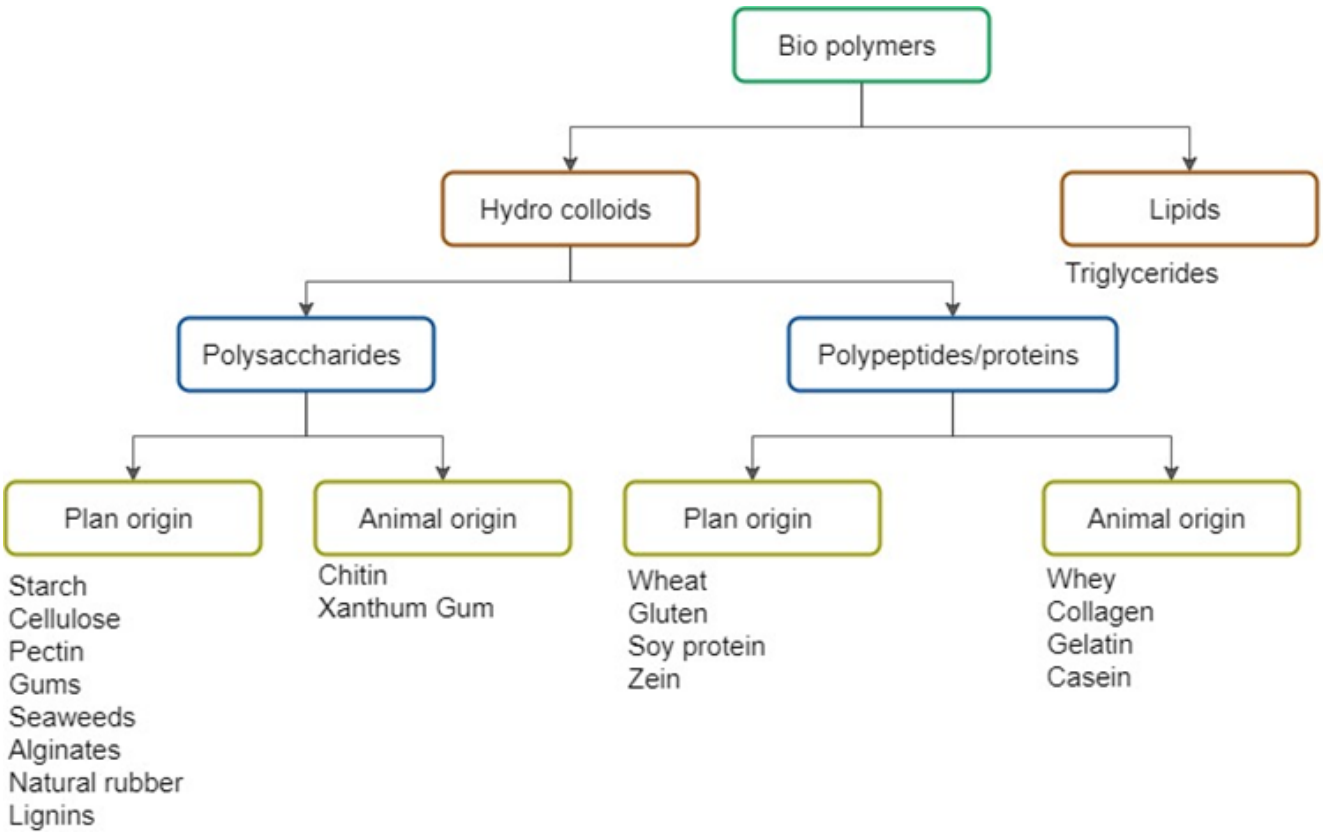

Figure 4: Types of biopolymers [23].

Table 2: Commercially available biopolymers.

Polymer	Feedstock, Method of process
Polyhydroxy Alkenoates (PHAs)	Direct synthesis from sugar, Microorganism/bacterial fermentation
Polylactic acid (PLA)	L-Lactic Acid, D-Lactic acid, Chemical and biological synthesis
Poly (Acrylic acid) (PAA)	3-Hydroxypropionic acid, Radical polymerization
Polyethylene (PE)	Ethanol, Dehydration and polymerization
Polyvinylchloride (PVC)	Ethanol, Dehydration and polymerization
Polyamide 11 (PA11)	Ricin oleic acid, Condensation reaction
Polyisoprene (Natural Rubber)	Isoprene, Mini-emulsion polymerization
Polyacrylic acid	3-hydroxy propionic acid, Dehydration, purification and Crystallization
Cellulosic	Cellulose, Dissolving, Extrusion and Precipitation
Thermoplastic starch (TPS)	Starch, Twin screw extrusion, mixing method
Aliphatic Polyester	1,3-propanediol, succinic acid, fatty acids, Copolymerization
Polyether	1,3-propanediol, fatty acids, Super acid-catalyzed condensation
Furan resins	Xylose, Polycondensation under the presence of weak acids
Epoxy resins	Triglycerides, Epoxidation
Bio-based Polyethylene Terephthalate (PET)	Sugarcane -Sugar, Fermented and distilled to ethanol, Monoethylene glycol (MEG) from bioethanol, MEG is combined with purified Terephthalic acid (PTA)
Bio-based Polyethylene (PE)	Sugarcane -Sugar, Fermented and distilled to ethanol, Dehydrated to ethylene, Polymerization
Bio-Polycarbonate (PC)	Corn-Isosorbide, Hydrogenation of Glucose to produce sorbitol, Isosorbide is obtained from double dehydration of sorbitol
Bio-Polyamide (PA 4,10/ PA 6,10)	Castor oil -Sebacic acid, The Dicarboxylic acid (Sebacic acid) part of Polyamide is produced from a renewable resource (Castor oil)

The scientific identification of green materials

ASTM D6866 is a standard test method for determining bio-based/biogenic carbon content or the percentage of bio-based contents of the given substances using radiocarbon analysis. The analysis is the percentage calculation of the relative amount of 14C in the carbon content of the material. In general, fossil-based carbon does not contain a 14C isotope, whereas materials that belong entirely or particularly to renewable resources have a significant amount of carbon isotope material. The tests reveal the results with a maximum total error of ±3% (absolute). This method does not elaborate on environmental impact, product performance, functionality or geological origin and is only applicable to compostable material which can produce CO_2 by-products. The major limitations of plant fibers compared to synthetic fibers are their non-uniformity, dimensional variations and variant mechanical property due to the variations between two fibers (though from the same cultivation), and the majority of composites comprised of natural materials are susceptible to performance and dimension changes when they come into contact with water.

4 Mechanical Characterization of Green Composites

Composites are the mixture of different constituents to form a single substance which is often intended to produce superior material performance compared to its sole materials. It is the mixture of substances wherein physical bond makes it compact. Those constituents are namely the continuous phase (matrix), dispersed phase (reinforcement) and interfacing phase (contagious coatings). As the fibers in a GC are hollow and lignocellulosic substances, they have very good thermal and acoustic insulation properties compared to synthetic fibers. But still, the mechanical properties of natural fibers are lagging compared to synthetic fibers. Studies report that chemical and mechanical surface treatments can overcome mechanical performance deficiencies of natural fibers and enhance the surface roughness of the subjective fiber material. However, due to the low-density factors and the specific mechanical modulus, the gravity is comparable to or even better with synthetic fibers. Table 3 tabulates green fibers' mechanical and physical properties that reinforce the green composites. Nevertheless, a study on hemp fiber elaborated on the changes in the mechanical properties with fiber separation wherein the hemp fiber separated with the 'steam explosion separation' method showed superior tensile properties compared to the fibers separated using the 'biological separation' method for the same fiber [10]. Material elongation is one of the critical considerations when choosing the right materials. As the materials are usually subjected to high strain and harsh environmental conditions, the fracture strain of the green composites increases larger than that of room temperatures. Generally, these composites demonstrate high elasticity with high temperatures [24]. The fiber aspect ratio is majorly dependent on how the fibers are extracted and processed, and both fiber orientation and the aspect ratio strongly influence the composite formulation. In a nutshell, it affects the mechanical properties of overall composite performance in return. The impact performance of the composites ensures the degree of usability of composites in the harsh environment, which is the primary sake for the usage. Yet, the crucial element of green composites is fiber/matrix adhesion which promotes good stress transfer. In general, cellulose in the fibers has a strong hydrophilic character due to three hydroxyl groups per monomeric unit, but biopolymers like PLA and poly (hydroxybutyrate) are generally hydrophobic [26, 25].

Table 3: Mechanical and physical properties of natural fiber [13, 24, 25]

Natural fiber	Tensile Strength (MPa)	Young's modulus (GPa)	Specific modulus (GPa)	Failure strain (%)	Length, l (mm)	Diameter, d (μm)	Density (kg/m3)	Microfiber angle (J)
Cotton	300-700	6-10	4-6.5	6-8	20-64	11.5-17	1550	20-30
Kapok	93.3	4	12.9	1.2	8-32	15-35	311-384	-
Bamboo	575	27	18	-	2.7	10-40	1500	-
Flax	500-900	50-70	34-48	1.3-3.3	27-36	17.8-21.6	1400-1500	5
Hemp	310-750	30-60	20-41	2-4	8.3-14	17-23	1400-1500	6.2
Jute	200-450	20-55	14-39	2-3	1.9-3.2	15.9-20.7	1300-1500	8.1
Kenal	295-1191	22-60	-	-	2-61	17.7-21.9	1220-1400	-
Ramie	915	23	15	3.7	60-250	28.1-35	1550	-
Abaca	12-400	41	-	3.4	4.6-5.2	17-21.4	1500	-
Banana	529-914	27-32	20-24	1-3	2-3.8	-	1300-1350	11-12
Pineapple	413-1627	60-82	42-57	0-1.6	-	20-80	1440-1560	6-14
Sisal	80-840	9-22	6-15	2-14	1.8-3.1	18.3-23.7	1300-1500	10-22
Coir	106-175	6	5.2	15-40	0.9-1.2	16.2-19.5	1150-1250	39-49
Oil palm	248	3.2	-	25	-	-	0.7-1.55	-

So, the material adhesion properties are to be ensured to the better stress transfers among the fiber & matrix.Mechanical characterization is one of the prevalent methods to predict the mechanical performance of any composites. It enables researchers to classify the composites according to their tensile strength, young's modulus, flexural strength, compressive strength, flexural modulus and impact strength. Mechanical property measurements of composites and fibers must adhere to a standard testing procedure, preferably the one prescribed by the American Society of Testing Materials (ASTM). The mechanical properties of green composites depend upon various parameters such as fiber aspect ratio, percentage of fiber content, surface treatment of fibers, coupling agents to increase the bonding between fiber and matrix and fabrication techniques [27–30]. It is to be noted that the mechanical performances of the composite materials also largely rely on the fabrication process. The materials' tensile moduli and tensile strength show slight increments with the compression pressures applied during the molding process. Table 4 summarizes the mechanical properties of the most common green composites.

5 Morphological Study of Bioresin-based Composites

The physicochemical orientation of the intrinsic constituent governs and differentiates composites' properties. Fiber reinforcements in the composites have two different forms, (a) woven and (b) non-woven (bulk fiber /fiber bundle). Different techniques can categorize the physio-chemical properties. Structural properties are analyzed by spectroscopic and microscopic techniques such as scanning electron microscopy (SEM), environmental electron microscope (ESEM), confocal laser scanning microscopy (CLSM), small-angle X-ray scattering (SAXS), atomic force microscopy (AFM), and wide-angle X-ray diffraction (WAXD) [27–29]. On the other hand, the measurement of other properties of the composite films is very extensive and depends on the individual applications [30]. The surface morphology micrograph analysis widely varies with the purpose of the subject content. The fractured surface morphology is one of the popular usages of micrographs for observing the intrinsic behavior of composites during tensile/impact/fracture and toughness testing, [16, 29–34]. The next significant importance following the fractured surface morphology is given to fiber surface pre-treatments morphology to confirm the level of roughness, smoothness, cavity and voids on the surface [35, 36]. Also, water absorption testing measurement practices outlined with standard ASTM D570-81 have often been seen to use micrograph analysis Liu2005,Lee2006. In some instances, surface micrographs were used to examine the soil burial test of biodegradability [29].

6 Chemical Treatment

The primary disadvantage of using natural fibers as reinforcement in GC is their incompatibility with the matrix due to their surface impurities and affinity for water absorption. Thus, modification of the fibers into a compatible structure becomes essential. Generally, chemical modification is a process that utilizes chemicals to refurbish the surface of the fibers to perform better. Cellulose-based fibers are compacted with lignin, wax, pectin or crystalline constituents that rush the chemical penetration/matrix to fiber interfacial adhesion. So natural fibers undergo some modification, making them feasible for composite production. The chemical modifications can be classified into five methods: mercerization/alkaline treatment, oxidation, crosslink, grafting and coupling agent treatment [1].

Table 4: Mechanical and physical properties of green composites.

Constituents(Fiber /matrix)	Molding Pressure (MPa)	Fiber content (%)	Tensile strength (MPa)	Fracture strain (%)	Young Modulus (GPa)	Reference
Curaua/cornstarch-based	-	30.1	327	1.16	36	[33]
Abaca/PLA	-	30	74.0 ± 0.7	1.44 ± 0.1	8.0 ± 0.34	[13]
Jute/PLA	-	30	81.9 ± 2.9	1.8	9.6 ± 0.36	[13]
Lyocell/PBS	5	60	117.4	9.9	3.16	[28]
Abaca/(PHBV/Eco-flex)	-	30	28.0 ± 1.3	0.9 ± 0.1	4.4 ± 0.06	[13]
Ramie/Eco flex	9.8	44-52	75.9	8	1.67	[24]
Lyocell/PHBV	10	63.2	108.8	10.6	2.46	[28]
Lyocell/PLA	10	62.1	100.5	6.4	5.55	[28]
Hemp/PHBV	2.03	32	27	1.1	-	[9]
Coir dust/PHB	-	30	7.4	2.2	0.4712	[37]
Wood/PHBV	0.551	30	18.08	-	1.94	[34]
Bamboo/PHBV	0.551	30	18.9	-	1.71	[34]
Flax/Soy-protein	8	-	18.6	16.4	0.448	[38]
Hemp/Cashew nutshell	6	-	43.82 ± 6.36	0.89 ± 0.12	8.7 ± 1.46	[39]

Hydrophobicity and hydrophilicity are the two concerns regarding the chemical treatment of fibers or the fiber's compatibility preparation. In particular, hydrophile fibers do not promote adhesion compared to hydrophobic polymers; thus, they are called dispersed matrix. So, the poor wetting of fibers causes the non-uniform distribution of fibers and the void formation, leading to crack initiation and moisture penetration to the composites, resulting in anisotropy eventually. As a result of their hydrophilic nature, natural fibers also absorb moisture from the surrounding air and thus can be a serious problem, particularly for the thermosetting resins, as it inhibits the curing processes when the manufacturing process is being done, leading to the low mechanical performance of the entire composite materials. The chemical treatment of the natural fibers is one of the effective ways to compromise the interfacial bond impairments between the fibers and the resin matrix as it holds on to reduce the OH (Hydroxy) functional group from the fiber surface (ionic hydroxy groups have the thirsts of water) and improves the surface roughness that enhances the interfacial interaction. Numerous treatment methods were reported to improve fiber/matrix compatibility. Nevertheless, the adhesion between two materials is the function of several factors, including surface polarity and roughness. A study with Curaua fiber green composites held an experiment with untreated and 10% alkali-treated fibers, which showed considerable changes in the mechanical properties of the compact material [33]. In yet another study, the chemical treatment of jute fiber with pyridine showed an improvement in the surface structure, and complementary scanning electron microscope images of treated jute fibers proved the modification of natural fiber using chemical agents. Table 5 lists numerous chemical treatment methods used to enhance the properties of the fibers by altering the chemical groups, surface morphology, inherent wettability, and tensile strength. In a study, the mechanical treatment of wheat straw fibers was compared with the chemical treatment [40]. The authors concluded that chemical treatment provides way better results than mechanical treatment. As per the SEM photomicrographs, as depicted in Figure 5, wheat straw fibers processed by mechanical and chemical means, chemically treated fibers show a homogeneous, uniform surface texture while comparing mechanically processed fibers in which surface irregularities are more prevalent even after the treatment.

Table 5: Chemical treatment of different natural fibers.

Natural fiber	Chemical reactants	Reference
Pineapple leaf	c-aminopropyl trimethoxy silane (Z-6011) and c-methacrylate propyl trimethoxy silane (Z-6030)	[41]
Green coconut	NaOCl, NaOCl/NaOH, or H2O2	[41]
Sisal	NaOH	[42]
Bamboo	NaOH	[43]
Alfa	NaOH	[44]
Carica Papaya	NaOH	[45]
Kenaf	NaOH	[46]
Hemp	(3-glycidyloxypropyl) trimethoxy silane	[47]
Ramie	NaOH, NaOH-Saline, Silane	[48]
Pineapple leaf	NaOH and KOH	[49]
Sisal	Stearic acid	[50]
Sisal	NaOH	[42]
Okra bas	NaClO2	[51]

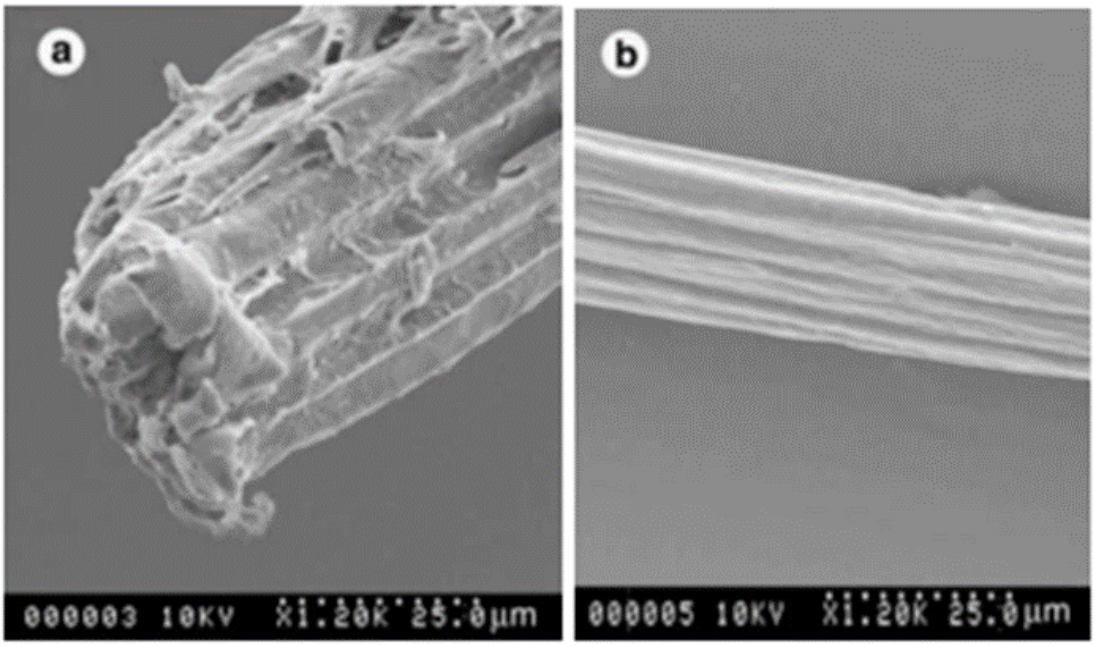

Figure 5: Surface of wheat straw fibers after (a)mechanical processing (b) chemical processing [40].

6.1 Alkaline treatment

As it removes a certain amount of lignin, wax, and vegetable oils from the surface of natural fibers, mercerization or alkaline treatment is one of the most common chemical treatments and the least expensive method of treating natural fibers [18]. It is a process in which natural fibers are immersed in an aqueous solution of sodium hydroxide (NaOH) over a period of time and at a specific temperature. The treatment time plays a significant role in the degree of modification [35]. As the concentration of NaOH(aq) increases, the fiber's color turns yellow despite disrupting hydrogen bonds and improving surface roughness[20]. As the treatment varnish the lignin, pectin and hemicellulose from the fiber, the density of the fiber matrix increases [52]. Usually, alkali treatment of the natural fibers changes its crystallinity, orientation of fibrils and unit cell structure [53]. The sophisticated alkaline treatment requires optimized treatment parameters; if not, it deviates the final results through fiber embrittlement, pore formation and fiber defibrillation [54]. In one study, the impact of alkali treatment on pineapple leaf fiber for pineapple leaf fiber/PLA composites has shown that alkali-treated fiber-reinforced composites offered superior mechanical performance [26, 46] as the treatment increased the crystallinity of the cellulose and thereby the mechanical performance of the composites. In addition, the alkalized fiber composites have a high storage modulus corresponding to their high flexural modulus.

6.2 Saline treatment

The hydrophilic fibers and hydrophobic matrix often show incompatibility while combining. So, one option would be coupling the fibers and resin matrix through the coupling agents. At a rough glance, silane is a chemical compound with the referring chemical formula of SiH4. Saline molecules with bi-functional groups are the choices in this context that link the fibers and resins through the siloxane bridge, which gives molecular continuity across the interfacial region of the composite. These coupling agents are of the general chemical structure, R(4-n)-Si-(R1X)n, where R is alkoxy, R1 is an alkyl bridge connecting silicon atoms, and X represents organofunctionality [55]. These organofunctionalities of silanes are typically amino, mercapto, glycidoxy, vinyl, or methacryloxy groups. For instance, the reaction of saline treatment can be referred to as follows:

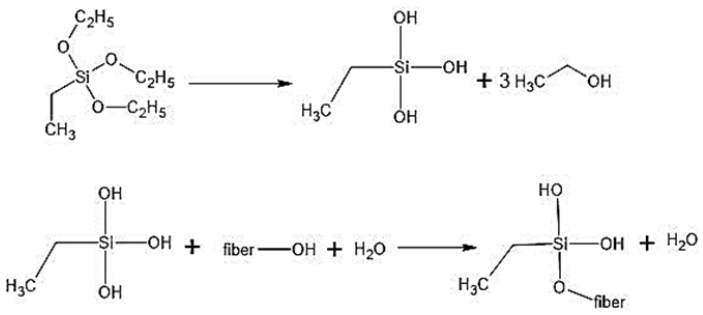

6.3 Graft polymerization

The graft polymerization onto lignocellulosic fibers is important in the physio-chemical modification of the natural fibers [56, 57]. This reaction is usually carried out in desirable temperatures while maintaining the standard. The cellulose is treated with an aqueous solution with selected ions and is exposed to high-energy radiation. In a study, redox activation was done to graft the copolymers into the natural fibers used in the composites at the end [58]. Redox catalysis is an effective method for generating free radicals under mild conditions. Grafting copolymerization of biofibers for biocomposites can be done in three ways: (a) grafting with a single monomer, (b) grafting with two or more monomers, and (c) grafting with the polymer directly [59]. There are plenty of techniques being used as a redox catalytic [41–43, 50, 56–65]. Among other graft copolymerization techniques, CuSO4-NaIO4-based treatment is quite popular as no acidic agents are used during graft copolymerization, as the use of acidic substances diminishes the quality of the outcomes. However, some researchers addressed the suitability of ceric-ion-induced redox initiation for the starch-based substrates validating that ceric-ions can effectively oxidize starch. As graft yield is a function of temperature, increasing temperature increases graft yield. [57, 60].

6.4 Acetylation

Acetylation is one of the chemical treatments in which fibers are exposed to the Acetyl function groups (CH3COO-) to replace the hydrogen bond held points into the hydrophobic Acetyl group (CH3CO), which improves properties such as dimensional stability, biological inertness, and UV-induced degradation [55]. Usually, before the treatment with glacial acetic acid (CH3COOH), the natural fibers are alkali-treated/bleached. The treated fibers are immersed in glacial acetic acid for 1h and later soaked in acetic anhydride for 2-5 minutes, containing two drops of H2SO4(conc). Hydrophobic acetyl groups trigger the hydrophobic nature of the fibers. Acetylation facilitates the removal of non-crystalline constituents, improves surface topography, changes surface free energy and improves the stress transfer efficiency in the fibers.

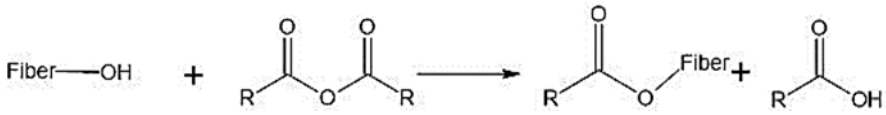

6.5 Isocyanate treatment

The Isocyanate group can react with the hydroxyl groups on the fiber surface, which improves the interfacial adhesion with the polymer matrix. The process is usually held in intermediate temperature ranges. The functional group of Isocyanates, –N=C=O, actively reacts with the fibers' hydroxyl group and produces strong covalent bonds. The reaction of natural fiber with isocyanate groups of polymeric di-Phenyl methane diisocyanate (PMDI) is as follows [61].

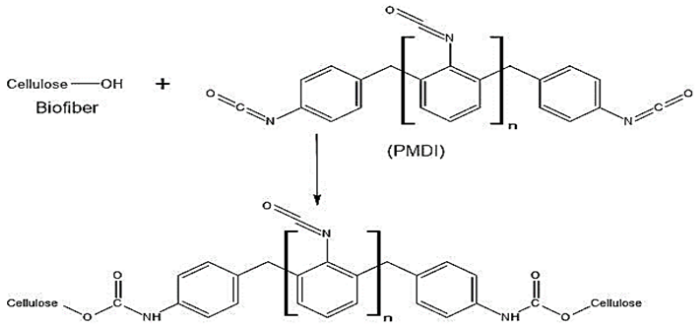

6.6 Benzoylation treatment

Benzoyl chloride is most often used in fiber treatment. Benzyl ($C_6H_5C=O$) in the benzyl chloride is designated to eliminate the hydrophilic nature of the natural fibers that improve the adhesion with the hydrophobic resin matrix. The fiber is usually pretreated with alkali to activate the fiber's cellulose and lignin hydroxyl groups. Later, it is left to the reaction with benzyl chloride (15 minutes usually). Then the fiber is isolated and treated with ethanol (around 1 min), then oven dried. An example reaction of a cellulosic hydroxyl group of fiber with benzyl chloride is as follows [55].

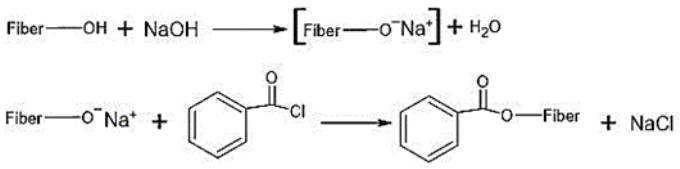

6.7 Permanganate treatment

Most permanganate treatments are conducted (1-3 minutes) with potassium permanganate ($KMnO_4$) resolved in acetone in different concentrations (typical concentrations in the range of 0.005%- 0.205%) [62] after alkaline pre-treatment [50, 63, 64]. Permanganate treatment tends to form a cellulose free radical through the MnO3- ion formation. The highly reactive Mn3+ irons are later responsible for graft copolymerization as follows:

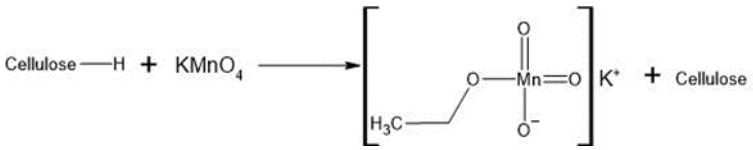

6.8 Maleic anhydride treatment (coupling agents)

Maleic anhydride agents are widely used to strengthen the interfacial impairments in fillers and reinforced fibers. The process also proceeds after following alkalization treatment. The use of maleic anhydride treatment as a coupling agent reduces the ability of moisture absorption and improves hydrophobicity. The weight percentage of fiber determines the amount of maleic anhydride required. An example treatment is as follows [65]. Table 5 below tabulates all the possible chemical reaction techniques in common for natural fibers

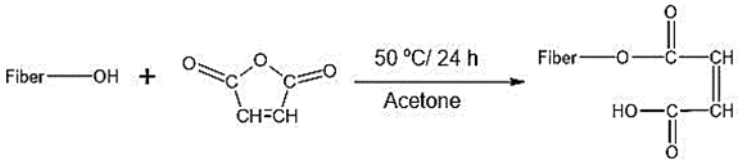

7 Processing of green composites

Several composite fabrication methods are being practiced producing the desired composite material performance, such as injection molding, compression molding, pultrusion, resin transfer molding, extrusion and thermoforming. Generally, the selection of processing technique depends on materials to be processed, quality of desired outcome, complexity of parts, cost of production and capital investments [7]. The resin transfer molding (RTM) technique is used in complex components with large surface areas. Composites having vinyl ester and unsaturated polyester resins are usually processed with RTM. The main drawback of RTM is that fiber to resin ratio is hard to be controlled. Pultrusion techniques are used in the fabrication of long fat sheets and channels. The process material is usually polyurethane (PU). Injection molding is a more prevalent process of fabricating one-piece objects and storage containers. Usually, polybutylene succinate (PBS), polypropylene (PP) and polybutylene adipate terephthalate (PBAT) are the fabrication materials. On the other hand, material wastage is high, and the production rate is low in compression molding. Thermoforming is for fabricating and disposing of polypropylene cups, containers, and blister trays. The production rate is high in the thermoforming process. Table 6 synthesizes the processing methods of the most common, commercially available fiber matrixes. Generally, the processing techniques are constituent-specific with the materials as discussed above.

8 Conclusion

Composites are tailored-made materials that show unique qualities in pursuing sophisticated material production. Synthetic composites have been boasted as cradle-to-grave lightweight materials used ever since. However, widespread environmental concerns in conceiving sustainability and ecological friendliness have increased significantly recently. Thus, the production of environmentally friendly materials emerged. Among the most viable solutions, green materials stood alone among the crowd while showing the greatest responses in automotive, aviation, building materials, household appliance and biomedical applications after the abundant advantages perceived from bio-based materials. A subject's life cycle assessment (LCA) reveals the overall potential environmental impacts on the surroundings. Substituting natural fibers for synthetic fibers has been seen as a prevalent method for improving the sustainability of the composites, as the energy consumption associated with natural fiber production is around half that of synthetic fiber production's carbon dioxide emissions. Although the product is said to be biodegradable, it doesn't mean that it can be thrown straight into the environment. Generally, any products at their end life, particularly industrial wastes, need to be gone through the right treatments with specific conditions before it is swept away. Green materials cannot be the solution for littering and should be regulated with standard practices. Thus, biodegradability or composability barely means the product will degrade in any environment. Degradation demands certain factors such as humidity, temperature, time and bacterium/fungi in a specific environment. Industrial composting facilities avail these triggered degradability and specific conditions. Besides environmental concerns, green composites are rich with some user, and industry-friendly advantages, encompass good electrical resistance, friendly processing, no wear of tools, eliminated skin irritation, low specific weight, higher specific strength, good thermal & acoustic insulations and low

Table 6: Processing methods of different natural fiber biocomposites.

Fiber	Matrix	Fiber content(%)	Processing method	Reference
Flax yarn	Vinyl ester	24	Resin transfer molding	[66]
Flax silver	Unsaturated polyester	58	Compression molding	[67]
Flax yarn	Unsaturated polyester	34	Resin transfer molding	[66]
Kenaf	PLA	80	Compression molding	[68]
kenaf	PHB	40	Compression molding	[69]
Hemp	PLA	30	Compression molding	[70]
Flax	Poly (l-lactic acid)	30	Film stacking	[71, 72]
Flax (Uni-directional)	Soy protein	-	Resin transfer molding	[38]
Chicken feather	Acrylated epoxidized soybean oil + styrene	5-20	Vacuum-assisted resin transfer molding	[72]
Luffa Cylindrica	Castor oil + dihenylmethane di-isocyanate	10	Sheet molding compound	[73]
Wheat straw	Linseed oil, maleic anhydride, and divinylbenzene	50–90	Compression molding	[74]
Coconut, sisal	Castor oil + diphenylmethane di-isocyanate	14–30	Compression molding	[75]
Jute	Polylactide	30	Injection molding	[76]

initial investments. These favorable likings of green materials upsurge their application throughout various manufacturing sectors. Numerous fibers and bioresins are available abundantly without any cost or at low cost showing different mechanical and impact performances, and they can be combined to alter the varying reinforcement/matrix combinations. The main disadvantage of using green fiber is that it is fond of water/moisture. Thus, it must be modified to a standard structure to retard the ability to absorb water and moisture. Therefore, for the green composites' desired performance, the ingredients, especially natural fibers, must be pretreated to yield their best performances. Among those alkalis, treatments have been seen frequently with most natural fibers. The main objective of this research study was to reduce the time potent researchers surf scholarly articles to get data and information for future studies. This review paper is believed to reach its zenith in comprehending the aspects of each constituent of various & most common bioresin-based composites and elucidating the research community in a single paper. Thus, a researcher can find all necessary information in one place and further developments and contributions to field can be done without further delays.

Declaration of Competing Interests

The authors declare that they have no known competing financial interests or personal relationships that could have appeared to influence the work reported in this paper.

Funding Declaration

This research did not receive any grants from governmental, private, or nonprofit funding bodies.

Author Contribution

Nithesh Naik: Conceptualization and Writing- Reviewing and Editing; **Nilakshman Sooriyaperakasam**, **Yashoda K. Abeykoon**, **Yomali S.Wijayarathna**, **Pranesh G**, **Soumik Roy**, **Rovin Negi** and **Aakif Budnar Kunjibettu**: Data curation, Writing–original draft preparation **Asela Kulatunga** and **Jayakrishna Kandasamy**: Writing- reviewing and editing.

References

[1] H. S. Shekar and M. Ramachandra, "Green Composites: A Review," *Materials Today: Proceedings*, vol. 5, no. 1, pp. 2518–2526, 2018.

[2] M. Mariano, F. Pilate, F. B. De Oliveira, F. Khelifa, P. Dubois, J. M. Raquez, and A. Dufresne, "Preparation of Cellulose Nanocrystal-Reinforced Poly(lactic acid) Nanocomposites through Noncovalent Modification with PLLA-Based Surfactants," *ACS Omega*, vol. 2, pp. 2678–2688, jun 2017.

[3] M. Nagalakshmaiah, N. El Kissi, and A. Dufresne, "Ionic Compatibilization of Cellulose Nanocrystals with Quaternary Ammonium Salt and Their Melt Extrusion with Polypropylene," *ACS Applied Materials and Interfaces*, vol. 8, pp. 8755–8764, apr 2016.

[4] M. A. Anwer, H. E. Naguib, A. Celzard, and V. Fierro, "Comparison of the thermal, dynamic mechanical and morphological properties of PLA-Lignin & PLA-Tannin particulate green composites," *Composites Part B: Engineering*, vol. 82, pp. 92–99, dec 2015.

[5] A. Keller, "Compounding and mechanical properties of biodegradable hemp fibre composites," *Composites Science and Technology*, vol. 63, pp. 1307–1316, jul 2003.

[6] R. U. Halden, "Plastics and health risks," in *Annual Review of Public Health*, vol. 31, pp. 179–194, Palo Alto: Annual Reviews, 2010.

[7] A. Ashori, "Wood-plastic composites as promising green-composites for automotive industries!," *Bioresource Technology*, vol. 99, pp. 4661–4667, jul 2008.

[8] G. S. Mann, L. P. Singh, P. Kumar, and S. Singh, "Green composites: A review of processing technologies and recent applications," *Journal of Thermoplastic Composite Materials*, vol. 33, pp. 1145–1171, aug 2020.

[9] M. McNutt, "Climate change impacts," *Science*, vol. 341, p. 435, aug 2013.

[10] D. Salarbashi, J. Bazeli, and E. Fahmideh-Rad, "Fenugreek seed gum: Biological properties, chemical modifications, and structural analysis– A review," *International Journal of Biological Macromolecules*, vol. 138, pp. 386–393, oct 2019.

[11] S. Raghavendra, T. Aravinda, and S. Sarapure, "Nano green composites-an overview," *International Journal of Applied Engineering Research*, vol. 13, no. 1, pp. 115–116, 2018.

[12] M. Nagalakshmaiah, S. Afrin, R. P. Malladi, S. Elkoun, M. Robert, M. A. Ansari, A. Svedberg, and Z. Karim, "Biocomposites: Present trends and challenges for the future," in *Green Composites for Automotive Applications*, pp. 197–215, Elsevier, 2018.

[13] O. Faruk, A. K. Bledzki, H. P. Fink, and M. Sain, "Biocomposites reinforced with natural fibers: 2000-2010," *Progress in Polymer Science*, vol. 37, pp. 1552–1596, nov 2012.

[14] S. Prasad, A. Singh, N. E. Korres, D. Rathore, S. Sevda, and D. Pant, "Sustainable utilization of crop residues for energy generation: A life cycle assessment (LCA) perspective," *Bioresource Technology*, vol. 303, p. 122964, may 2020.

[15] D. B. Pal, A. Singh, and A. Bhatnagar, "A review on biomass based hydrogen production technologies," *International Journal of Hydrogen Energy*, vol. 47, pp. 1461–1480, jan 2022.

[16] A. Ashori and A. Nourbakhsh, "Bio-based composites from waste agricultural residues," *Waste Management*, vol. 30, pp. 680–684, apr 2010.

[17] S. L. Fávaro, M. S. Lopes, A. G. Vieira de Carvalho Neto, R. Rogério de Santana, and E. Radovanovic, "Chemical, morphological, and mechanical analysis of rice husk/post-consumer polyethylene composites," *Composites Part A: Applied Science and Manufacturing*, vol. 41, pp. 154–160, jan 2010.

[18] R. Prithivirajan, S. Jayabal, and G. Bharathiraja, "Bio-based composites from waste agricultural residues: Mechanical and morphological properties," *Cellulose Chemistry and Technology*, vol. 49, no. 1, pp. 65–68, 2015.

[19] C. Nyambo, A. K. Mohanty, and M. Misra, "Polylactide-based renewable green composites from agricultural residues and their hybrids," *Biomacromolecules*, vol. 11, pp. 1654–1660, jun 2010.

[20] N. Reddy and Y. Yang, "Properties and potential applications of natural cellulose fibers from cornhusks," *Green Chemistry*, vol. 7, no. 4, pp. 190–195, 2005.

[21] D. Y. Kim, T. Lütke-Eversloh, K. Elbanna, N. Thakor, and A. Steinbüchel, "Poly(3-mercaptopropionate): An nonbiodegradable biopolymer?," *Biomacromolecules*, vol. 6, pp. 897–901, mar 2005.

[22] L. Zimmermann, A. Dombrowski, C. Völker, and M. Wagner, "Are bioplastics and plant-based materials safer than conventional plastics? In vitro toxicity and chemical composition," *Environment International*, vol. 145, sep 2020.

[23] P. C. Srinivasa and R. N. Tharanathan, "Chitin/chitosan - Safe, ecofriendly packaging materials with multiple potential uses," *Food Reviews International*, vol. 23, pp. 53–72, jan 2007.

[24] R. Nakamura, K. Goda, J. Noda, and J. Ohgi, "High temperature tensile properties and deep drawing of fully green composites," *Express Polymer Letters*, vol. 3, no. 1, pp. 19–24, 2009.

[25] G. Cicala, G. Cristaldi, G. Recca, and A. Latteri, "Composites Based on Natural Fibre Fabrics," in *Woven Fabric Engineering* (P. D. Dubrovski, ed.), pp. 317–342, editor. books.google.com. IntechOpen; 2010 [cited 2021 Aug 25]. p. Available from: Sciyo, aug 2010.

[26] M. S. Huda, L. T. Drzal, A. K. Mohanty, and M. Misra, "Effect of chemical modifications of the pineapple leaf fiber surfaces on the interfacial and mechanical properties of laminated biocomposites," *Composite Interfaces*, vol. 15, pp. 169–191, jan 2008.

[27] I. Živković, C. Fragassa, A. Pavlović, and T. Brugo, "Influence of moisture absorption on the impact properties of flax, basalt and hybrid flax/basalt fiber reinforced green composites," *Composites Part B: Engineering*, vol. 111, pp. 148–164, feb 2017.

[28] M. Shibata, S. Oyamada, S. I. Kobayashi, and D. Yaginuma, "Mechanical properties and biodegradability of green composites based on biodegradable polyesters and lyocell fabric," *Journal of Applied Polymer Science*, vol. 92, pp. 3857–3863, jun 2004.

[29] W. Liu, M. Misra, P. Askeland, L. T. Drzal, and A. K. Mohanty, "'Green' composites from soy based plastic and pineapple leaf fiber: Fabrication and properties evaluation," *Polymer*, vol. 46, pp. 2710–2721, mar 2005.

[30] P. J. P. Espitia, N. d. F. F. Soares, J. S. d. R. Coimbra, N. J. de Andrade, R. S. Cruz, and E. A. A. Medeiros, "Zinc Oxide Nanoparticles: Synthesis, Antimicrobial Activity and Food Packaging Applications," *Food and Bioprocess Technology*, vol. 5, pp. 1447–1464, jul 2012.

[31] H. Takagi and Y. Ichihara, "Effect of fiber length on mechanical properties of "green" composites using a starch-based resin and short bamboo fibers," *JSME International Journal, Series A: Solid Mechanics and Material Engineering*, vol. 47, no. 4, pp. 551–555, 2004.

[32] M. A. Sawpan, K. L. Pickering, and A. Fernyhough, "Improvement of mechanical performance of industrial hemp fibre reinforced polylactide biocomposites," *Composites Part A: Applied Science and Manufacturing*, vol. 42, pp. 310–319, mar 2011.

[33] A. Gomes, T. Matsuo, K. Goda, and J. Ohgi, "Development and effect of alkali treatment on tensile properties of curaua fiber green composites," *Composites Part A: Applied Science and Manufacturing*, vol. 38, pp. 1811–1820, aug 2007.

[34] S. Singh, A. K. Mohanty, T. Sugie, Y. Takai, and H. Hamada, "Renewable resource based biocomposites from natural fiber and polyhydroxybutyrate-co-valerate (PHBV) bioplastic," *Composites Part A: Applied Science and Manufacturing*, vol. 39, pp. 875–886, may 2008.

[35] F. Corrales, F. Vilaseca, M. Llop, J. Gironès, J. A. Méndez, and P. Mutjè, "Chemical modification of jute fibers for the production of green-composites," *Journal of Hazardous Materials*, vol. 144, pp. 730–735, jun 2007.

[36] C. Asasutjarit, S. Charoenvai, J. Hirunlabh, and J. Khedari, "Materials and mechanical properties of pretreated coir-based green composites," *Composites Part B: Engineering*, vol. 40, pp. 633–637, oct 2009.

[37] J. D. S. Macedo, M. F. Costa, M. I. Tavares, and R. M. Thiré, "Preparation and characterization of composites based on polyhydroxybutyrate and waste powder from coconut fibers processing," *Polymer Engineering and Science*, vol. 50, no. 7, pp. 1466–1475, 2010.

[38] X. Huang and A. Netravali, "Characterization of flax fiber reinforced soy protein resin based green composites modified with nano-clay particles," *Composites Science and Technology*, vol. 67, pp. 2005–2014, aug 2007.

[39] L. Y. Mwaikambo and M. P. Ansell, "Hemp fibre reinforced cashew nut shell liquid composites," *Composites Science and Technology*, vol. 63, pp. 1297–1305, jul 2003.

[40] S. Panthapulakkal, A. Zereshkian, and M. Sain, "Preparation and characterization of wheat straw fibers for reinforcing application in injection molded thermoplastic composites," *Bioresource Technology*, vol. 97, pp. 265–272, jan 2006.

[41] P. Threepopnatkul, N. Kaerkitcha, and N. Athipongarporn, "Effect of surface treatment on performance of pineapple leaf fiber-polycarbonate composites," *Composites Part B: Engineering*, vol. 40, pp. 628–632, oct 2009.

[42] G. L. Prasad, B. S. Gowda, and R. Velmurugan, "Comparative Study of Impact Strength Characteristics of Treated and Untreated Sisal Polyester Composites," *Procedia Engineering*, vol. 173, pp. 778–785, 2017.

[43] X. Zhang, F. Wang, and L. M. Keer, "Influence of surface modification on the microstructure and thermo-mechanical properties of bamboo fibers," *Materials*, vol. 8, pp. 6597–6608, sep 2015.

[44] M. Rokbi, H. Osmani, A. Imad, and N. Benseddiq, "Effect of chemical treatment on flexure properties of natural fiber-reinforced polyester composite," *Procedia Engineering*, vol. 10, pp. 2092–2097, 2011.

[45] A. Saravanakumaar, A. Senthilkumar, S. S. Saravanakumar, M. R. Sanjay, and A. Khan, "Impact of alkali treatment on physico-chemical, thermal, structural and tensile properties of Carica papaya bark fibers," *International Journal of Polymer Analysis and Characterization*, vol. 23, pp. 529–536, aug 2018.

[46] O. M. Asumani, R. G. Reid, and R. Paskaramoorthy, "The effects of alkali-silane treatment on the tensile and flexural properties of short fibre non-woven kenaf reinforced polypropylene composites," *Composites Part A: Applied Science and Manufacturing*, vol. 43, pp. 1431–1440, sep 2012.

[47] R. Sepe, F. Bollino, L. Boccarusso, and F. Caputo, "Influence of chemical treatments on mechanical properties of hemp fiber reinforced composites," *Composites Part B: Engineering*, vol. 133, pp. 210–217, jan 2018.

[48] D. K. Debeli, Z. Qin, and J. Guo, "Study on the Pre-Treatment, Physical and Chemical Properties of Ramie Fibers Reinforced Poly (Lactic Acid) (PLA) Biocomposite," *Journal of Natural Fibers*, vol. 15, pp. 596–610, jul 2018.

[49] K. Senthilkumar, N. Rajini, N. Saba, M. Chandrasekar, M. Jawaid, and S. Siengchin, "Effect of Alkali Treatment on Mechanical and Morphological Properties of Pineapple Leaf Fibre/Polyester Composites," *Journal of Polymers and the Environment*, vol. 27, pp. 1191–1201, jun 2019.

[50] A. Paul, K. Joseph, and S. Thomas, "Effect of surface treatments on the electrical properties of low-density polyethylene composites reinforced with short sisal fibers," *Composites Science and Technology*, vol. 57, pp. 67–79, jan 1997.

[51] G. M. Arifuzzaman Khan, M. Shaheruzzaman, M. H. Rahman, S. M. Abdur Razzaque, M. S. Islam, and M. S. Alam, "Surface modification of okra bast fiber and its physico-chemical characteristics," *Fibers and Polymers*, vol. 10, pp. 65–70, feb 2009.

[52] K. J. Vardhini, R. Murugan, C. T. Selvi, and R. Surjit, "Optimisation of alkali treatment of banana fibres on lignin removal," *Indian Journal of Fibre and Textile Research*, vol. 41, pp. 156–160, aug 2016.

[53] X. Colom and F. Carrillo, "Crystallinity changes in lyocell and viscose-type fibres by caustic treatment," *European Polymer Journal*, vol. 38, pp. 2225–2230, nov 2002.

[54] S. K. Ramamoorthy, *Properties and Performance of Regenerated Cellulose Thermoset*. PhD thesis, 2015.

[55] R. M. Rowell, "Acetylation of natural fibers to improve performance," *Molecular Crystals and Liquid Crystals*, vol. 418, pp. 153–164, jan 2004.

[56] A. K. Mohanty, P. C. Tripathy, M. Misra, S. Parija, and S. Sahoo, "Chemical modification of pineapple leaf fiber: graft copolymerization of acrylonitrile onto defatted pineapple leaf fibers," *Journal of Applied Polymer Science*, vol. 77, pp. 3035–3043, sep 2000.

[57] P. C. Tripathy, M. Misra, S. Parija, S. Mishra, and A. K. Mohanty, "Studies of Cu(II)-IQ-4 initiated graft copolymerization of methyl methacrylate from defatted pineapple leaf fibres," *Polymer International*, vol. 48, pp. 868–872, sep 1999.

[58] J. Rout, M. Misra, and A. K. Mohanty, "Surface modification of coir fibers I: Studies on graft copolymerization of methyl methacrylate on to chemically modified coir fibers," *Polymers for Advanced Technologies*, vol. 10, pp. 336–344, jun 1999.

[59] L. Wei and A. G. McDonald, "A review on grafting of biofibers for biocomposites," *Materials*, vol. 9, p. 303, apr 2016.

[60] M. E. Carr, "Preparation and Application of Starch Graft Poly(vinyl) Copolymers as Paper Coating Adhesives," *Starch - Stärke*, vol. 44, no. 6, pp. 219–223, 1992.

[61] A. K. Mohanty, M. Misra, and L. T. Drzal, "Surface modifications of natural fibers and performance of the resulting biocomposites: An overview," *Composite Interfaces*, vol. 8, pp. 313–343, jan 2001.

[62] E. Zini and M. Scandola, "Green composites: An overview," *Polymer Composites*, vol. 32, pp. 1905–1915, dec 2011.

[63] K. Joseph, S. Thomas, and C. Pavithran, "Effect of chemical treatment on the tensile properties of short sisal fibre-reinforced polyethylene composites," *Polymer*, vol. 37, pp. 5139–5149, nov 1996.

[64] M. S. Sreekala, M. G. Kumaran, and S. Thomas, "Water sorption in oil palm fiber reinforced phenol formaldehyde composites," *Composites - Part A: Applied Science and Manufacturing*, vol. 33, pp. 763–777, jun 2002.

[65] A. Bessadok, S. Marais, F. Gouanvé, L. Colasse, I. Zimmerlin, S. Roudesli, and M. Métayer, "Effect of chemical treatments of Alfa (Stipa tenacissima) fibres on water-sorption properties," *Composites Science and Technology*, vol. 67, pp. 685–697, mar 2007.

[66] S. Goutianos, T. Peijs, B. Nystrom, and M. Skrifvars, "Development of flax fibre based textile reinforcements for composite applications," *Applied Composite Materials*, vol. 13, pp. 199–215, jul 2006.

[67] M. Hughes, J. Carpenter, and C. Hill, "Deformation and fracture behaviour of flax fibre reinforced thermosetting polymer matrix composites," *Journal of Materials Science*, vol. 42, pp. 2499–2511, apr 2007.

[68] S. Ochi, "Mechanical properties of kenaf fibers and kenaf/PLA composites," *Mechanics of Materials*, vol. 40, pp. 446–452, apr 2008.

[69] S. Phillips and L. Lessard, "Application of natural fiber composites to musical instrument top plates," *Journal of Composite Materials*, vol. 46, pp. 145–154, jan 2012.

[70] M. S. Islam, K. L. Pickering, and N. J. Foreman, "Influence of alkali treatment on the interfacial and physico-mechanical properties of industrial hemp fibre reinforced polylactic acid composites," *Composites Part A: Applied Science and Manufacturing*, vol. 41, pp. 596–603, may 2010.

[71] E. Bodros, I. Pillin, N. Montrelay, and C. Baley, "Could biopolymers reinforced by randomly scattered flax fibre be used in structural applications?," *Composites Science and Technology*, vol. 67, pp. 462–470, mar 2007.

[72] C. K. Hong and R. F. Wool, "Development of a bio-based composite material from soybean oil and keratin fibers," *Journal of Applied Polymer Science*, vol. 95, pp. 1524–1538, mar 2005.

[73] B. N. Melo, C. G. Dos-Santos, V. R. Botaro, and V. M. Pasa, "Eco-composites of polyurethane and Luffa aegyptiaca modified by mercerisation and benzylation," *Polymers and Polymer Composites*, vol. 16, pp. 249–256, may 2008.

[74] D. P. Pfister and R. C. Larock, "Green composites from a conjugated linseed oil-based resin and wheat straw," *Composites Part A: Applied Science and Manufacturing*, vol. 41, pp. 1279–1288, sep 2010.

[75] R. V. Silva, D. Spinelli, W. W. Bose Filho, S. Claro Neto, G. O. Chierice, and J. R. Tarpani, "Fracture toughness of natural fibers/castor oil polyurethane composites," *Composites Science and Technology*, vol. 66, pp. 1328–1335, aug 2006.

[76] A. K. Bledzki and A. Jaszkiewicz, "Mechanical performance of biocomposites based on PLA and PHBV reinforced with natural fibres - A comparative study to PP," *Composites Science and Technology*, vol. 70, pp. 1687–1696, oct 2010.